Part 1 Synthesis of a potent histone deacetylase inhibitor
Part 2 Studies towards a stabilized helix-turn-helix peptide

by

Tao Liu

Dissertation submitted to the faculty of the Virginia Polytechnic Institute and State University in partial fulfillment of the requirements for the degree of

Doctor of Philosophy
in
Chemistry

Dr. Felicia A. Etzkorn, Committee Chair
Dr. Mark R. Anderson
Dr. Paul R. Carlier
Dr. David G. Kingston
Dr. James M. Tanko

January 15, 2007
Blacksburg, Virginia

Keywords: helix-turn-helix, histone deacetylase inhibitors, mimic, conformation, peptidomimetics, assay, inhibition, cyclization.

Part 1 Synthesis of a potent histone deacetylase inhibitor
Part 2 Studies towards a stabilized helix-turn-helix peptide

Tao Liu

ABSTRACT

The first part of this work describes the synthesis of a new histone deacetylase (HDAC) inhibitor (HDI). HDAC enzymes modify core histones, influence nucleosome structure and change gene transcription by removing the acetyl groups from lysine residues on proteins. HDIs are showing exciting potential as a new class of drugs for cancer and a variety of other diseases. A new HDAC inhibitor based on the hydroxamic acid motif has been synthesized. Two characteristic structural features were incorporated into the design of the novel inhibitor. A cyclic peptide mimetic of known structure was fused to a hydroxamic acid moiety through an aliphatic chain. The HDAC inhibitor provided significant inhibitory activity against HDACs with an IC_{50} value of 46 ± 15 nM, and against HDAC8 with an IC_{50} value of 208 ± 20 nM. The potent HDAC inhibitory activity of the HDAC inhibitor demonstrates the importance of the rim recognition region in the design of HDIs. The hydrophobic cyclic turn mimic allows the formation of a tight complex between HDI and HDAC enzymes.

The second part of this work is to synthesize secondary structure mimics and incorporate them into the helix-turn-helix (HTH) motif. One of the important methods to study the conformation of the biologically active peptides is to incorporate the rigid peptidomimetics into the relevant peptides. Important information can be obtained from the study of conformationally constrained peptides. HTH proteins are well characterized and found in many organisms from prokaryotes to eukaryotes. The relatively small size,

simple structure, and significance in stabilizing tertiary structures make the HTH peptide an attractive target to mimic. Both a Gly HTH turn mimic and a Ser HTH turn mimic were synthesized using stereoselective hydrogenation and macrocyclization starting from unnatural amino acids in a yield of 33% and 14%, respectively. The synthesis of Fmoc protected HTH turn mimics allowed incorporation into HTH peptides using Fmoc chemistry on solid phase. The incorporation of the HTH turn mimics into the peptides proved to be challenging, either by sequential elongation or by segment condensation. Alternative peptide synthesis strategies were employed in attempts to solve the problems.

Dedicated to my parents, my wife and my sister

ACKNOWLEDGMENTS

I would like to acknowledge my advisor, Dr. Felicia A. Etzkorn, for her guidance, constant encouragement, intellectual support, and for providing excellent working environment for her students. I am very fortunate to carry out this research under her supervision. I would also like to express my sincere appreciation to my committee members, Dr. Mark R. Anderson, Dr. Paul R. Carlier, Dr. David G. Kingston, and Dr. James M. Tanko for their excellent teaching and help. I also thank Dr. David G. Kingston for allowing me to use the fluorescence spectrometer. I thank all of the faculty, administrators and staff for providing the excellent environment in the Chemistry Department of Virginia Tech.

I also deeply thank my former and current lab colleagues, Dr. Galina Kapustin, Dr. Bailing Xu, Dr. Xiaodong Wang, Mr. Song Zhao, Mr. Chao Yang, Ms. Guoyan Xu, Mr. Nan Dai, Ms. Ashley Mullins, Mr. Keith Leung, Ms. Ana Mercedes, Mr. Boobalan Pachaiyappan for helping with all kinds of experimental details and invaluable discussion about a variety of scientific topics. Financial support from Virginia Tech and NIH are appreciated.

I will always be indebted to my sister for willingly covering my contributions to family matters while I have been studying abroad. Most of my thanks are reserved for my parents, who have provided consistent encouragement and support for my graduate study despite the hardships of geographical separation. Finally but most importantly, words cannot express my gratitude to my wife, Ru Lu. I want her to know how much I love her and appreciate the love and support she has given me.

Table of Contents

List of Figures

List of Schemes

List of Tables

List of Abbreviations

Amino Acid

A	Ala	Alanine
C	Cys	Cysteine
D	Asp	Aspartic acid
E	Glu	Glutamic acid
F	Phe	Phenylalanine
G	Gly	Glycine
H	His	Histidine
I	Ile	Isoleucine
K	Leu	Leucine
L	Lys	Lysine
M	Met	Methionine
N	Asn	Asparagine
P	Pro	Proline
Q	Gln	Glutamine
R	Arg	Arginine
S	Ser	Serine
T	Thr	Threonine
V	Val	Valine
W	Trp	Tryptophan
Y	Tyr	Tyrosine
Xaa	X is used for an undetermined amino acid	

Abbreviations

AA	amino acid
Ac	acetyl
Acm	acetamidomethyl
AMC	7-amino-4-methylcoumarin
AML	acute myeloid leukemia
Antp	Antennapedia type homeodomain
APL	acute promyelocytic leukemia
Bn	benzyl
Boc	*tert*-butoxycarbonyl
bp	base pairs
cavitand	rigid organic molecules that contain enforced cavities
Cbz	benzyloxycarbonyl
CD	circular dichroism
CTB	cyclotribenzylene
DCC	1,3-dicyclohexylcarbodiimide
DMAP	4-dimethylamino pyridine
DMF	dimethylformamide
DMSO	dimethyl sulfoxide
DNA	deoxyribonucleic acid
DPPA	diphenylphosphoryl azide

EDC	1-[3-(dimethylammino)propyl]-3-ethylcarbodiimide hydrochloride
FDDP	pentafluorophenyl diphenylphosphinate
Fmoc	fluorenylmethoxycarbonyl
G1	preparation for chromosome replication
G2	preparation for mitosis
HAT	histone acetyltransferase
HATU	*O*-(7-azabenzotriazol-1-yl)-*N,N,N′,N′*-tetramethyluronium hexafluorophosphate
HBTU	*O*-(benzotriazol-1-yl)-*N,N,N′,N′*-tetramethyluronium hexafluorophosphate
HDAC	histone deacetylase
HDLP	histone deacetylase-like protein
HDI	histone deacetylase inhibitor
HOAt	1-hydroxy-7-azabenzotriazole
HOBT	1-hydroxybenzotriazole
hr	hour
HTH	helix-turn-helix
IC_{50}	the concentration required for 50% inhibition in determination of receptor binding affinity of a ligand using a competitive binding curve
k_{cat}	catalyzed rate constant
K_m	Michaelis constant
min	minute
NK	neurokinin
N-CoR	nuclear co-repressor

NOESY	nuclear Overhauser and exchange spectroscope
PyAOP	(7-Azabenzotriazol-1-yloxy)tripyrrolidinophosphonium hexafluorophosphate
rms	root mean square
SAHA	suberoylanilide hydroxamic acid
SIR2	silent information regulator 2
TASP	template assembled synthetic proteins
TBS	*tert*-butyldimethysilyl
TBAF	tetrabutylammonium fluoride
TEA	triethylamine
TES	triethyl silane
TFFH	tetramethyl fluoro formamidinium hexafluorophosphate
THF	tetrahydrofuran
TIS	triisopropyl silane
TMG	tetramethyl guanidine
TMSCl	chlorotrimethylsilane
TMSE	trimethylsilylethyl
TSA	trichostatin A
SAR	structure activity relationships

Part 1
Synthesis of a potent histone deacetylase inhibitor

Chapter 1
Histone deacetylase

1.1 Epigenetic regulation of histones

Increasing evidence shows that cancer is not only operated by genetic mechanisms, but also operated by epigenetic mechanisms. Epigenetic refers to a heritable change in gene expression that is mediated by mechanisms that do not affect the DNA sequence. Epigenetic mechanisms include DNA and histone modification, such as methylation and acetylation.[1] Epigenetic changes can induce abnormal expressions of genes that regulate cell proliferation, differentiation, and apoptosis, which can increase the potential of cellular transformation.

The DNA is assembled into nucleosomes, which are the fundamental repeating subunits of all eukaryotic chromatin. Nucleosomes are made up of DNA (146 base pairs) wrapped around an octamer of histones: two copies of H2A, H2B, H3, and H4 each (Figure 1-1).[2, 3] The association of histone H1 with linker DNA compacts the structure of nucleosomes by forming a helical structure named the 30-nm fiber.[4] More condensed chromatin is called higher-order chromatin structure. The chromatins have dynamic

structures that can be changed according to environmental changes.[5] Remodelling studies reveal that the gene activity is affected by the structures of chromatin.[4] Modification can cause the changes of the structure of chromatin, including ATP-dependent chromatin remodeling complexes, DNA methylation and histone modifications.[6-10]

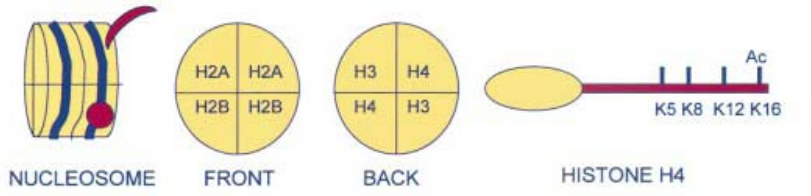

Figure 1-1. Schematic structure of nucleosomes. (Reproduced with permission from de Ruijter et al. 2003, *Biochemical Journal,* **370**, 737-749. © the Biomedical Society.[10])

Post-translational modifications of core histone *N*-terminal tails can modify the structure of chromatin and then regulate gene expression. The *N*-terminal tails of histones are subjected to a variety of post-translational modifications including acetylation/deacetylation of lysine, methylation of lysine and arginine, phosphorylation of serine, and ubiquitination of lysine.[6,7] Most mechanisms of these post-translational modifications are unclear. Histone tails provide the binding sites for chromatin-associated proteins from the study of the identification of chromatin proteins and their native complexes.[6] Modifications of histone amino terminal form code that can control whether the gene is turned on of off.[8] The histone codes can act as epigenetic marks which are heritable and can be translated into biological functions.

Histones bind to negatively-charged DNA through the positively-charged lysine residues in their *N*-terminal tails (Figure 1-1). The *C*-terminal domain of histones lies buried inside of the nucleosome core, and the lysine tails of the *N*-terminal domain lies

outside of the nucleosome.[9] Lysine residues of the histone *N*-terminal tails can be reversibly acetylated or deacetylated, as controlled by histone acetyltransferases (HATs) and histone deacetylases (HDACs), respectively. The competing action of HAT and HDAC determines the histone acetylation levels that ultimately affect the higher-order chromatin structure and gene activities at a particular chromosomal region. Acetylation of histones neutralizes the positive charge on lysine and relaxes nucleosome structures, facilitating access of transcription factors to their targeted DNA. Nucleosomes are tightly compacted in the hypoacetylated state, leading to a condensed chromatin structure, and resulting in transcriptional repression due to restricted access of transcription factors to their targeted DNA (Figure 1-2).[10] Generally speaking, transcriptional activation is associated with histone acetylation, while transcriptional silencing is associated with histone deacetylation. The equilibrium between HATs and HDACs alters the status of the lysine residues, therefore, affects the structure of chromatin and gene activities.[6]

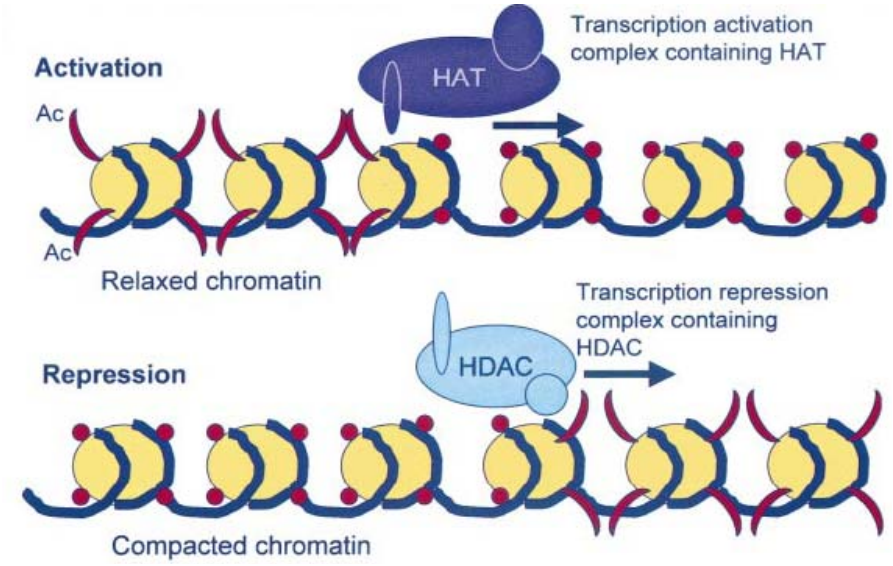

Figure 1-2. HAT and HDAC regulate gene transcription through the modulation of nucleosomal packaging of DNA.[10] (Reproducted with permission from de Ruijter et al. 2003, *Biochemical Journal,* **370**, 737-749. © the Biomedical Society.)

1.1.1 Histone acetyltransferases (HATs)

Histone acetyltransferases (HATs) catalyze the transfer of an acetyl group from acetyl coenzyme A to the lysine ε-amino groups on the *N*-terminal tails of histones. The modification of histones H3 and H4 have been more extensively characterized than that of the other histones. Important positions for acetylation are Lys9 and Lys14 on histone H3, and Lys5, Lys8, Lys12 and Lys16 on histone H4.[10] Histone acetylation opens the chromatin transcriptional regulators by neutralizing the positive charge of histone tails and thus decreasing their affinity for the negatively charged DNA.[11] Thus, histone hyperacetylation loosens the chromatin structure and activates genes.

The histone acetyltransferases are divided into five families, including over twenty enzymes.[11-13] GNAT (Gcn5-related *N*-acetyltransferases), the first family described, includes proteins involved with transcriptional initiation, such as Gcn5 and PCAF. The second family is the MYST family, named after the monocytic leukemia zinc-finger protein (MOZ), YBF2/SAS3, SAS2 and the HIV-1 TAT-interactive protein 60 (TIP60). The third family is comprised of two closely related proteins p300 and CBP (cyclic adenosine monophosphate response element-binding protein), which act as co-activators for a number of transcription factor complexes. Another two HAT families include general transcription factors, comprised of the TFIID complex subunit TAF250, and nuclear hormone-receptor cofactors, such as ACTR and SRC1.[14] HATs not only acetylate histone tails, but also acetylate transcription co-activators and co-repressors, including E2F, p53 and GATA1.[15] HATs therefore play an important role in gene activation and in the gene repression. HATs do not bind directly to DNA, instead, they form complex with other HATs and transcription factors.[16]

1.1.2 Histone deacetylases (HDACs)

Histone deacetylases (HDACs) reverse the activity of HATs and catalyze the removal of acetyl groups from lysine residues in the *N*-terminal tails of histones, leading to chromatin condensation and silencing the gene post transcription. HDACs are evolutionarily conserved and expressed in organisms from archaebacteria to humans.

Similar to HATs, HDACs do not bind to DNA sequences directly, but are recruited as a complex with other transcription co-repressors. Different HDACs form different complexes. The activity of HDACs is regulated by post-translational modification. Phosphorylation of HDAC1 and HDAC2 causes an increase in HDAC activity.[17, 18] HDACs not only deacetylate histone proteins, but also deacetylate non-histone proteins, such as p53[19] and GATA-1.[20] Acetylated p53 shows higher binding affinity to its target sequence.[21]

Mammalian HDAC1 is the first histone deacetylase identified.[22] Currently, 18 HDACs have been identified, of which eleven HDACs have been identified in humans. These HDACs differ in their sequence homology, substrate specificity and requirement for cofactors.[23] HDACs are divided into 3 classes based on their homology to yeast histone deacetylases.

Class I and II HDACs are mediated by Zn-dependent mechanism, class III HDACs are mediated by an NAD-dependent mechanism. The Class I HDACs includes HDAC 1, 2, 3 and 8, expressing high sequence homology to the yeast protein Rpd3 (Reduced potassium dependency protein 3).[23] Class II HDACs share homologies with the yeast HDA1 protein and consists of HDAC 4, 5, 6, 7, 9, and 10.[24] HDAC 11, identified in human, is most likely a class I enzyme, but it has not been classfied.[24] Class I HDACs are

relatively small size enzymes ranging between 42–45 kDa, exclusively expressed in the nucleus. Class II HDACs are larger proteins (120–130 kDa), shuttling between the cytoplasm and the nucleus (Figure 1-3).[9] Class III HDACs are structurally unrelated to the human class I and class II HDACs, and share homology with Sir2 (Silent information regulator 2) protein.[25]

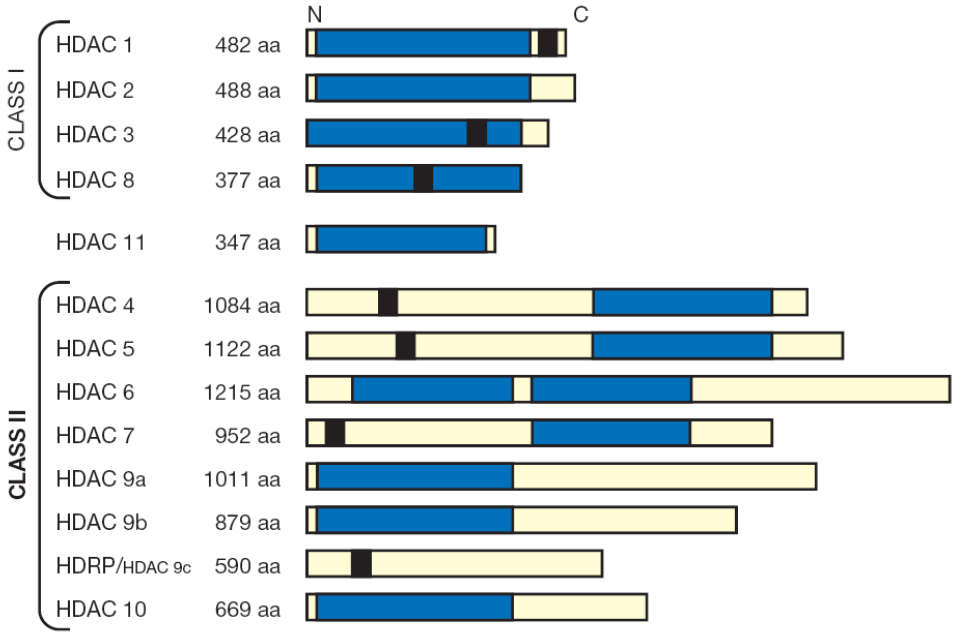

Figure 1-3. Schematic depiction of HDAC isoforms. Bars depict the length of the protein. N represents *N*-terminus. C represents *C*-terminus. The black box represents a NLS. The blue box represents the catalytic site conserved in Class I and Class II HDACs. Two catalytic sites are present in HDAC6.[10] (Reproduced with permission from de Ruijter et al. 2003, *Biochemical Journal,* **370**, 737-749. © the Biomedical Society.)

1.1.2.1 Class I HDACs

Class I HDACs contain a large conserved domain homologous to the *N*-terminal region of yeast Rpd3 and a short *C*-terminal region with a more variable sequence.[26] In yeast and mammalian cells, the Rpd3-type HDACs have been shown to regulate

transcriptional factors by interacting with specific DNA-binding proteins or associated corepressors and by recruitment to target promoters.[27]

Class I HDACs exist in yeast, mammals, and plants. Rpd3 HDAC1 forms a complex with Sin3 in yeast, where it regulates the gene activities involved, including meiosis, cell-type specificity, potassium transport, phosphate and phospholipid metabolism, and methionine biosynthesis.[28, 29] In plants, the first Rpd3 homolog is identified in maize and it complements the phenotype of a Rpd3 null mutant of yeast.[30] In mammals, class I HDACs include HDAC 1, 2, 3, 8 and 11, which are divided into subclasses, HDAC 1/2 and HDAC 3.

The sequences of HDAC1 and HDAC2 are highly conserved, exhibiting an 82% sequence similarity. The catalytic domain is located in the *N*-terminus of HDAC1 and HDAC2, occupying the major part of the protein.[31] HDAC1 and HDAC2 only are inactive when produced by recombinant techniques, implying that cofactors are necessary for HDAC activity. HDAC1 and HDAC2 show activity to form complexes, including the SIN3, NuRD/NRD/Mi2, and CoREST complexes.[32, 33] Cofactors are needed to maximize the HDAC activity.[34, 35] Phosphorylation of Ser on the HDAC1 and HDAC2 regulates their activity and formation of the complex with other cofactors.[17, 18] The activity of HDAC1 and HDAC2 increases, and the formation of the complexes decreases when the proteins are hyperphosphorylated.

HDAC3 is found in corepressor complex called N-CoR (nuclear receptor corepressor) that has been shown to inhibit JNK activation through an integral subunit, GPS2.[36] HDAC3 has the same domain structure as class I HDACs. The 181-333 amino acid domain of HDAC3 shares an only 68% identity with HDAC1 and HDAC2.[10] The

non-conserved *C*-terminal region of HDAC3 is required for both deacetylase activity and transcriptional repression.[37]

HDAC8 is not categorized as a single subclass because it mainly appears in vertebrates.[38] HDAC8 shows a 37% similarity with HDAC3. The activity of HDAC8 decreases when phosphorylated by protein kinase A, whereas HDAC1 and HDAC2 are activated by phosphorylation.[39] HDAC8 was the first mammalian HDAC that had a three-dimensional structure.[40]

1.1.2.2 Class II HDACs

Class II HDACs, also called HDA1-like HDACs, share sequence homology with Rpd3-type HDACs in their catalytic domain, but they have distinct structural and functional features.[31] In yeast, Hda1 is the primary class I HDAC. In *Arabidopsis*, 6 putative class II HDAC genes were identified but their functions and characterization are poorly studied. Class II HDACs are divided into two subclasses, Iia (HDAC4, 5, 7, 9) and Iib (HDAC6 and 10), based on their sequence homology and domain organization.[24]

HDAC4, HDAC5 and HDAC7 share more similarity with each other than they do with HDAC9.[24] The catalytic domains of HDAC4, 5, and 7 are located at the *C*-terminus of the protein, whereas the catalytic domain of HDAC9 is located on the *N*-terminus, as in class I HDACs.[10] Class Iia HDACs shuttle between the nucleus and the cytoplasm.[41] Class Iia HDACs binding to 14-3-3 proteins, a family of highly conserved acidic proteins that is regulated by the phosphorylation of *N*-terminal serine residues in class Iia HDACs.[42] Class Iia HDACs bind to SMRT and N-CoR through their *C*-terminal domains, and only show enzymatic activities when they form a complex with SMRT/N-CoR–HDAC3.[43]

HDAC6 is mostly identified in testis.[44] HDAC10 is mostly expressed in liver, spleen, and kidney.[45] HDAC6 has two catalytic sites, while other HDACs have only one. HDAC10 shares 37% sequence homology with HDAC6.[46] The enzymatic activities of HDAC6 and HDAC10 are more resistant to trapoxin and sodium butyrate inhibitors than those of class I and class Iia HDACs.[47] HDAC10 interacts with HDACs 1, 2, 3, 4, 5, 7, and SMRT, but not with HDAC6, indicating that HDAC10 may act as a recruiter rather than a deacetylase.[48]

Histone is not the only protein that can be regulated by HDAC, a growing number of non-histone proteins influenced by the function of HDACs.[49]

1.1.3 Aberrant HDAC or HAT activity associated with cancer

Acetylation of histones by HATs neutralizes the positive charge on lysine and relaxes nucleosome structures, facilitating the access of transcription factors to their targeted DNA. HDACs catalyze the removal of acetyl-groups from histones and non-histones, increasing the positive charge on histone tails. Hypoacetylated nucleosomes are tightly compacted, leading to a condensed chromatin structure and resulting in transcriptional repression due to restricted access of transcription factors to their targeted DNA.[10] Therefore, acetylation and deacetylation of chromatin play an important role in chromatin remodeling and in transcriptional regulation of gene expression. Increasing evidence shows alteration of HATs and HDACs may cause aberrant gene expression and the development of cancer.[50-52]

HAT activity is associated with translocation, amplification, overexpression, or mutation in a variety of cancers, both hematological and epithelial in origin.[53] Two closely related HATs, p300 and CBP, are altered in some tumors by either mutation or

translocation. Mutations and truncations in p300 have been identified in a number of glioblastomas, hepatocellular carcinomas and leukemias.[54] The Rubinstein Taybi syndrome, tending to develop into a cancer, is correlated with the mutation in CBP.[25] The CBP gene has been found in association with the MOZ gene in acute myeloid leukemia (AML).[55] In addition, the CBP gene has also been identified in fusions with the mixed lineage leukemia gene (MLL), therefore resulting in disrupted histone acetylation and inappropriate gene silencing.[16] The oncogenic viral proteins E1A and SV40 can bind to CBP and antagonize CBP-dependent transcription either by direct inhibition of HAT activity or through blockage of the interaction of the co-activators with specific transcription factors.[56]

No evidence shows alterations of HDACs are directly related with the pathogenesis of human cancer. However, HDACs associate with oncogenic translocation products and tumor suppressor genes, such as p53, p21, and gelsolin, in a number of human carcinoma cell lines and various tumors.[57] In acute promyelocytic leukemia (APL), the association between the retinoic acid receptor α gene (RARα) and either the promyelocytic leukemia gene (PML) or the promyelocytic leukemia zinc finger gene (PLZF) produces the fusion proteins PML-RARα and PLZF-RARα, which repress transcription by HDAC recruitment.[58] Thus the cancer cell is unable to undergo differentiation, leading to excessive proliferation. Translocation of t(8;21) chromosomal of acute myeloid leukemia (AML) yields the AML1-ETO fusion protein, which represses transcription through recruitment of a HDAC-containing multiprotein complex.[59] In non-Hodgkin's diffuse large cell lymphoma, chromosomal rearrangements within the promoter region result in an overexpression of the transcriptional repressor LAZ3/BCL6

(lymphoma-associated zinc finger-3/B cell lymphoma 6) that induces inappropriate transcriptional repression through recruitment of HDACs.[25]

Apparently, transcriptional repression is regulated the recruitment of HDACs. It is possible to control cancer by inhibition of HDAC activities. HDIs may block cancer cell growth by restoring the histones to their normal acetylated state, turning on transcription of important regulatory genes.

1.2 Histone deacetylase inhibitors (HDIs)

1.2.1 Mechanism of HDACs

The interaction between histone deacetylase inhibitors and the HDAC enzyme was studied in detail by Finnin in 1999.[60] The enzyme used in the structural study was histone deacetylase-like protein (HDLP), a homolog from the hyperthermophilic bacterium *Aquifex aeolicus*. HDLP shares a 35.2% sequence identity with HDAC1.

The structure of the complexes of TSA and SAHA with HDLP were elucidated to 2.0 Å resolution.[60] The study of the crystal revealed that the region interacting with TSA or SAHA of HDLP contains three characteristics feathers, a surface recognition region, a tube-like, 11 Å deep channel and a 14 Å long, narrow pocket which attaches to the channel. All these structural characteristics of HDLP derived from sequence alignment are in excellent agreement with the crystal structure of HDAC8.[61]

The binding study of four HDIs with HDAC8 illustrated that the surface of HDAC8 in the vicinity of the active site is fairly flexible and can change conformation according to the structural properties of the different HDIs.[40] The hydrophobic and

aromatic residues that make up the channel in HDLP are identical in HDAC1, HDAC2, HDAC3, and HDAC8.[60] With one exception, the residues making up the 14 Å tunnel are either identical or conservatively substituted in all four class I HDACs. In HDLP, the opening of the tunnel is between 4.5 and 5.5 Å, and it becomes wider at the bottom.

The structure of the complex shows that TSA inserts its hydroxamic acid into the pocket by the aliphatic chain that contacts hydrophobic residues in the channel. The hydroxamic acid binds Zn^{2+} in a bidentate fashion. The zinc ion is located near the bottom of the pocket. The proposed catalytic mechanism for the deacetylation of acetylated lysine is analogous to the amide hydrolysis mechanism for zinc proteases.[62] The zinc ion is five-fold coordinated with Asp 168 (2.1 Å), His 170 (2.1 Å), Asp 258 (1.9 Å) and a water molecule (2.5 Å), which presumably acts as a nucleophile. The zinc ion polarizes the carbonyl group to make it more electrophilic. By forming hydrogen bonds with negatively charged Asp 166-His 131, the water would have an increase in its nucleophilicity.[60] The nucleophilic attack of the water on the carbonyl carbon forms a tetrahedral intermediate which is stabilized by the zinc-oxygen interaction. The bond breaking between carbon and nitrogen releases acetate and lysine, which are protonated by Asp 173-His 132.

However, experimental studies indicate the transition state of HDACs may not be analogous to zinc proteases.[63] Phosphonamidates were demonstrated as transition-state analogue inhibitors of thermolysin.[64] Phosphorous was proposed to be tetrahedrally positioned with heteoatoms to mimic the tetrahedral intermediate of amide bond hydrolysis. The phosphorous containing compounds that are analogous to SAHA were synthesized to mimic the histone deacetylation. However, the compound showed a weak

inhibitory activity against HDACs, suggesting HDACs follow another mechanism to remove the acetyl group.

A density functional theory QM/MM study demonstrates that zinc prefers to be four-fold coordinated during the deacetylation.[65] A water molecule does not bind to zinc in the presence of the substrate. However, the nucleophilic water molecule binds to H131, H132, and D168. The binding of zinc to the substrate makes the carbonyl of the amide more susceptible to the nucleophile attack. The nucleophilic attack of the water on the carbonyl carbon forms a tetrahedral intermediate, which is stabilized by Y297, D166, and D173. The formation of the amine of the lysine and the acetate is facilitated by the transfer of one proton from His132 to the amide nitrogen.

The function of the pocket was hypothesized to remove the cleaved acetate and transfer it out of the pocket, consequently, restoring the activity of the active site.[66] The postulation was based on the necessity to regenerate the activity of the active site. The acetate or acetic acid remains in the 14 Å pocket after the deacetylation. While the channel is still occupied by the deacetylated lysine side chain, the acetate or acetic acid needs to find a route to exit the pocket. The large temperature factor (B-factor) of the amino acids composing the pocket indicates they have considerable mobility which can help remove the acetate out of the pocket. The acetate binds first to Arg27, which is in equilibrium with Arg16, the second binding site for the acetate. The side chain movement of Arg16 moves the acetate out of the pocket by exchanging it with water. The water is moved in the opposite direction and the activity of the active site is restored. The acetate would block the active site and hinder the substrate binding if it can not leave the pocket.[66]

1.2.2 Classification of HDIs

Many reviews about HDIs have been published.[9, 49-52, 67-74] These will be summarized in this section. The structural characteristic of HDIs is summarized in Figure 1-14 based on the study of inhibitor-enzyme complexes and the SAR of various inhibitor classes. The efficient HDIs must have three features: 1) a coordinating group (such as hydroxamic acid) to chelate to Zn^{2+} at the bottom of the tubular active site, 2) a hydrophobic region that binds the surface of the active site and caps the entrance, and 3) a 5 to 7 carbon linker from the hydrophobic region to the coordinating group.[74] The aliphatic linker helps the inhibitor insert into the tube-like channel.

HDIs come from either natural sources or from synthetic routes. HDIs can be divided into several structural classes, including hydroxamates, cyclic peptides, aliphatic acids, benzamides and electrophilic ketones.

Trichostatin A (TSA), the first natural product hydroxamate isolated from a *Streptomyces hygroscopicus* strain, was discovered to inhibit HDACs directly,[75] providing evidence that the hydroxamate is required for activity. Only (*R*)-TSA, which was obtained by total synthesis, was active against HDACs.[75] SAHA, containing relatively less structural complexity, has recently entered phase II clinical trials.[16] Cinnamic acid bishydroxamic acid (CBHA) has been shown to be a potent HDAC inhibitor.[76] Oxamflatin exhibited a potent HDAC inhibition of partially purified mouse HDAC (IC_{50}= 15.7 nM).[77] Scriptaid was identified via high throughput screening for transcriptional activators, acting as a HDAC inhibitor.[78]

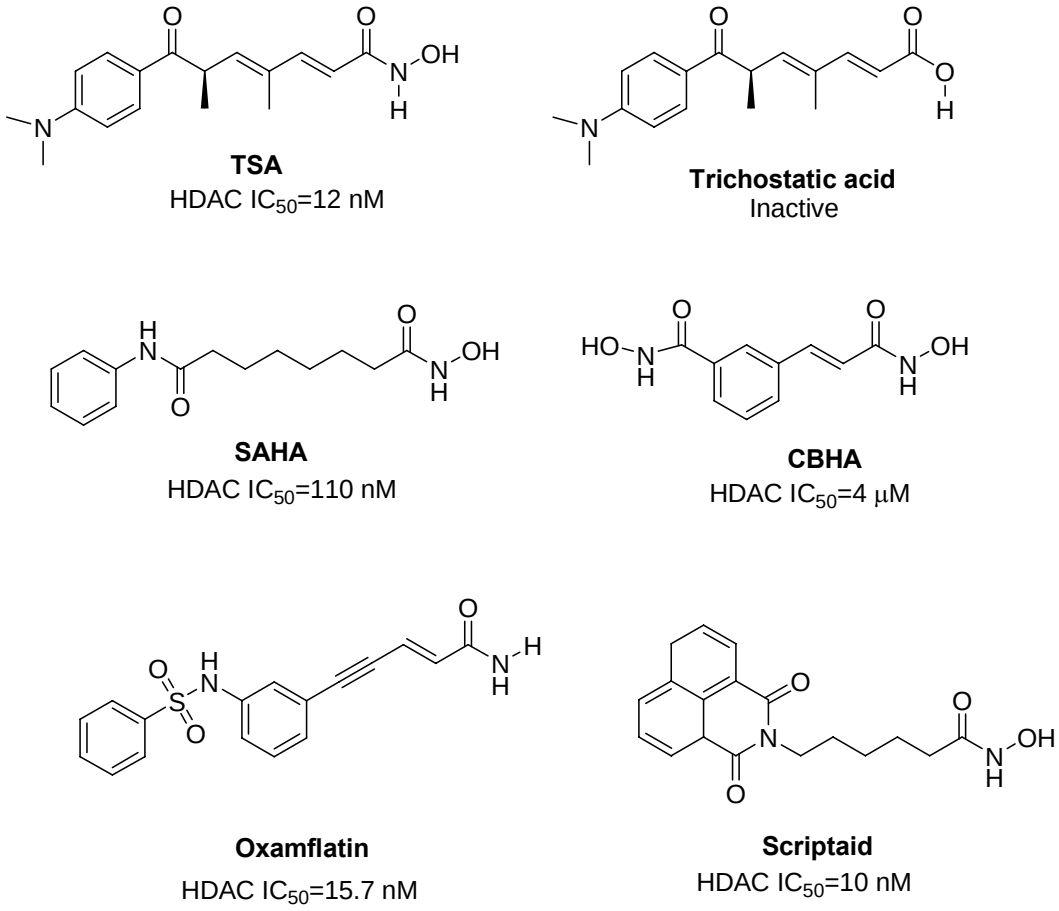

Figure 1-4. Hydroxamate HDIs.

Cyclic tetrapeptides comprises the most structurally complex class of HDIs, including depsipeptide (FK-228),[79] apicidin,[54] and CHAPs (cyclic hydroxamic acid-containing peptides).[47] Almost all the compounds in this class inhibit the activity of HDACs at nanomolar levels. Depsipeptide FK228 is a naturally occurring polypeptide which was isolated from *Chromobacterium violaceum.*[79] FK228 is only one of the cyclic peptides under clinical investigation. It has progressed through phase II clinical trials on cutaneous T-cell lymphoma leading to complete or partial response at the end of the phase I study (Figure 1-5).[80]

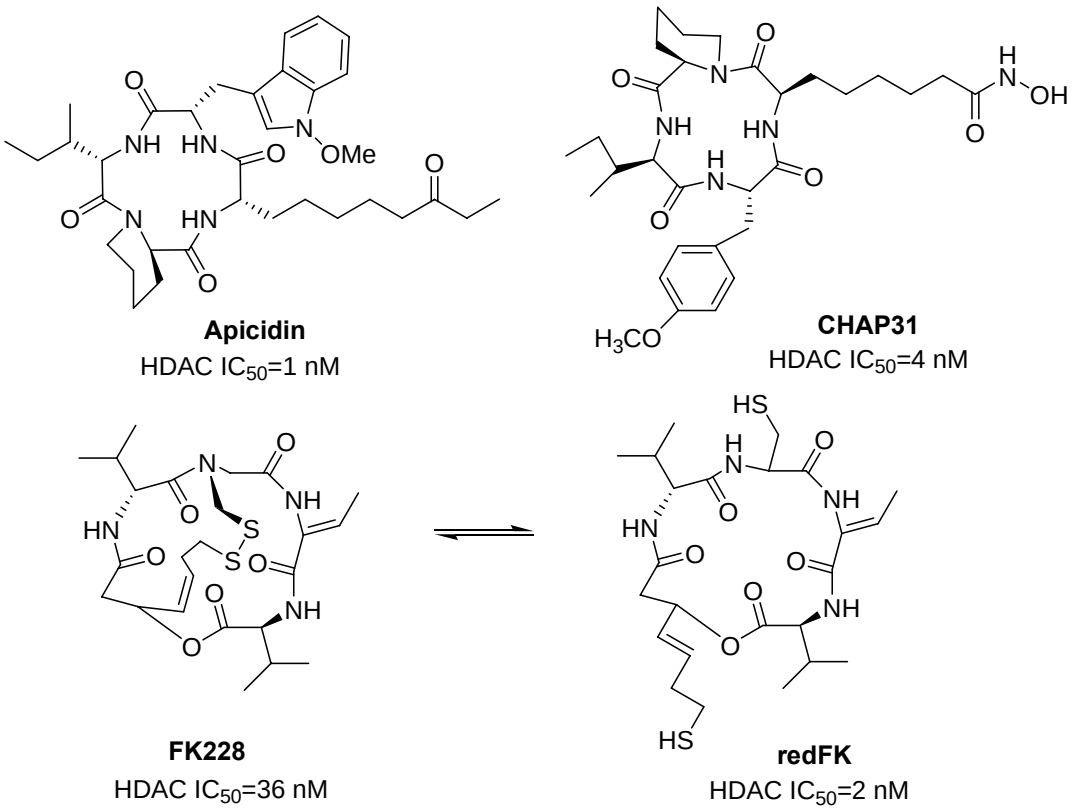

Figure 1-5. Cyclic tetrapeptide HDIs.

Mechanistic studies have shown that FK228 is only activated by reduction with glutathione after entering the cells.[81] The reduced form of FK228, redFK, is the active form, which was proven by the enhancement of HDAC inhibition after reduction with DTT, and the stronger inhibition of redFK compared to FK228 against class I HDACs (Figure 1-5). The SH of RedFK between the sulfhydryl and the cyclic depsipeptide core can react with a cysteine residue in the pocket to form a covalent disulfide bond. The stability of FK228 and its hydrophobic nature helps its penetration through the cell membrane to afford the active species, making it more effective than other HDIs. Investigations of the binding interactions on the recognition region of the HDAC

enzymes with cyclic peptide HDIs helps to understand the essential inhibitor-enzyme contacts and leads to the identification of selective inhibitors with higher efficiency.

The aliphatic acids are the least potent class of HDIs (active at millimolar levels), including valproic acid and butyric acid (Figure 1-6).[82,83] Butyric acid is a natural product generated in man by metabolism of fatty acids and bacterial fermentation of fiber in the colon. These inhibitors require careful study because they can modulate gene expression in subtle ways.[67] Valproic acid and butyric acid are under clinical investigation for cancer treatment.

Butyric acid

HDAC IC_{50}=1 mM

Valproic acid

HDAC IC_{50}=3 mM

Figure 1-6. The aliphatic acid HDIs.

The benzamide class, including MS-275 and CI-994, is generally less potent than the corresponding hydroxamates and cyclic tetrapeptides, inhibiting HDACs at micromolar level.[84, 85] Both MS-275 and CI-994 are in phase II clinical trials (Figure 1-7).

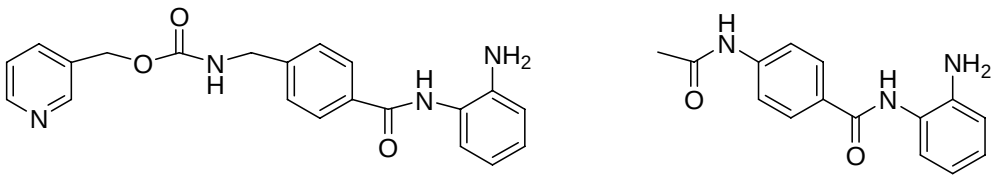

MS-275

HDAC IC_{50}=4.8 μM

CI-994

HDAC IC_{50}=1 μM

Figure 1-7. The benzamide HDIs.

A great number of electrophilic ketones form another class of HDIs. This class of inhibitors includes various trifluoromethyl ketones[86] and α-ketoamides.[87] These inhibitors inhibit HDAC activity at micromolar levels (Figure 1-8).

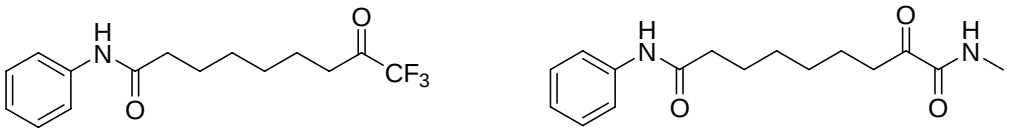

Trifluoromethyl ketone
HDAC IC_{50}=6.7 μM

α-Ketoamide
HDAC IC_{50}=340 nM

Figure 1-8. The electrophilic ketone HDIs.

Based upon the structure of TSA, SAHA and oxamflatin, a great number of HDIs were designed and synthesized. Most of these inhibitors contain a zinc binding group, and a 5-6 carbon chain attached to a hydrophobic group. The hydroxamic acid derivatives are the most studied HDIs. Cyclic peptide HDIs are among the most potent HDIs. Modifications of HDIs can be rim region, connecting unit, the length of aliphatic chain, and zinc bind functional group. While, at the same time, HDAC inhibitor with weak inhibitory activities also provide a useful tool to evaluate the SAR of HDIs and to give insight into the conformational features of HDACs. Both successful and failed cases not only reveal details of the active site, but also direct study to more potent HDIs.

Although class I and II HDACs exhibit homologous structures, their functions in modulating gene activities are different. Therefore, identification of HDIs with specific HDAC inhibitory activity is necessary. Butyric acid and MS-275 inhibit HDAC1 more efficiently than HDAC6 by 50-fold and 40000-fold factors, respectively. TSA does not exhibit any selectivity over HDAC1 and HDAC6. The results of the selectivity studies

are coincident with the observation of the sequence alignment of HDACs, demonstrating that residues in the channel and active site domains are not completely conserved.[74] Cyclic peptides, such as FK228 and CHAP, show selectivity of HDAC1 over HDAC6 or HDAC4. To design and synthesize HDIs which are selective over different enzymes is a major target at present. However, several compounds exhibit selectivity over different HDACs. The selectivity and high potency shown by cyclic peptides inspires us to design new class of HDIs by incorporating the cyclic peptides into the newly designed HDIs.

1.2.3 Mechanisms of action of HDIs

HDIs inhibit the enzymatic activity of HDACs and cause hyperacetylation of histones of nucleosomes. HDIs can induce cell cycle arrest in the G1 and/or G2 phases, apoptosis, terminal differentiation and to stop proliferation in virtually all transformed cell types, including epithelial (neuroblastoma, glioma, melanoma, lung, breast, pancreas, ovary, prostate, colon and bladder) and hematological (lymphoma, leukemia and multiple myeloma) tumors.[71,72] Several factors, such as the specific inhibitor being used, concentration of HDIs, the duration of exposure and the cell type change the cellular effects of these HDIs.[14] The precise mechanisms underlying these cellular responses are still not clear. These effects were either caused by an altered gene-expression profile or were caused by toxic effects of these substances. HDIs not only induce the transcriptional expressor, but also recruit of transcriptional repressor.[88]

Transcriptional profiling studies by microarrays show that only a small fraction (2%-9%) of genes are modulated by HDIs. Lymphoid cell lines treated with TSA showed that only ~2% of 340 genes being examined were affected.[89] By using differential display detection, the result of the cell transcriptional response to HDIs varies, for example, ~7%

(over 8000 genes assayed) of gene alterations in two colon carcinoma cell lines are affected and >9% (12000 genes assayed) in two leukemia cell lines are effected upon treatment with TSA.[90] The ratio between the upstream regulated genes and the down stream regulated genes is close to 1:1.[70] HDIs show low toxicity towards the whole organism in clinical trials due to the fact that a relatively small percentage of genes are affected by these inhibitors.

HDIs have different effects on different transformed cells including cell arrest, terminal differentiation, apoptosis, and cell death.[91]

HDIs display different effects on normal and cancer cells. Normal cells are found to be less sensitive to the effects caused by HDIs. SAHA and MS-275 cause an accumulation of reactive oxygen species (ROS) and caspase activation in transformed but not normal cells.[91] Although SAHA and MS-275 can arrest the growth of both normal (WI38- human embryonic lung fibroblast and Hs578Bst, human breast fibroblast) and transformed cells (ARP-1, human multiple myeloma and VA13- SV40 transformed WI38 cells) but only induce cell death of the transformed cells.

HDIs regulate the acetylation state of the cell cycle control protein, such as E2F, pRb, and p53. The accumulation of acetylated histone or non-histone proteins will either repress or activate the transcription factor leading to either the repression or activation of transcription, respectively. For example, acetylation of p53 increases DNA binding and transcription,[92] while acetylation of high mobility group I (HMGI) transcription factors inhibit their binding to DNA.[93]

The cell cycle kinase inhibitor $p21^{WAF1}$ is one of the most commonly induced genes by HDIs.[69] Induced expression of $p21^{WAF1}$ was up-regulated by almost all HDIs.[68]

$p21^{WAF1}$ is one of cell cycle cyclin-dependent kinase (cdk) inhibitors whose expression results in arrest of cell cycle progression. $P21^{WAF1}$ inhibits both the cyclin D associated cdk4 and cdk6 kinases and the cyclin E- and cyclin A-associated cdk2 kinases.[94] $p21^{WAF1}$ gene expression is stimulated by the tumor suppressor gene p53 in the process of DNA damage repair process. The transcriptional induction of $p21^{WAF1}$ is modulated by a p53-independent manner.[69] Other commonly induced genes include gelsolin, p16ink4a and p27kip1.[95] Gene expression is not only induced, but also expressed, as in cyclin D1.[95] A gene could be repressed because acetylation of histones or non-histones proteins cause the recruitment of a transcriptional repressor rather that an activator.

Cell cycle checkpoints are often defective in cancer cells. The G2 checkpoint is activated by HDIs in normal cells, causing the cell cycle to arrest. However the G2 checkpoint is defective in cancer cells. Consequently, treatment of the cancer cell with HDIs causes the cancer cell to go through aberrant mitosis and to cell death.[96]

HDIs can induce apoptosis of the cancer cells either by relaxing chromatin to increase accessibility of DNA to apoptotic endonucleases or inducing expression of p21, c-myc and gelsolin.[50] HDIs can induce cell antiproliferation by repressing the telomerase gene.[97] HDIs inhibit angiogenesis by the repression of angiogenic stimulating factor VEGF from tumor cells, and consequently inhibition of endothelial cells migration and proliferation.[73] The possible mechanisms of the cellular responses induced by HDIs, including inhibition of proliferation, cell cycle arrest in G1 phase, and induction of differentiation and/or apoptosis in tumor cell lines.

1.2.4 HDIs in clinical trials

Several HDIs, including butyric acid derivatives, depsipeptide FK228, *N*-acetyl dinaline, pyroxamide, SAHA and valproic acid, are under clinical investgation. These HDIs exhibit impressive anti-tumor activity and little toxicity. HDIs either act as monotherapy or work with cytotoxics and differentiation agents.[71]

Short chain fatty acids, such as phenylbutyrate are the most investigated of the butyric acid derivatives. Clinical trials with PB include intravenous and oral routes. These agents showed limited anti-cancer activity and were associated with toxicities, including central nervous system symptoms, fatigue and hypocalcemia. Another short chain fatty acid, valproic acid, is under phase I and phase II clinical trials.[14] Hydroxamate-based HDIs have been tested extensively in clinical trials. SAHA is in phase I and phase II clinical trials. SAHA shows anti-cancer activity in a broad range of hematologic and solid tumors at doses that are well tolerated. SAHA has induced responses in patients with refractory cutaneous T cell lymphomas (CTCL).[14] Treatment with SAHA relieves the symptomatic relief of the pruritus associated with cutaneous lymphoma in the majority of patients. Depsipeptide FK228 completed phase I evaluation, and it showed activity against cutaneous T cell lymphoma. Fk228 is being tested in a range of solid and hematological malignancies in phase II.[57] MS-275 is in Phase I clinical trials. MS-275 markedly suppressed the growth of tumors such as neuroblastoma, undifferentiated sarcoma and Ewing's sarcoma with few side effects.[98]

1.3 Conclusions

HDIs have become a new class of targeted anticancer agents, which mediate the regulation of gene expression and induces growth arrest, cell differentiation, and apoptosis of tumor cells. Aberrant histone deacetylation may cause changes in chromatin structure, leading to transcriptional factor repression. HDIs can induce the proper expression of genes by restoring the balance of histone acetylation. Although HDIs regulate the conformation of almost all the chromatins, they only alter a very limited number of genes. More than a dozen HDIs are either in phase I or phase II clinical trials to test their anti-cancer efficacy against various haematological and solid malignancies. The data from clinical trial have shown that HDIs have little toxicity towards normal cells and can inhibit cancer cells at nanomolar concentration. HDIs not only regulate the acetylation of histones, but also modulate the acetylation of non-histone proteins. Combinations of HDIs with retinoic acid have been shown to decrease leukemic cells in bone marrow, which is resistant to mono effect from retinoic acid alone. The combination therapy can not only extend the therapeutic range of HDIs, but also synergize the effects of HDIs. Finding the specific HDIs for the individual HDAC is an important goal since HDACs are found to maintain different biological activities. However, the mechanisms behind HDIs modulating gene expression are not clear. The cytotoxic effects of HDIs can not only be explained by histone acetylation. More understanding of the biological functions of HDACs inhibitors on the level of molecular are needed to facilitate the discover of the more specific HDI.

Chapter 2
Synthesis of a potent histone deacetylase inhibitor

2.1 Design of the histone deacetylase inhibitor

A great number of HDIs have been reported, either naturally occurring, such as TSA,[75] apicidin,[54] and trapoxin,[75] or chemically synthesized, such as SAHA (Figure 2-1).[76] These HDIs can be divided into several categories according to their structural characteristics, such as hydroxamates, carboxylates, benzamides, and cyclic peptides. Most of these inhibitors are hydroxamic acid derivatives. Quite a few compounds are in phase I or II clinical trials, including SAHA, MS-275,[84] butyrate, and FK-228.[79] Based on the X-ray crystal structure of HDLP (histone deacetylase-like protein) co-crystallized with inhibitors, such as TSA and SAHA, and from SAR studies, efficient HDIs must have three features: 1) a coordinating group (such as hydroxamic acid) to chelate to Zn^{2+} at the bottom of the tubular active site, 2) a hydrophobic region that binds the surface of the active site and caps the entrance, and 3) a 5 to 7 carbon linker from the hydrophobic region to the coordinating group. The aliphatic linker helps the inhibitor insert into the tube-like channel.

Not all inhibitors show efficient activity against HDACs; most of them exhibit IC_{50} values against HDACs in the micromolar range.[74] However, some inhibitors containing a large surface recognition element, such as trapoxin, apicidin and cyclic

tetrapeptides,[47] give nanomolar IC_{50} values against HDACs. The high potency of these tetrapeptides suggests it would be promising to introduce a cyclized peptide into a HDAC inhibitor (Figure 2-1).

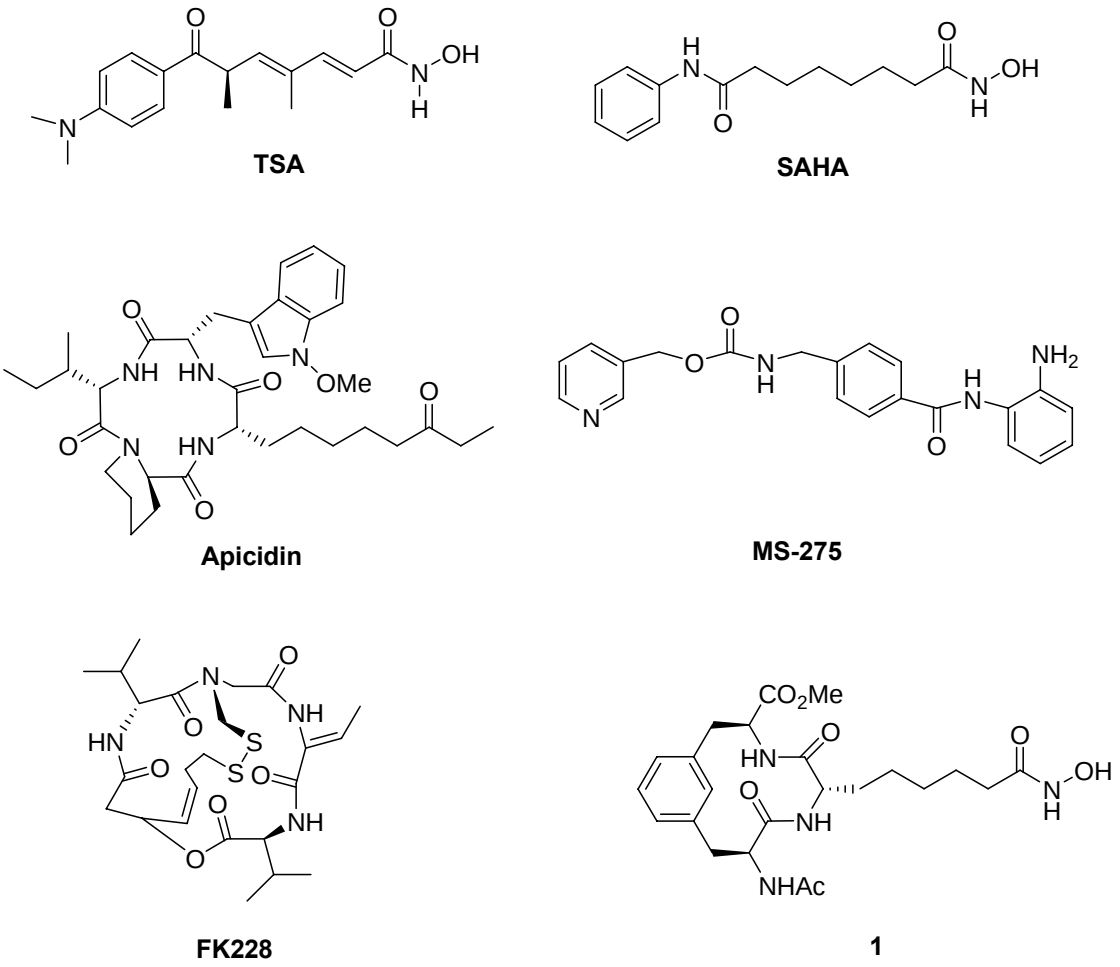

Figure 2-1. Naturally occurring and synthesized HDIs. The hydroxamic acid derivatives (TSA and SAHA) are most studied HDI. Cyclic tetrapeptides, such as apicidin, and trapoxin, are another class of potent HDIs.

The new HDAC inhibitor **1** was designed based on a cyclic peptide mimic **2** previously synthesized in our laboratory,[99] to which a hydroxamic acid motif was

introduced. The NMR study of the derivative with stereospecifically deuterated β-protons determined the three-dimensional structure of the cyclic peptide mimic **2** (Figure 2-2).[100] Incorporating hydroxamic acid functionality into the cyclic peptide mimic not only keeps the hydrophobic property of the cyclic peptide mimic, but also introduces the linker and zinc binding functional groups into the targeted molecule **1**. Target molecule was designed by molecular modeling and docking. The known cyclic peptide mimic **2** was attached to the linker and hydroxamic acid of SAHA from the X-ray structure of the HDLP complex to form the compound **1**. Compound **1** was docked manually by superposition onto SAHA in the HDLP active site using Sybyl 7.1.

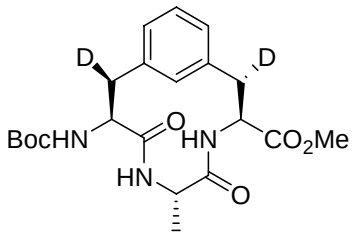

2

Figure 2-2. Deuterated cyclic peptide mimic **2**.

The design of HDAC inhibitor **1** was studied using Sybyl 7.1. The dockings using **3** capped with a Boc group at the amine end demonstrated that the bumping between the Boc and the side chains of the recognition region of the active site prevented the effective binding of **1** to HDLP. The ligand **1** binds to the pockets on the recognition region by the aromatic ring and 12- membered ring of the cyclic peptide mimic. However, the bulky Boc causes the repulsion between the mimic and side chains of the surface region of the

active site. The ligand **1** capped with acetyl on the amine end gave a stronger binding with HDLP (Figure 2-3).

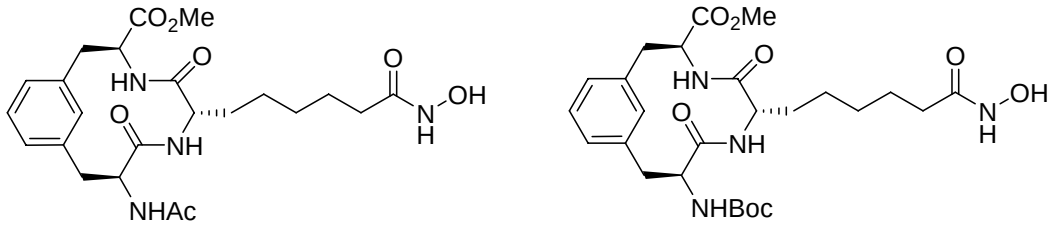

Figure 2-3. Two designed HDIs **1** and **3** capped with Ac and Boc on the amine end, respectively. The design of the compound **3** protected with the Boc group at the amine group of the recognition region was based on the usefully synthesized compounds **4** and **5**. The binding of **3** into the active site of the HDLP was repulsive because the bulky size of the Boc group. Compound **1**, protected with acetyl group on the amine produced an excellent docking into the active site of the HDLP.

The binding mode of **1** revealed that the structure of molecule **1** is compatible with the SAHA-binding cavity of HDLP. The surface shown in Figure 2-4 was created using the MOLCAD option in SYBYL. Molecular surface visualization shows that there are several pockets on the HDLP surface (Figure 2-4). The aromatic group and the 12-membered ring of compound **1** are predicted to make good contact with the enzyme surface recognition site, and the hydroxamic acid group is predicted to bind tightly to Zn^{2+}. The results of the computational study demonstrated that the newly designed HDAC inhibitor could be an efficient HDAC inhibitor.

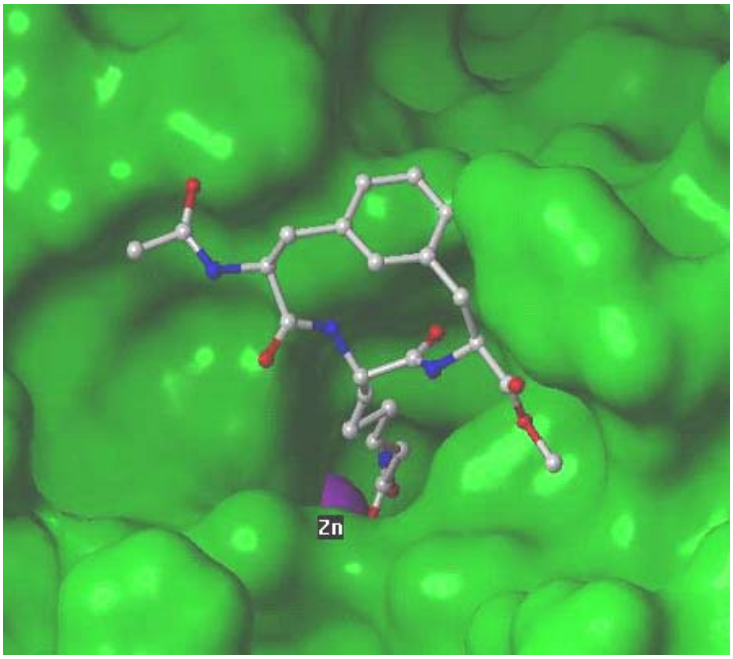

Figure 2-4. Molecular model of the surface and the active site of the complex of compound **1** (ball and stick) and HDLP (green surface).

The cyclic peptide mimics **4** and **5**, which contain Gly and Ala in the middle of the molecule, respectively, were successful synthesized by J. M. Travins (Figure 2-5).[99] The synthesis of **4** was repeated by the author in larger quantities (1.5g).

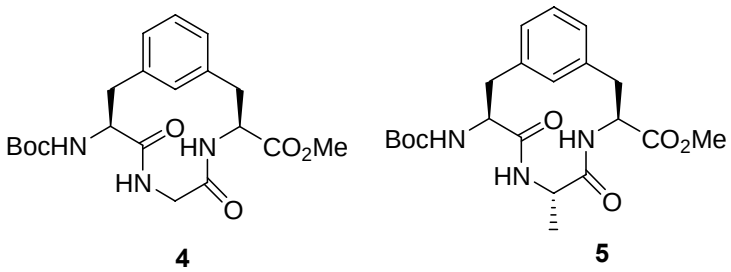

4 **5**

Figure 2-5. Two cyclic peptide mimics containing Gly and Ala in the position of Cys, respectively.

However, the synthesis of HDAC inhibitor **1** was extraordinarily difficult. To find a practical method for synthesizing the HDAC inhibitor **1**, several strategies were tried, including a two-allyl strategy, a solid-phase strategy, and a Boc-TMSE strategy. Each synthetic route will be discussed in detail here.

Retrosynthesis analysis reveals that the cyclic HDI must be synthesized through macrocyclization. The fusion of 12-membered ring can take place at either side of the central α-(*S*)-aminosuberic acid (Figure 2-6). Two synthetic routes had been proposed by applying different protecting groups.

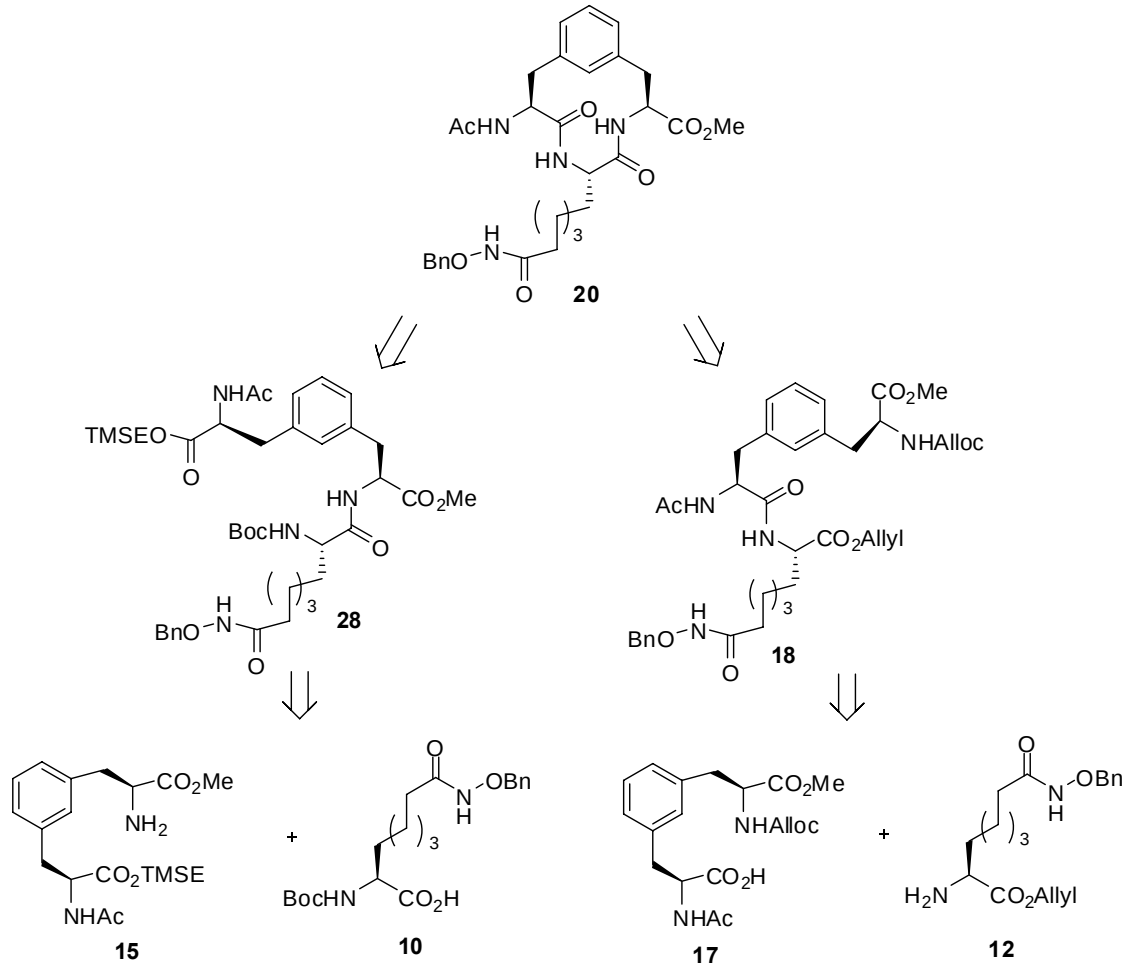

Figure 2-6. Retrosynthetic analysis of cyclic compound **20**

2.2 Attempts to synthesize HDI using two-allyl strategy

2.2.1 Synthesis of hydroxamate 12 from α-(*S*)-aminosuberic acid via oxazolidinone 8

The hydroxamate **12** from α-(*S*)-aminosuberic acid was synthesized via oxazolidinone **8**.[101-105] The amine group of α-(*S*)-aminosuberic acid **6** was protected with the Boc protecting group by treatment with Boc_2O in dioxane-water solution to afford **7**. The formation of oxazolidinone **8** was carried out by treatment with paraformaldehyde and TsOH as a catalyst by removing water formed during the reaction with a Dean-Stark trap. The Boc group was stable in the presence of TsOH under heat. The solvents employed in the reaction were benzene, 1,1,3 trichloroethane, toluene, of which 1,1,3 trichloroethane produced best results because it had a good solubility towards compound **7**, but also formed an azeotrope with water. Oxazolidinone **8** coupled with benzyloxyamine to give the protected hydroxamate **9**. Saponification of **9** freed the carboxyl group by mild basic conditions (LiOH).[102-104, 106, 107] The hydrolysis of **9** with sodium hydroxide partly produced decomposed product due to the sensitivity of hydroxamate to the basic condition. The fully protected hydroxamate **11** was obtained by coupling the free acid **10** with an allyl alcohol using EDC as coupling reagent. Several reagents are available for allylation, including allyl bromide,[108,109, 110] allyl chloride,[111, 112] and allyl alcohol.[113, 114] All these allylation reagents show good reactivity during the coupling. Allyl alcohol was chosen to form the allyl ester because the reaction proceeded under neutral, mild conditions. Allyl ester **11** was obtained in good yield (65%). The Boc group was cleaved using TFA in CH_2Cl_2 giving free amine **12**, which was carried on to

the next coupling step without further purification.

Scheme 2-1. Synthesis of hydroxamate **12** from α-(*S*)-aminosuberic acid via oxazolidinone **8**.

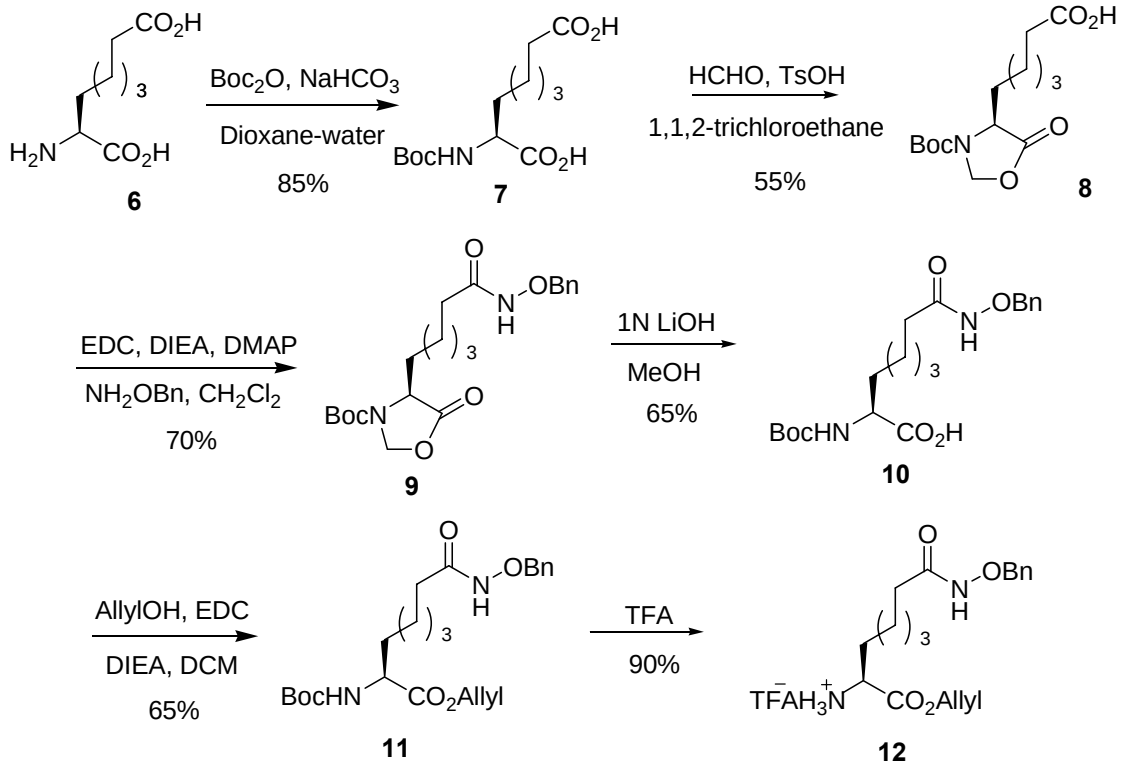

2.2.2 Synthesis of cyclization precursor 18

To apply the allyl strategy in our synthesis, we had to modify the known intermediate **13**.[99] The Boc group was removed with 4 M HCl in dioxane to give nearly quantitative yields of the hydrochloride salts,[115] followed by acetylation using an acetic anhydride and DIEA mixture. The transformation of the Cbz group to allyl carbamate on the amine was accomplished by hydrogenation with 10% Pd/C under 30-psi hydrogen atmosphere, followed by coupling with allyl chloroformate (Scheme 2-2).[111, 112] The

TMSE group of the fully protected intermediate **16** was removed by TBAF in wet DMF, giving the free acid **17**. Racemization was observed previously under strictly anhydrous conditions.[99] Water (0.4%v/v) was added to the reaction to suppress racemization. PyAOP ((7-Azabenzotriazol-1-yloxy)tripyrrolidinophosphonium hexafluorophosphate) coupling of fragments **12** and **17** gave fully protected tripeptide **18**. Phosphonium derivatives of HOAt, such as PyAOP, are useful in solid-phase peptide synthesis, including incorporating hindered amino acids, difficult short sequences, and cyclic systems.[27] Another advantage of PyAOP is that excess PyAOP does not undergo side-reactions at the amino terminus that block further chain formation.[116, 117]

Scheme 2-2. Synthesis of compound **18**.

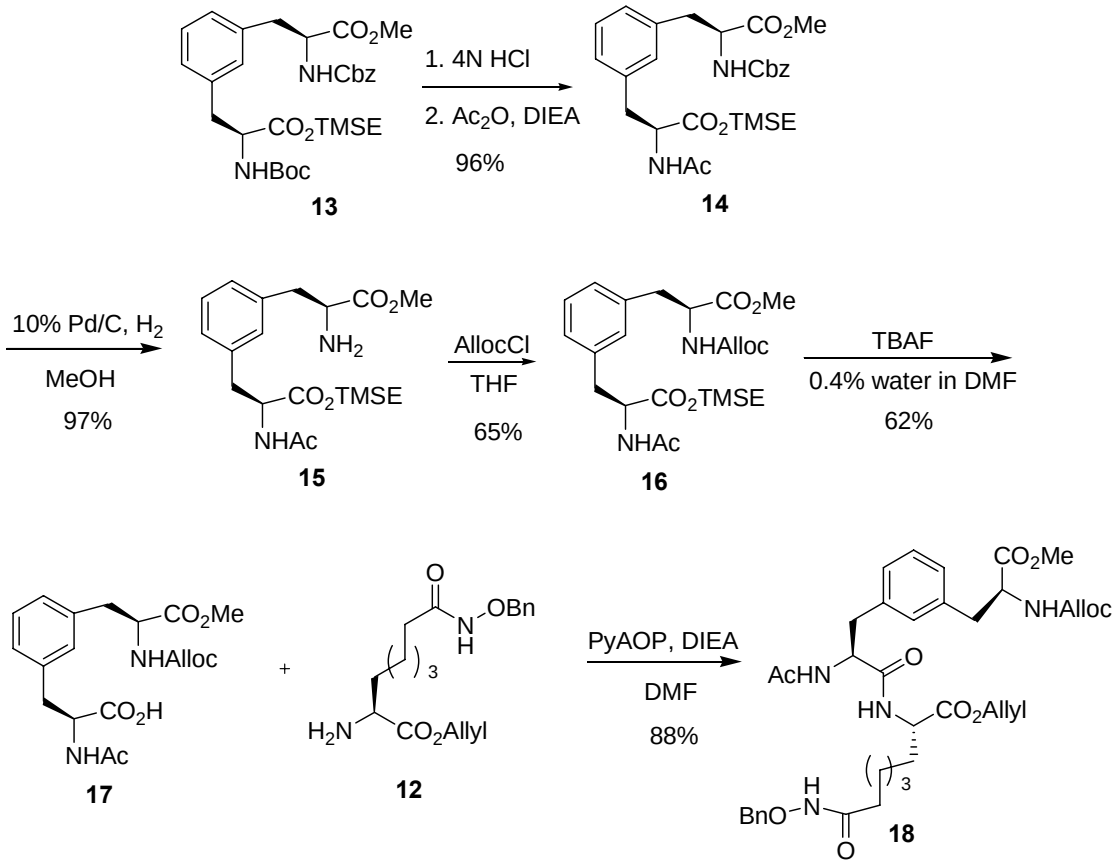

The steps of deprotection of two allyl groups and cyclization both limited the formation of cyclic HDI. The first difficulty met in the two-allyl route was how to improve the efficiency of simultaneous deprotection of two allyl groups (Scheme 2-3). The formation of allylamine as a side product during the deprotection was a major drawback of the reaction, although this could be trapped using an excess of scavenger.[118] Two kinds of scavengers, dimedone and morpholine, have been employed in the palladium catalyzed deprotection.[118-120] Although many successful cases of simultaneous removal of allyl esters and allyl carbamates in the presence of a catalytic amount of palladium complex have been reported,[121] the use of dimedone as an allyl scavenger in our case failed to give the desired amino acid **19**. The intermediate **19** was observed when morpholine was used as a scavenger only in the FAB+ mass spectrum. The yield was too low to isolate product.

Scheme 2-3. Simultaneous cleavage of allyl esters and carbamates in the presence of a palladium catalyst.

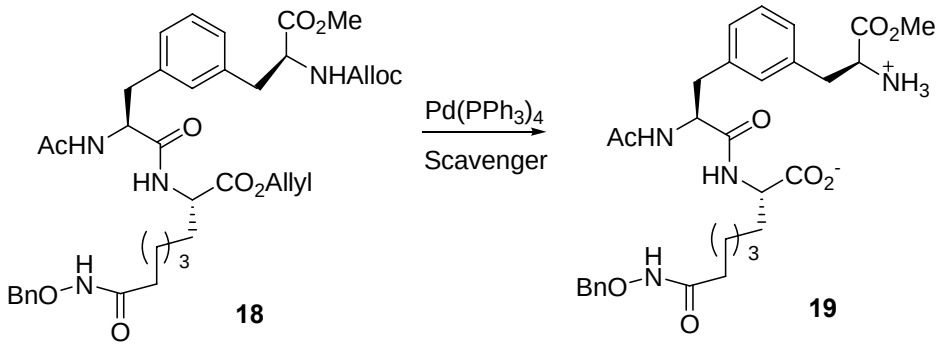

The quality of palladium catalyst surely played an important role in the allyl cleavage. The combination of dimedone as a scavenger and palladium catalyst from

different bottles and even from different sources failed to give the right precursor **19**. An example of using morpholine as a scavenger to cleave allyl and alloc groups simultaneously has been reported.[122, 123] Although the reported cases were carried out during resin-bound synthesis, we still employed morpholine as scavenger in the palladium catalyzed deprotection, which afforded the right precursor **19** as determined from the high resolution mass spectrum. The catalyst, which might interfere with the activity of the coupling reagent during the subsequent cyclization, was removed by reverse phase HPLC. Multiple by-products were observed on HPLC. The staring material could not be recovered after the treatment with catalyst, possibly due to hydrophobic interaction between cyclic peptide and the catalyst. The conditions of allyl ester and allyl carbamate deprotection are summarized in Table 2-1.

Table 2-1. Deprotection of two allyl groups by various catalysts.

Catalyst	Scavenger	Reaction time	Temperature	Yield of 19
$Pd(PPh_3)_4$ from Aldrich	Dimedone (10 equil)	2 h	rt	X
		4 h	rt	X
		2 h	0 C	X
$Pd(PPh_3)_4$ from STREM	dimedone	2 h	RT	X
		4 h	0 C	X
	morpholine (10 equil)	**3 h**	**0 C**	**35%**
		3 h	rt	30%

After separation of amino acid **19** by HPLC, many attempts were made to produce cyclized product **20** by employing different classes of coupling reagents, including phosphorus acid derivatives (DPPA and FDDP), phosphonium salt (PyAOP),

aminium salt (HATU), and acid fluorides formed from cyanuric acid or TFFH. Only DPPA or HATU coupling produced cyclized product **20**, but the yields were low. DPPA is the most widely used coupling reagent in peptide cyclization,[124] however, in our case; the highest yield of cyclization using DPPA was only 10% (Scheme 2-4). Although cyclization using DPPA produced detectable cyclized product **20** if the reaction was allowed to continue for 7 days, the best result was achieved using HATU for a 1 h coupling. Long-time coupling using HATU or PyAOP produced no product. The possible reaction of the secondary amine on hydroxamate was one of the side effects that caused the low yield of formation of cyclic HDI. The cyclization of **19** will be discussed alongside its amide bond structural isomer **30** in detail at the end of this chapter.

Scheme 2-4. Synthesis of cyclized product **20**.

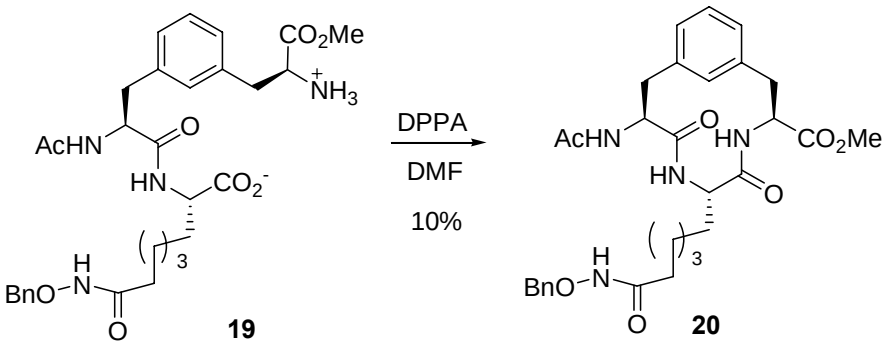

2.3 Attempts to synthesize cyclized HDI using two-allyl strategy on resin

The low efficiency of cyclization stated above enforced us to find an alternate route. The traditional methods of forming cyclic peptides in solution have some disadvantages, such as cyclodimerization and cyclo-oligomerization, which may happen even in highly diluted solutions. Cyclic peptides also may be prepared by attaching the linear precursor to a resin, cyclizing the peptides by coupling reagents, and cleaving the cyclized peptides from the resin after cyclization.[125] The linear peptide is attached to a low loading resin to produce *pseudodilution*, which suppresses the formation of cyclodimerization and cyclo-olimerization. The cyclization can be easily carried out while the linear peptide still remains attached the resin. The cyclization happening on the solid phase preferentially undergoes intramolecular reactions over intermolecular side reactions.[125]

Compound **24** was synthesized following a similar procedure that used for **18** (Scheme 2-5)**.** Large amounts of the Boc protected intermediate **13** that were on hand were used in this attempt. The Cbz group was changed to the allyl carbamate by hydrogenation, following by treatment with allyl chloroformate.[111, 112] The TMSE group was cleaved by TBAF in wet DMF to afford acid **23**.[99] The condensation between two segments, **23** and **12**, produced linear peptide precursor **24** by PyAOP coupling.

Scheme 2-5. Synthesis of linear precursor **24**.

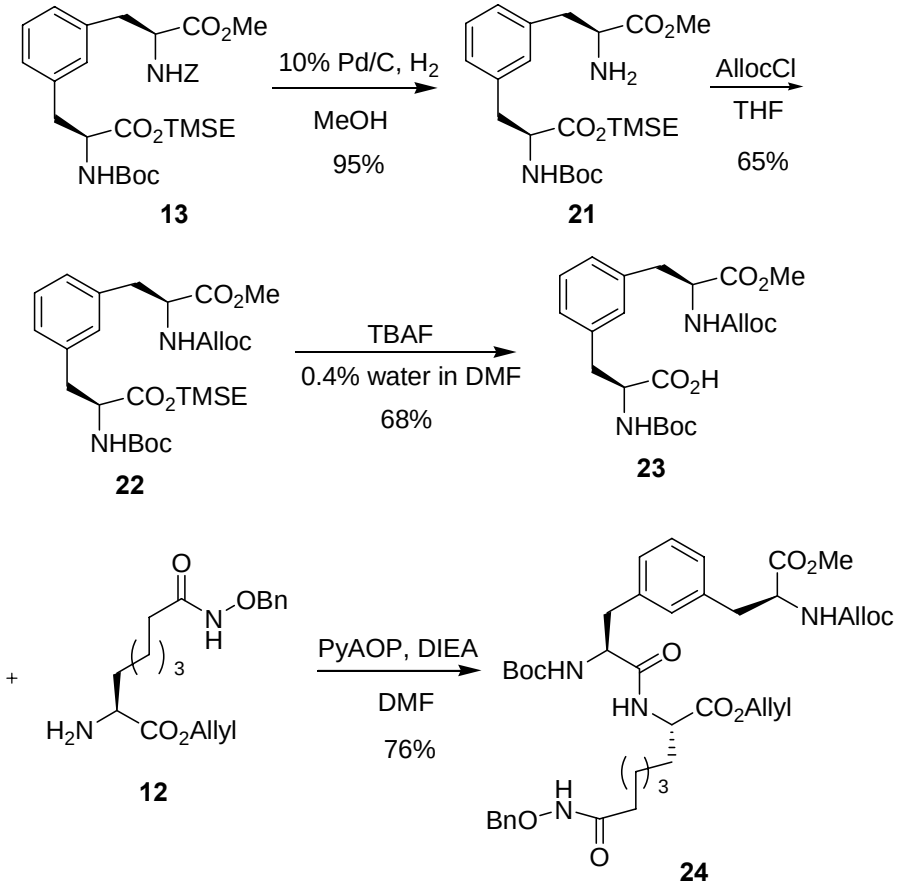

Compound **24** was treated with TFA to remove the Boc group. The 2-chlorotrityl chloride resin was chosen to anchor the amine because of its properties of high loading, high acid-lability, and it is capable of releasing a free amine.[126, 127] The allyl and alloc protecting groups were removed using $Pd(PPh_3)_4$ simultaneously (Scheme 2-6). The resulting amino acid was cyclized with DPPA. The reaction was traced by HPLC to monitor its completeness. Release of the cyclized product from the resin was accomplished by mild acidic conditions with AcOH to give a free amine. Acetylation of the amine with acetic anhydride gave rise to cyclized compound **20**. The conditions for

cyclization still need to be optimized because only a mass spectrum of the small amount of **20** produced showed that the cyclized product was obtained. This was the first time that the cyclic peptide mass peak showed up in the FAB+ mass spectrum.

Scheme 2-6. Cyclization to make **20** by solid-phase synthesis.

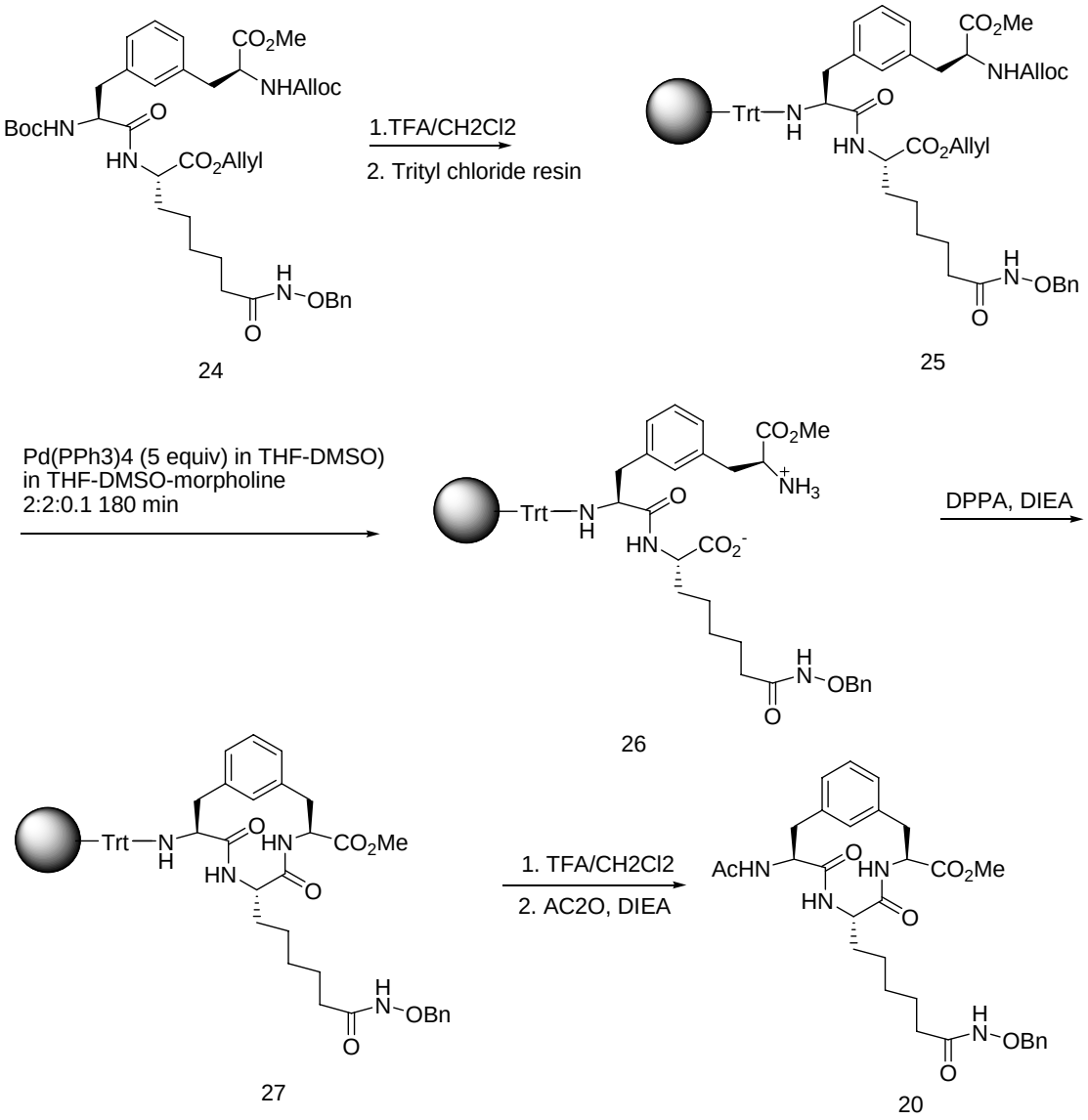

The synthesis of compound **20** was successfully accomplished both in solution phase and solid phase. Although the yield of HDAC inhibitor was quite low, which may have been due to the sterically hindered precursor at the α carbon of α-(*S*)-aminosuberic acid, it did prove that the synthesis of cyclized HDI was possible. Solution phase synthesis has undergone optimization because it gave a better yield.

2.4 Attempts to synthesize cyclized HDI using Boc-TMSE strategy

The fact that only a low yield of **19** was obtained by the two-allyl route and only trace amounts of compound **20** were obtained by cyclization of **19** enforced us to develop a more effective route. Two questions were asked: whether the amide at the site of cyclization could not be formed, or whether this amide bond was not stable enough to exist. To test the stability of the amide bond and to find a more productive route to synthesize the cyclized compound **20**, the method of employing Boc to protect the amine and TMSE to protect the carboxylic acid was investigated (Scheme 2-7).

Scheme 2-7. Synthesis of compound **28**

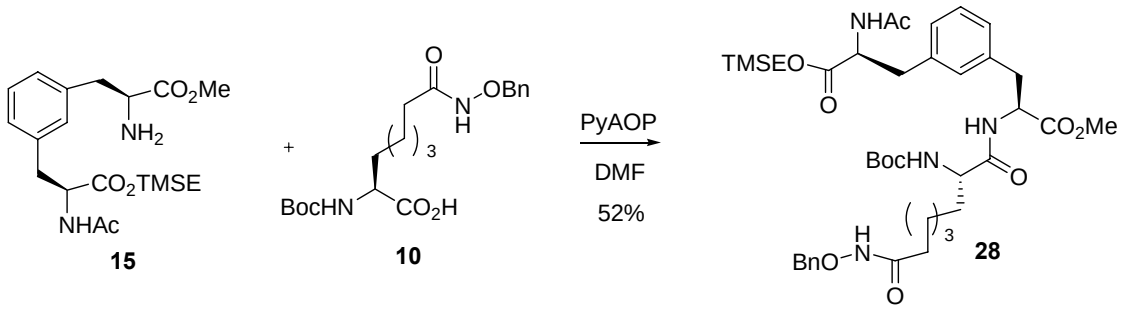

The segment condensation between **10** and **15** produced tripeptide **28** by PyAOP coupling. The synthesis of compound **18** alongside compound **28** indicated that amide bond could be formed at either side of the α-(*S*)-aminosuberic acid residue of compound **20**. However, the low yield of formation of the second amide bond to furnish the cyclized product **20** from both **18** and **28** suggested that either the hindrance from the long chain of the α-(*S*)-aminosuberic acid had a negative effect on the amide bond formation to fuse the ring or the cyclized product may have decomposed during the purification. The deprotection of the TMSE ester was unexpectedly difficult. The F^- ion came from TBAF (*tert*-butyl ammonium fluoride), either in solid state or in solution, but none of **29** was obtained after TMSE cleavage (Scheme 2-8). Although deprotection carried out using TBAF on silica gel gave **29** in a yield of 60%,[128] the purified acid **29** was contaminated by the impurities from TBAF. Acidolysis using TFA on **29** followed by cyclization using DPPA as coupling reagent and DIEA as base did not afford cyclized product **20**. The acid **29** might react with the hydroxylamine at the end of the side chain of α-(*S*)-aminosuberic acid to form dimer or polymer even before the cyclization occurs.

Scheme 2-8. Cleavage of Boc and TMSE in two steps.

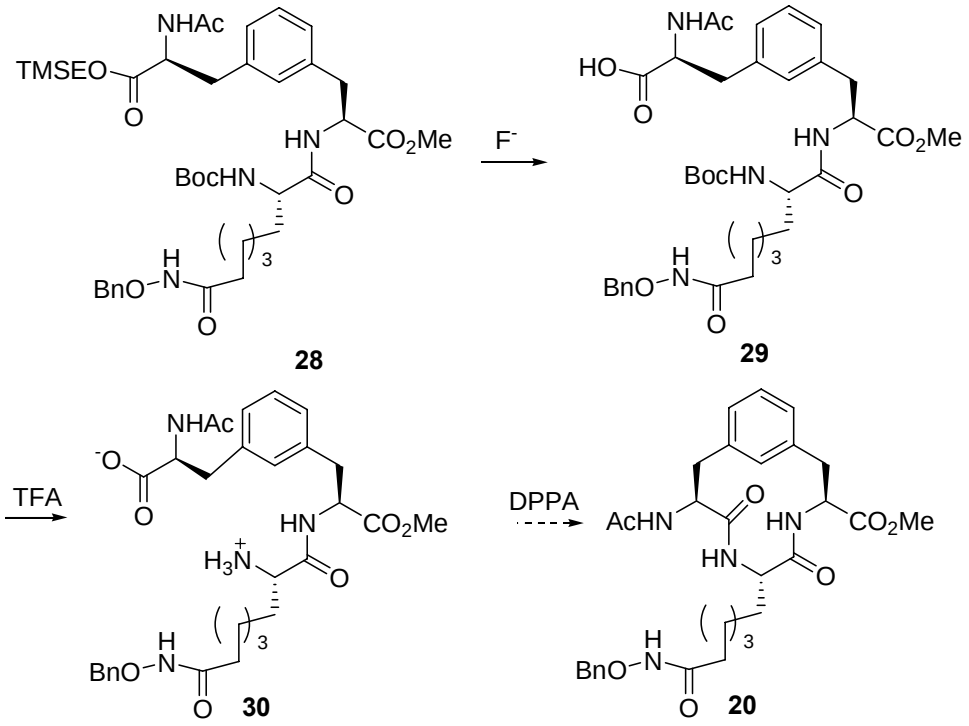

The two-step process to produce amino acid **30** was abandoned because TMSE was found to be labile to acid and could by cleaved simultaneously with Boc by TFA treatment (Scheme 2-9).[129-133] To trap the carbocation formed during the TFA treatment, TES (triethylsilane) was used as a scavenger.[134] TIS (triisopropylsilane), which is used often as a scavenger in solid-phase peptide synthesis,[135 136] was also tried as a scavenger in our cleavage, and it gave almost the same yield as TES did. The Boc cleavage by 20% TFA was complete in 30 min, while the TMSE cleavage needed more time and more concentrated TFA to finish. The incomplete TMSE cleavage was observed when a more dilute TFA solution was used for a quick deprotection. The best yield to produce **30** was obtained by treatment of **28** with 80% TFA in CH_2Cl_2 at rt for 3 h with TES acting as a scavenger (Table 2-2).

Scheme 2-9. Simultaneous cleavage of Boc and TMSE by TFA treatment.

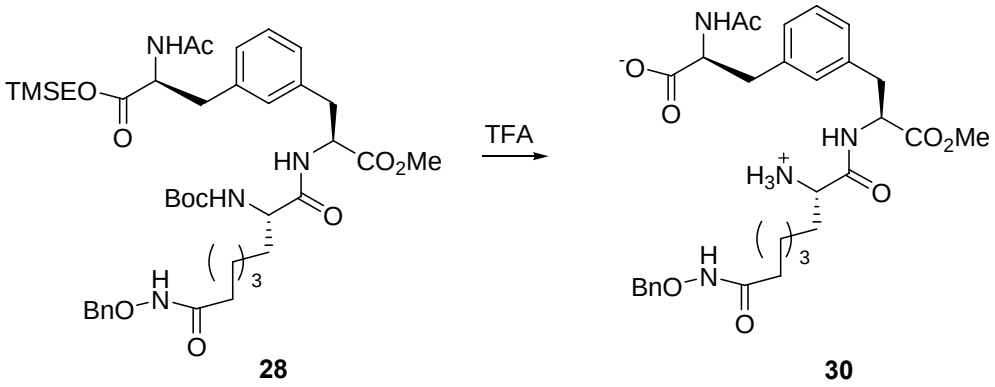

The results of cleaving Boc and TMSE either in two-step or simultaneously to form amino acid **30** are summarized in Table 2-2**.**

Table 2-2. Conditions for deprotection to make intermediate **30**.

TMSE removal			**Reaction time**	**Temperature**	**Yield of 30**
	TBAF		12 h	0 ºC (30min) to rt	X
	TBAF on SiO_2		12 h	0 ºC (30min) to rt	40%
	TFA (after TMSE removal)		30 min	rt	X
Boc and TMSE removed simultaneously	TFA	Scavenger	Reaction time	Temperature	**Yield of 30**
		TIS	30 min, 60% TFA	rt	20%
			2 h, 30% TFA	rt	15%
			4 h, 50% TFA	0 ºC	10%
		TES	30 min, 60% TFA	rt	12%
			3 h, 80% TFA	**rt**	**22%**

2.5 Cyclization

With intermediates **19** and **30** in hand, several attempts were made to produce cyclized peptide **20** by employing different coupling reagents, including using DPPA as a coupling reagent and DIEA as base, DPPA as a coupling reagent and inorganic salt $NaHCO_3$ as base, the combination of FDDP and DIEA, HATU and DIEA, PyAOP and DIEA, and fluoride and DIEA (Table 2-3).

Scheme 2-10 Macrocyclization from intermediate **19** or **30** to afford **20**.

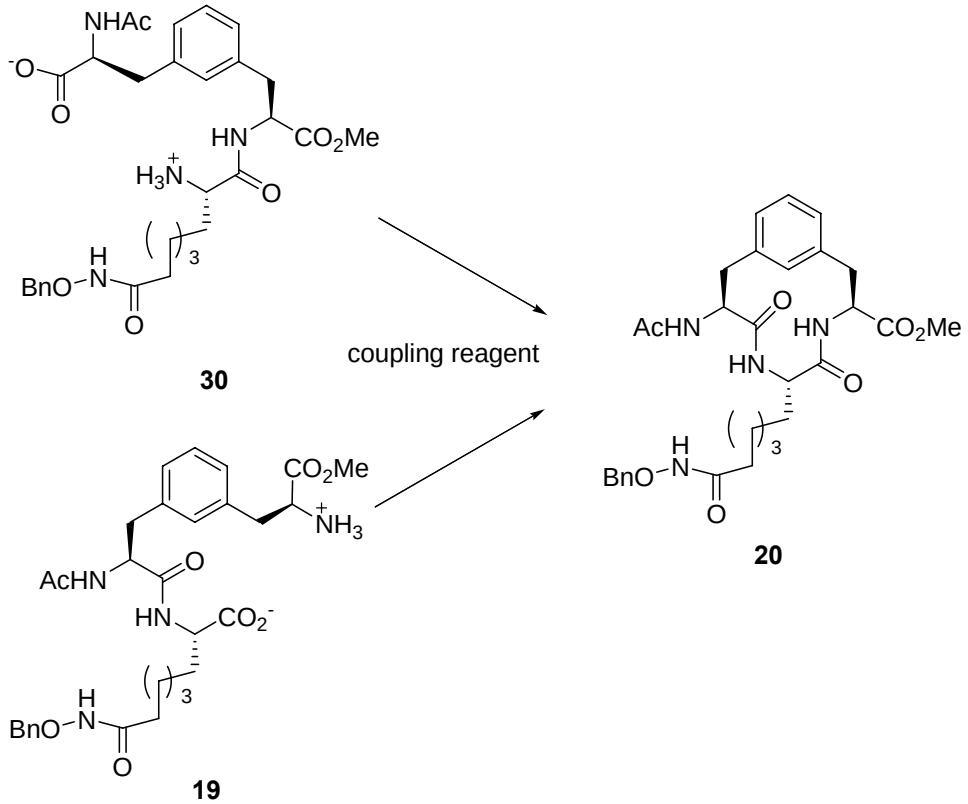

All of the conditions listed in Table 2-3 were applied to both **19** and **30** intermediates. The formation of the amide bond on either side of α-(*S*)-aminosuberic acid

to afford **20** have shown almost the same results when the same coupling conditions were employed, but only the best results are listed in Table 2-3.

DPPA has been widely used as a coupling reagent in cyclization,[124] however, in our case, the highest yield of cyclization using DPPA was only 10%. The attempts using HATU or PyAOP as coupling reagents failed to give any product when the reaction was carried out for 7 d, which was the standard length of time for cyclization. Although these coupling reagents can lead to cyclization in a short time compared to milder coupling reagents, such as DPPA and FDDA, more byproducts formed during the long-time reaction, which might be the reason why no product **20** was observed using HATU or PyAOP as coupling reagents. Better results were obtained when the HATU coupling finished in one hour.

FDDP (pentafluorophenyl diphenylphosphinate) was reported to produce more efficient macrocyclization than DPPA coupling by forming pentafluorophenyl esters of the carboxylic acids.[137] In our case, the FDDP coupling did not show any advantage over DPPA coupling. Almost the same or even lower yield was obtained by FDDP coupling. Amino acid fluorides have shown excellent coupling reactivity both in solution and in solid phase synthesis; especially good results were obtained in cases of sterically hindered amino α,α-disubstituted amino acids.[138, 139] To improve the yield of our cyclization, two types of fluorinating reagents, cyanuric fluoride[138] and TFFH[140] (fluoro-*N*,*N*,*N*'',*N*''-tetramethylformamidinium hexafluorophosphate) have been used respectively for the ring-closure step. Unfortunately, no desired product **20** was observed using either of these two fluorination reagents. It was suspected that the benzyloxy amide at the end of side chain in intermediate **19** or **30** might react with fluoride formed in situ,

as NBD fluoride (4-fluoro-7-nitrobenzo-2-oxa-1,3-diazole) reacts with secondary amines and it is therefore capable of derivatizing proline and hydroxyproline.[141]

Table 2-3. Conditions for cyclization.

Coupling reagent	Base	Yield of 20
DPPA 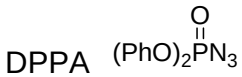	DIEA	10%
DPPA 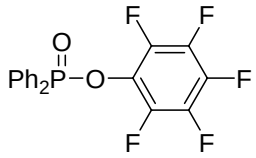	$NaHCO_3$	5%
FDPP	DIEA	7%
HATU 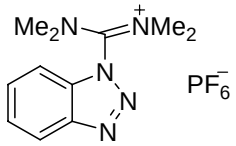	DIEA	Trace for seven days **10% for one hour**
PyAOP 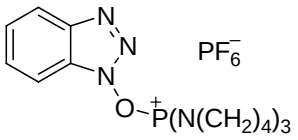	DIEA	X
Cyanuric fluoride 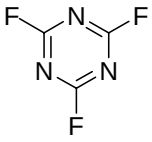	Pyridine	X
TFFH 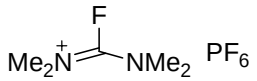	DIEA	X

DPPA is one of the most widely used cyclization reagents due to its milder coupling ability to depress the formation of dimer or polymer. The cyclization by DPPA always needs days to complete; however, more byproduct formation occurred along with the extension of the reaction time in our case. Two factors limited the formation of the cyclic HDI, the reactivity of hydroxylamine at the end of the α-(*S*)-aminosuberic acid and the steric hindrance coming from the long chain at α carbon of the α-(*S*)-aminosuberic acid. The second factor proven to be the most important one in effecting the yield of

cyclization from the synthesis of **20a**, a derivative **20** (Figure 2-7). The yield of cyclization of compound **20a** was almost same as the yield of cyclization of **20**. Both these two factors caused the accumulation of byproducts for a long time reaction by DPPA coupling. Therefore, HATU was chosen to make a quick coupling, and produced the best result so far.

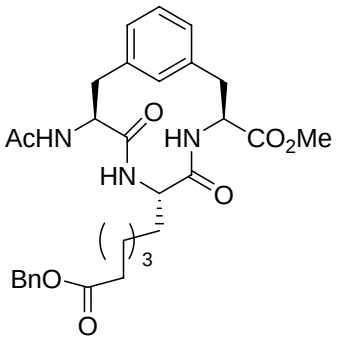

20a

Figure 2-7. The low yield of **20a**, a derivative of **20**, demonstrated the steric hindrance is the most important factor that affects the efficiency of cyclization.

2.6 Hydrogenation

To produce the free hydroxamic acid **1**, the cyclic HDAC inhibitor, catalytic hydrogenolysis was carried out on **20**. With the more reactive catalysts Pd/C (5%, 10%), only the amide **31** was formed (Scheme 2-11). The same phenomenon were observed in the synthesis of *N*-methyl *D*-aspartate (NMDA) receptor antagonist HA-966.[142]

Scheme 2-11 Hydrogenation by Pd/C on **20** produced amide **31**.

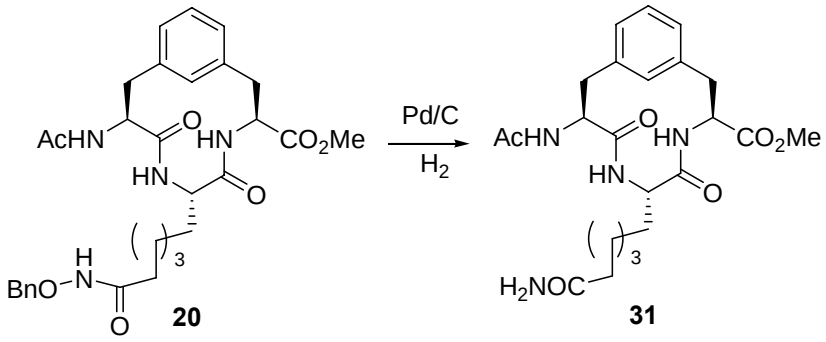

Milder catalysts, such as $Pd(OH)_2$[143] and $Pd/BaSO_4$,[142] produced the HDAC inhibitor **1** as expected (Scheme 2-12).

Scheme 2-12 Hydrogenation using $Pd/BaSO_4$ of **20** to give HDAC inhibitor **1**.

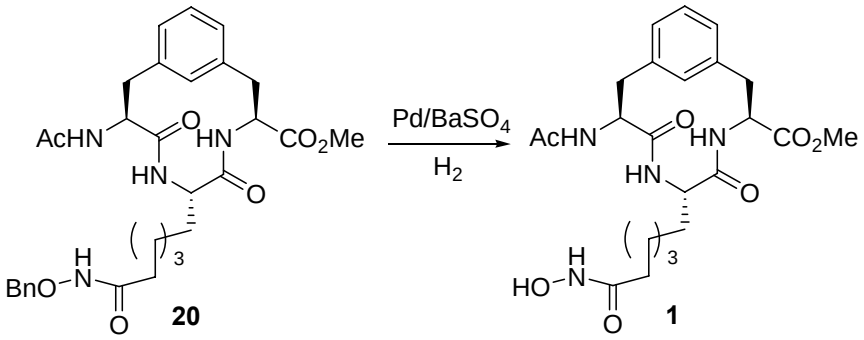

The results of hydrogenolysis using a variety of palladium catalysts were summarized in the Table 2-4.

Table 2-4. Conditions for hydrogenation of **20**.

	H_2	**Result**
10%Pd/C	20 psi	Amide formed
5%Pd/C	15 psi	Amide formed
5% $Pd(OH)_2$	15 psi	40% yield of **1**
5% $Pd/BaSO_4$	15 psi	60% yield of **1**

2.7 Conclusions

Molecular modeling studies of the HDLP-SAHA complex reveal HDIs bind to the zinc in the active site through a channel. Characterized HDIs typically contain three structural features: an aromatic cap group, an aliphatic chain and a metal binding functional group that is necessary for the activity. To increase the interaction between the rim region of HDACs and the recognition group of the HDIs, the cyclic HTH peptide was fused to a hydroxamic acid moiety to produce a new class of HDIs were. The HDI **1** was synthesized through macrocyclization through a quick coupling to avoid side reactions. Although only a small amount of HDI **1** was obtained (5 mg), we can still test its efficiency against HDAC activity. The successful synthesis of the HDI **1** not only allows us to evaluate the efficiency of the compound but also give us an opportunity to test our hypothesis. Forming the cyclic peptide was the most difficult part in the HDI **1** synthesis, which may result from the steric hindrance of the long chain at α carbon of the α-(*S*)-aminosuberic acid and/or the reactivity of hydroxylamine at the end of the α-(*S*)-aminosuberic acid. The new class of the HDIs containing the cyclic HTH peptide will be explored using the same design strategy.

2.8 Experimental

General Experiment. Unless specified otherwise, all chemicals were used as received. THF was freshly distilled under nitrogen from sodium/benzophenone ketyl immediately prior to use. Dichloromethane was freshly distilled under nitrogen from calcium hydride. DMF and MeOH were used from SureSeal^{TM} bottles. DIEA was distilled from CaH_2 under nitrogen. Brine (NaCl), $NaHCO_3$ and NH_4Cl refer to saturated aqueous solutions. ^1H NMR were recorded at 500, or 400 MHz. ^{13}C NMR were determined at 125, or 75 MHz. Flash column chromatography was performed using 230-400 mesh, EM Science silica gel. Analytical reverse phase liquid chromatography (RPHPLC) was performed on a RP C18 column, 250 × 4.4 mm, 5 μm, 100 × 21.2 mm. Preparative HPLC was performed using on a RP C18, 250 × 21.4 mm, 5 μm. HPLC solvents were A: water, B: CH_3CN. UV detection was performed at 220 nm unless otherwise noted.

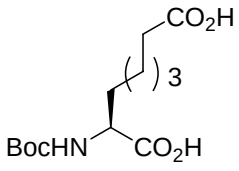

Acid 7. L-α-aminosuberic acid **6** (0.67 g, 3.0 mmol) was dispensed in a mixture of dioxane-water (10mL, 1:1) and $NHCO_3$ (0.76 g, 9.0 mmol) was added to obtain a solution and then cooled to rt. Boc_2O (1.96g, 9.00 mmol) was added dropwise with stirring. The reaction was stirred for 3.5 h. Water was added (30 mL) and the mixture was extracted with Et_2O (20mL) to remove unreacted Boc_2O. The aqueous layer was acidified with 1M HCl under cooling in ice bath to pH 2 and extracted with EtOAc (50 mL × 2). The organic layer was dried over Na_2SO_4, the volatiles were evaporated to

afford 0.72g (80%) of a white solid. $[\alpha]_D^{20}$= +8.7 (c=2, $CHCl_3$). ^{1}H NMR (CD_3OD): δ 12.14 (s, 2H), 3.78 (m, 1H), 3.29 (s, 1H), 2.45 (m, 2H), 2.13 (t, 2H), 1.65 (m, 3H), 1.11-1.64 (m, 16H). ^{13}C NMR ($CDCl_3$):δ174.9, 174.7, 156.0, 78.3, 53.8, 33.9, 31.0, 28.6, 28.5, 25.7, 24.7.

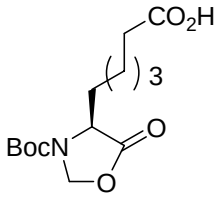

Acid 8. A suspension of **7** (140 mg, 0.48 mmol) in 1,1,2-trichloroethane was heated to 80 ºC to obtain a clear solution and tolunesulphonic acid (TsOH) (9.0 mg, 0.048 mmol) was added followed by paraformaldehyde (116 mg, 3.84 mmol). The mixture was heated to 100 ºC with a Dean-Stark trap until the reaction was completed and no more water formed. The solvent was evaporated under reduced pressure. The residue was dissolved in EtOAc and the solution was extracted with water. The organic layer was dried over Na_2SO_4 and concentrated. The product was purified by silica gel to give a colorless oil 108 mg (55%). $[\alpha]_D^{20}$= +93.6 (c=2, $CHCl_3$). ^{1}H NMR ($CDCl_3$): δ 5.29 (s, 1H), 4.06 (s, 1H), 1.91 (s, 2H), 1.78 (s, 2H), 1.65 (s, 2H), 1.46 (s, 2H), 1.31 (s, 9H), 1.21 (s, 2H). ^{13}C NMR ($CDCl_3$): δ 178.7, 172.8, 152.2, 82.0, 81.9, 54.7, 33.6, 30.2, 28.4, 28.0, 24.1, 23.8. HRMS calcd. For $C_{14}H_{23}NO_6$ (MH^+) *m/z* = 302.1604, found *m/z* = 302.1611. Anal. Calcd for $C_{14}H_{23}NO_6$: C, 55.80; H, 7.69; N, 4.65. Found: C, 56.06; H, 7.53; N, 4.58.

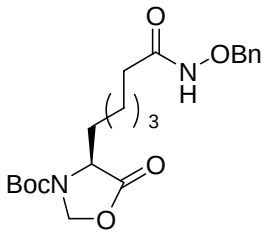

Hydroxamate 9. To a solution of **8** in THF cooled in ice bath was added DIEA (1.36 mL, 7.98 mmol) and EDC (560 mg, 2.9 mmol). The reaction mixture was stirred for 30 min at 4 ºC, then allowed to warm to rt and stirring was continued for another 30 min. *O*-benzyl hydroxylamine (552 mg, 3.46 mmol) was added and the resulted mixture was stirred 16 h. The THF was added to quench the reaction. The solution was washed with 0.3 N HCl (3 × 15 mL) and water (10 mL). The organic layer was dried over Na_2SO_4. Concentration followed by chromatography gave a colorless oil 750 mg (70 %). $[\alpha]_D^{20}$= +59.8 (c=2, $CHCl_3$). ^{1}H NMR (CDCl3): δ 7.34 (s, 5H), 5.43 (s, 1H), 5.11 (d, 1H), 4.17 (s, 1H), 1.52-2.06 (br, 7H), 1.43 (s, 9H), 1.29 (m, 3H). ^{13}C NMR (CDCl3): δ 173.5, 173.1, 152.3, 136.3, 128.4, 82.1, 66.2, 55.0, 34.3, 30.7, 28.8, 28.4, 24.8, 24.3. HRMS calcd. For $C_{21}H_{30}N_2O_6$ (MH^+) *m/z* = 407.2182, found *m/z* = 407.2189.

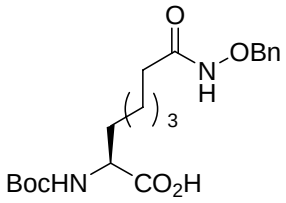

Acid 10. Fully protected hydroxamate **9** (110 mg, 0.27 mmol) was dissolved in MeOH (15 mL). The reaction was cooled to 0 ºC and 1N LiOH (0.54 mL, 0.54 mmol) was added dropwise. The reaction was traced by TLC and completed in 1 h. Methanol was removed under pressure. The aqueous solution was acidified with 1N HCl to pH 1 and extracted with EtOAc (3 × 30 mL). The EtOAc extract was washed with water and brine, and dried over Na_2SO_4. The solvent was concentrated, followed by

chromatography gave a colorless oil 101 mg (94%). $[\alpha]_D^{20}$= +5.92 (c=2, $CHCl_3$). ^1H NMR ($CDCl_3$): δ 7.32 (s, 5H), 5.45 (s, 1H), 4.87 (s, 2H), 3.93 (s, 1H), 2.03 (s, 2H), 2.04 (s, 2H), 1.77 (s, 2H), 1.54 (s, 2H), 1.40 (s, 9H), 1.29 (s, 2H). ^{13}C NMR ($CDCl_3$): δ 171.3, 170.1, 156.0, 135.3, 129.4, 128.9, 128.7, 80.7, 78.5, 51.9, 33.0, 32.2, 28.4, 24.9, 20.7. HRMS calcd. For $C_{20}H_{30}N_2O_6$ (MH^+) *m/z* = 395.2182, found *m/z* = 395.2150. Anal. Calcd for $C_{20}H_{30}N_2O_6$: C, 60.90; H, 7.67; N, 7.10. Found: C, 62.18; H, 7.60; N, 7.10.

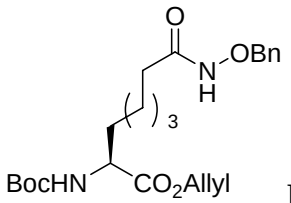

Hydroxamate 11. Acid **10** (101 mg, 0.260 mmol) was dissolved in CH_2Cl_2 (10 mL). The solution was cooled to 0 ºC in an ice bath, followed by the addition of allyl alcohol (0.18 mL, 2.6 mmol), EDC (73 mg, 0.38 mmol), and DMAP (3.0 mg, 0.026 mmol). The reaction was stirred at rt for 13 h. The solution was concentrated and then residue was dissolved in EtOAc (20 mL). The solution was washed with 10% citric acid (2 × 10 mL), $NaHCO_3$ (10 mL), water (10 mL), brine (20 mL), dried over $MgSO_4$, and then concentrated *in vacuo*. The residue was purified by chromatography, giving a colorless oil 87 mg (65%). ^1H NMR ($CDCl_3$): δ 8.74 (s, 1H), 7.33 (m, 5H), 5.87 (m, 1H), 5.23-5.31 (m, 2H), 4.87 (s, 2H), 4.59 (m, 2H), 4.22 (s, 1H), 2.28 (br s, 2H), 1.98 (s, 2H), 1.74 (s, 2H), 1.55 (s, 2H), 1.41 (s, 9H), 1.28 (s, 2H). ^{13}C NMR ($CDCl_3$): δ 173.0, 171.3, 158.2, 135.3, 131.5 129.0, 128.3, 126.4, 114.1, 82.0, 76.1, 65.7, 55.5, 32.7, 30.3, 28.2, 25.0, 23.9. HRMS calcd. For $C_{23}H_{34}N_2O_6$ (MH^+) *m/z* = 435.2495, found *m/z* = 435.2486. Anal. Calcd for $C_{23}H_{34}N_2O_6$: C, 63.57; H, 7.89; N, 6.45. Found: C, 62.55; H, 7.33; N, 6.72.

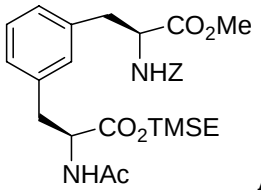

Amide 14. Compound **13** (1.27 g, 2.12 mmol) was dissolved in 4M HCl in dioxane (6 mL). The reaction mixture was stirred for 1h, and the solvent was evaporated. The remaining HCl was removed *in vacuo* at rt. Without further purification, the crude product was dissolved in a mixture of Ac_2O (2.00 mL, 19.6 mmol), DIEA (2.00 mL, 11.5 mmol) and CH_2Cl_2 (6 mL). The reaction was stirred for 1 h. The reaction mixture was diluted with EtOAc (30mL), washed with NH_4Cl (10 mL), brine (20 mL), dried over Na_2SO_4, and concentrated. Purification performed by chromatography on silica gel yielded a colorless oil 1.1 g (96%). $[\alpha]_D^{20}$= +17.83 (c = 2, $CHCl_3$). ^{1}H NMR ($CDCl_3$): δ 7.32 (m, 5H), 7.18 (t, 1H, *J* = 7.5Hz), 6.98 (d, 1H, *J* = 11.4Hz), 6.87 (s, 1H), 6.01 (d, 1H), 5.29 (d, 1H, *J* = 7.9Hz), 5.07 (s, 2H), 4.81 (d, 1H, *J*= 7.91Hz), 4.64 (d, 1H), 4.19 (m, 2H), 3.71 (s, 3H), 3.15-2.94 (m, 4H), 1.94 (s, 3H), 0.96 (t, 2H), 0.02 (s, 9H). ^{13}C NMR ($CDCl_3$): δ 173.5, 173.3, 171.3, 157.7, 137.9, 137.7, 136.41, 131.8, 130.3, 130.0, 129.7, 129.6, 129.5, 68.5, 65.4, 56.4, 54.7, 53.9, 39.7, 39.1, 24.5, 18.9, 0.00. HRMS calcd. For $C_{28}H_{38}N_2O_7Si$ (MH^+) *m/z* = 543.2527, found *m/z* = 543.2529.

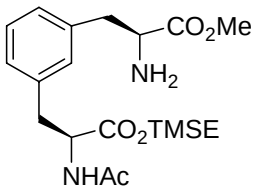

Amine 15. Compound **14** (800 mg, 1.48 mmol) was dissolved in MeOH (15 mL), then 10% Pd/C (100 mg) was added. The pressure in the Parr shaker was maintained at 45 psi after 3 vacuum/ H_2 cycles. The reaction was shaken for 16 h at rt. The catalyst was removed by filtration on a celite column and the filtrate was

concentrated to yield 700 mg (95%) **15** as a colorless oil. The crude product was carried into the next step without purifying.

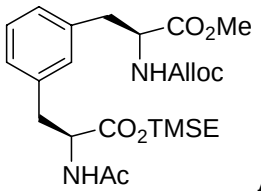

Allyl carbamate 16. Amine **15** (412 mg, 1.28 mm) was dissolved in THF (10 mL). The solution was cooled down to 0 ºC in an ice bath, followed by the addition of allyl chloromate (0.280 mL, 2.57 mmol), NHS (296 mg, 2.57 mmol), and DIEA (0.890 mL, 5.14 mmol). The reaction was stirred at rt for 14 h. The solution was concentrated and then residue was dissolved in EtOAc (20 mL). The solution was washed with 10% citric acid (2 × 10 mL), $NaHCO_3$ (10 mL), water (10 mL), brine (20 mL), dried on $MgSO_4$, and concentrated *in vacuo*. The residue was purified by chromatography, giving a colorless oil 316 mg (65 %). ^{1}H NMR ($CDCl_3$): δ 7.17 (m, 1H), 6.98 (m, 2H), 6.75 (d, 1H), 5.84 (m, 1H), 5.10-5.22 (m, 2H), 4.77 (d, 1H), 4.55 (d, 2H), 4.53 (d, 2H), 4.15 (m, 2H), 3.66 (s, 3H), 2.94-3.09 (m, 4H), 1.94 (s, 3H), 0.93 (t, 2H), 0.007 (s, 9H). ^{13}C NMR ($CDCl_3$): δ 173.74, 173.47, 171.72, 157.30, 138.24, 137.96, 134.29, 131,83, 130.16, 129.53, 129.44, 119.12, 61.19, 65.21, 61.84, 56.63, 55.00, 53.80, 39.48, 39.23, 24.29, 22.48, 18.84, 15.28. HRMS calcd. For $C_{24}H_{37}N_2O_7Si$ (MH^+) *m/z* = 493.2370, found *m/z* = 493.2339. Anal. Calcd for $C_{24}H_{37}N_2O_7Si$: C, 58.51; H, 7.37; N, 5.69. Found: C, 58.66; H, 7.23; N, 5.62.

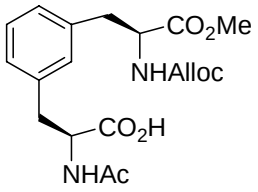

Acid 17. Allyl carbamate **16** (340 mg, 0.69 mmol) was dissolved in DMF (10 mL) and was cooled to 0 ºC in an ice bath. Five drops of water (0.4% in vol) were added. $Bu_4N^+F^-$ (472 mg, 1.50 mmol) was added to the solution and the color of the solution turned to yellow. The reaction was allowed to warm to rt and stirred for 17 h. DMF was removed *in vacuo* and the residue was redissolved in EtOAc (25 mL). The solution was acidified to pH 2 with HCl (1 N, 10 mL). The aqueous layer was extracted with EtOAc (3 × 30 mL). The extracts were combined, dried over Na_2SO_4, and concentrated. The residue was purified by chromatography, giving a colorless oil 176 mg (65%). ^{13}H NMR ($CDCl_3$): δ 7.17 (m, 1H), 6.98 (m, 2H), 6.75 (d, 1H), 5.84 (m, 1H), 5.10-5.22 (m, 2H), 4.77 (d, 1H), 4.55 (d, 2H), 4.53 (d, 2H), 4.15 (m, 2H), 3.66 (s, 3H), 2.94-3.09 (m, 4H), 1.94 (s, 3H), 0.93 (t, 2H), 0.007 (s, 9H). ^{13}C NMR ($CDCl_3$): δ 173.70, 172.54, 171.43, 156.17, 136.66, 136.38, 136.33, 132.62, 132.08, 131.13, 130,51, 128.92, 128.46, 128.30, 128.14, 118.86, 118.23, 67.06, 66.18, 60.66, 55.29, 55.06, 53.49, 52.67, 38.53, 38.16, 37.65, 37.55, 22.98, 22.91, 21.23, 14.38. HRMS calcd. For $C_{19}H_{25}N_2O_7$ (MH^+) *m/z* = 393.1662, found *m/z* = 393.1661.

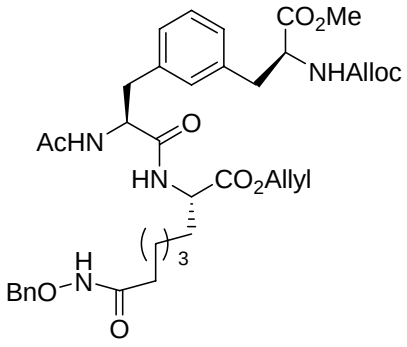

Tripeptide 18. Fully protected hydroxamate **11** (87.0 mg, 0.165 mmol) was dissolved in 10 mL CH_2Cl_2, and then was cooled to 0 ºC by an ice bath. TFA (3.5 mL) was added to the solution. The reaction was allowed to warm to rt and stirred for 30 min. The solution was concentrated under pressure. The excess TFA was removed with diethyl ether (3 × 5 mL), producing a white powder. The crude product **12** was dissolved in CH_2Cl_2 (10 mL) and coolded to 0 ºC, Acid **17** (101 mg, 0.260 mmol) were dissolved in DMF (10 mL). The solution was cooled down to 0 ºC in an ice bath, followed by the addition of DIEA (0.162 mL, 0.935 mmol) and PyAOP (292 mg, 0.561 mmol). The resulting solution was stirred for 2 min before the solution of **12** was added. The reaction was stirred at rt for 12 h. The reaction was quenched with EtOAc (20 mL), and was washed with $NaHCO_3$ (10 mL), water (10 mL), the aqueous solution was extracted with EtOAc 3 × 15 mL. The organic layer were combined and dried on $MgSO_4$. The filtrate was concentrated *in vacuo*. The residue was purified by chromatography, giving a colorless oil 126 mg (88%). ^{1}H NMR ($CDCl_3$): δ 8.74 (s, 1H), 7.33 (m, 5H), 5.87 (m, 1H), 5.23-5.31 (m, 2H), 4.87 (s, 2H), 4.59 (m, 2H), 4.22 (s, 1H), 2.28 (br s, 2H), 1.98 (s, 2H), 1.74 (s, 2H), 1.55 (s, 2H), 1.41 (s, 9H), 1.28 (s, 2H). ^{13}C NMR ($CDCl_3$): δ 172.6, 171.7.171.4, 170.5, 169.6, 155.2, 136.1, 135.9, 132.2, 129.7, 128.0, 127.4, 127.3, 117.0, 65.1, 63.1, 59.8, 54.5, 52.9, 51.7, 37.4, 24.9, 22.2, 20.4, 16.7, 13.6, -2.05.

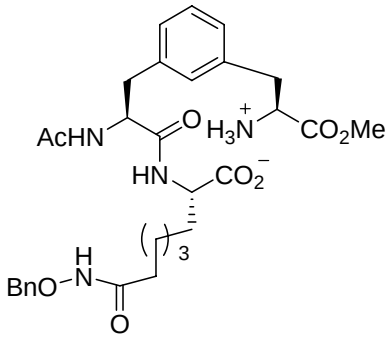

Amino acid 19. $Pd(PPh_3)_4$ (18 mg, 0.015 mmol) was added under nitrogen at rt to a solution of **18** (60 mg, 0.078 mmol) in THF (10mL), followed by the addition of morpholine (68 mg, 0.78 mmol). The resulting mixture was stirred for 1 h and then the solvent was evaporated. The amino acid **19** was purified by HPLC to afford a white powder 15 mg (30%). HRMS calcd. For $C_{29}H_{28}O_3N_6$ (MH^+) *m/z* = 514.2222, found *m/z* = 514.1978.

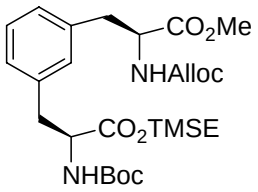

Alloc carbamate 22. Intermediate **13** (500 mg, 0.83 mmol) was dissolved in MeOH (15 mL), and 10% Pd/C (50 mg) was added. The pressure in the Parr shaker was maintained at 45 psi after 3 vacuum/ H_2 cycles. The reaction was shaked 15 h at rt. The catalyst was removed by filtration on a celite column and filtrate was concentrated to give 412 mg (97%) of a colorless oil. The crude product was carried into the next step without purifying. Amine **14** (412 mg, 1.28 mm) was dissolved in THF (10 mL). The solution was cooled to 0 ºC in an ice bath, followed by the addition of allyl chloromate (0.28 mL, 2.6 mmol), NHS (296 mg, 2.57 mmol) and DIEA (0.89 mL, 5.1 mmol). The reaction was stirred at rt for 16 h. The solution was concentrated and then

residue was dissolved in EtOAc (20 mL). The solution was washed with 10% citric acid (2 × 10 mL), $NaHCO_3$ (10 mL), water (10 mL), brine (20 mL), dried on $MgSO_4$, and concentrated *in vacuo*. The residue was purified by chromatography, giving 316 mg (65 %) of a colorless oil. ^{1}H NMR ($CDCl_3$): δ 7.17 (s, 1H), 6.98 (s, 2H), 6.87 (s, 1H), 5.86 (m, 1H), 5.16-5.24 (m, 2H), 4.98 (s, 1H), 4.74 (s, 1H), 4.53 (m, 2H), 4.17 (m, 2H), 3.71 (s, 3H), 2.98-3.08 (m, 4H), 1.39 (s, 9H), 0.94 (m, 2H), 0.04 (s, 9H). HRMS calcd. For $C_{27}H_{43}O_2N_8Si$ (MH^+) *m/z* = 551.2789, found *m/z* = 551.2800.

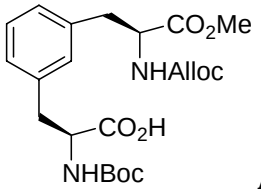

Acid 23. Fully protected intermediate **22** (319 mg, 0.530 mmol) was dissolved in DMF (10 mL) and was cooled down to 0 ºC in ice bath. Water (5 drops, 0.4% by vol) was added. $Bu_4N^+F^-$ (346 mg, 1.32 mmol) was added to the solution and the color of solution turned yellow. The reaction was allowed to warm to rt and was stirred for 14h. DMF was removed *in vacuo* and residue was redissolved in EtOAc (25 mL). The solution was acidified to pH 2 with HCl (1 N, 10 mL). The aqueous layer was extracted with EtOAc (3 × 30 mL). The extracts were combined, dried on Na_2SO_4, and concentrated. The residue was purified by chromatography, producing 147 mg (62 %) of a colorless oil. ^{1}H NMR ($CDCl_3$): δ 9.89 (br s, 1H), 7.20 (s, 1H), 6.98 (m, 2H), 6.88 (s, 1H), 5.86 (m, 1H), 5.05-5.51 (m, 3H), 4.53-4.63 (m, 4H), 3.67 (s, 3H), 2.98-3.08 (m, 4H), 1.40 (s, 9H).

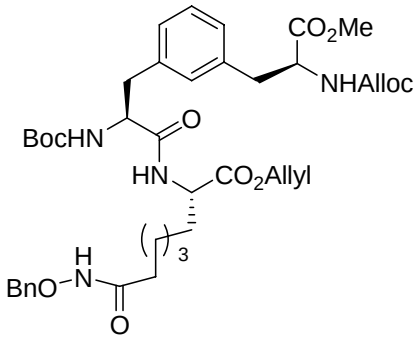

Tripeptide 24. Fully protected hydroxamate **11** (87.0 mg, 0.165 mmol) was dissolved in 10 mL CH_2Cl_2, and then was cooled to 0 ºC in an ice bath. TFA (3.5 mL) was added to the solution. The reaction was allowed to warm to rt and stirred for 30 min. The solution was concentrated under pressure. The excess TFA was removed with diethyl ether (3 × 5 mL) to give a white powder. Acid **23** (101 mg, 0.260 mmol) were dissolved in DMF (10 mL). The solution was cooled down to 0 ºC in an ice bath, followed by the addition of DIEA (0.162 mL, 0.935 mmol) and PyAoP (292 mg, 0.561 mmol). The resulting solution was stirred for 2 min before solution of amine **12** (84.0 mg, 0.187 mmol) was added. The reaction was stirred at rt for 12 h. The reaction was quenched with EtOAc (20 mL), and was washed with $NaHCO_3$ (10 mL), water (10 mL), the aqueous solution was extracted with EtOAc (3 × 15 mL). The organic layer were combined and dried on $MgSO_4$. The filtrate was concentrated *in vacuo*. The residue was purified by chromatography, giving 126 mg (88%) of a colorless oil. ^{1}H NMR ($CDCl_3$): δ 8.74 (s, 1H), 7.33 (m, 5H), 5.87 (m, 1H), 5.23-5.31 (m, 2H), 4.87 (s, 2H), 4.59 (m, 2H), 4.22 (s, 1H), 2.28 (br s, 2H), 1.98 (s, 2H), 1.74 (s, 2H), 1.55 (s, 2H), 1.41 (s, 9H), 1.28 (s, 2H). ^{13}C NMR ($CDCl_3$): δ 175.5, 172.5, 172.1, 170.2, 162.6, 150.8, 133.1, 132.0, 129.2, 128.8, 128.5, 120.6, 118.6, 117.6, 78.6, 78.1, 72.9, 65.5, 55.6, 52.2, 43.2, 36.7, 36.5, 31.4, 28.5.

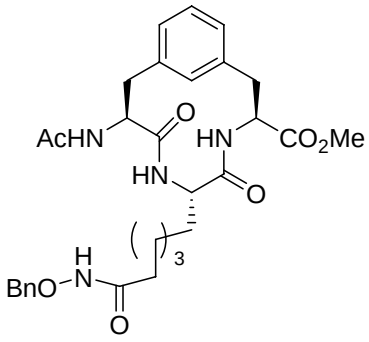

Cyclized peptide 20. The two allyl ester **24** (60mg) was dissolved in a mixture of DCM/TFA (1:1, v/v) and stirred for 1 h, and the solvent was evaporated *in vacuo*. The resulting residue was triturated with ether and dried *in vacuo*. The resulted amine and DIEA were dissolved in DMF (3mL), and the solution was mixed with 2-chlorotrityl chloride resin.[126, 127, 144] The mixture was stirred for 20 h. At the end of this time, the resin was washed with 3 × CH_2Cl_2/MeOH/DIEA (17:2:1), 3 × 10 min. Then, the mixture was successively washed with 3 × CH_2Cl_2; 2×DMF; 2 × CH_2Cl_2. After washing, the resin was dried *in vacuo* for 18 h. The resin was washed with DMF, 5×0.5 min; treated with $Pd(PPh_3)_4$ (5 equiv) in THF-DMSO-1,1,2-trichloroethane-morpholine (2:2:1:0.1) for 2 h. The resin was washed successively with THF, DMF, CH_2Cl_2, DIEA-CH_2Cl_2 (1:19), CH_2Cl_2, 3 × 2 min each, then sodium diethydithiocarbamate trihydrate (0.03 M in DMF), 3 × 10 min, DMF, 5 × 2 min, CH_2Cl_2, 3 × 2 min, and DMF, 3 × 1 min. The coupling was accomplished by DPPA/DIEA for 3 d. The cyclized product was cleaved from the resin under mild conditions, AcOH/ TFE/ CH_2Cl_2 (2:2:6) for 2 h, then the resin was removed by filtration. Hexane was added to the filtrate to help remove acetic acid by forming an azeotrope. The acetylation of the amine afforded cyclized product **20**. HRMS calculated for $C_{36}H_{44}O_7N_3Si$ (MH^+) *m/z* = 658.2949, found *m/z* = 658.2972.

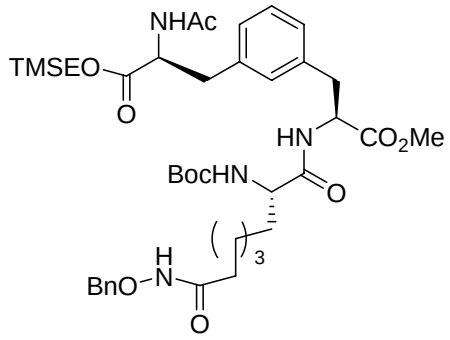

Tripeptide 28. The solution of acid **10** (68 mg, 0.17 mmol) was cooled down to 0 ºC in ice bath, followed by the addition of DIEA (110 mg, 0.86 mmol) and HATU (197 mg, 0.516 mmol). The resulting solution was stirred for 2 min before the solution of **15** (70.0 mg, 0.172 mmol) was added. The reaction was stirred at rt for 13 h. The reaction was quenched with EtOAc (20 mL), and was washed with $NaHCO_3$ (10 mL), water (10 mL). The aqueous solution was extracted with EtOAc (3 × 15 mL). The organic layer were combined and dried on $MgSO_4$. The filtrate was concentrated *in vacuo*. The residue was purified by chromatography, giving 70 mg (52%) of a colorless oil. $[\alpha]_D^{20}$= +45.27 (c=2, $CHCl_3$). ^{1}H NMR (CDCl3): δ 7.34 (m, 5H), 7.15 (m, 1H), 6.92 (m, 3H), 5.43 (s, 1H), 5.10 (d, 1H), 4.63-4.94 (m, 4H), 3.76 (m, 3H), 2.92-3.16 (m, 4H), 2.25 (br s, 2H), 1.94 (m, 3H), 1.77 (s, 2H), 1.57 (s, 2H), 1.45 (s, 9H), 1.29 (m, 2H), 0.95 (t, 2H), 0.01 (s, 9H).). ^{13}C NMR ($CDCl_3$): δ 176.8, 173.1, 171.4, 161.6, 138.9, 137.6, 131.7, 130.6, 130.4, 130.0, 129.4, 129.2, 83.5, 65.3, 62.2, 56.8, 54.8, 53.1, 48.6, 41.5, 40.1, 39.2, 29.8, 25.2, 24.5, 23.5, 18.9, 0.00. HRMS calcd. For $C_{40}H_{60}N_4O_{10}Si$ (MH^+) *m/z* = 785.4157, found *m/z* = 785.4117.

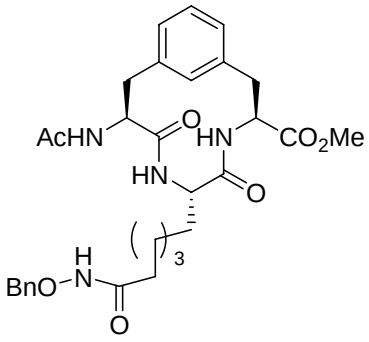

Cyclized peptide 20. Compound **28** (85.0 mg, 0.108 mmol) was dissolved in a mixture of TFA (4 mL) and CH_2Cl_2 (6 mL). Triethylsilane (37.0 mg, 0.324 mmol) was added via syringe. The reaction mixture was stirred for 1 h, and the solvent was evaporated. The remaining TFA and triethylsilane were removed *in vacuo*. Without further purification, the crude product was dissolved in DMF (5 mL) and transferred into a flask containing DPPA (89.0 mg, 0.324 mmol) and DIEA (81 mg, 0.65 mmol) in DMF (100 mL). The reaction was stirred under N_2 for 7 d at 4 ºC. The solution was concentrated followed by chromatography to give 2 mg (8%) cyclized product as a white solid. HPLC conditions: maintain 10% B for 5 min, then do a gradient from 10% B to 90% B over 12 min, keep 90% B for 4 min, do a gradient from 90% B to 10% B in 1 min on a Varian Polaris semipreparative C_{18} reverse phase analytical column at 20.0 mL/min. Retention time was 12.32 min. A solvent: H_2O; B solvent: CH_3CN. ^{1}H NMR (CDCl3): δ 6.73-7.45 (m, 9H), 4.71 (s, 2H), 4.45 (br, s, 1H), 4.29 (br, s, 1H), 3.97 (m, 1H), 3.63 (s, 3H), 2.68-3.09 (m, 4H), 2.45 (s, 2H), 1.90 (s, 3H), 1.03-1.85 (m, 6H), 0.82 (m, 2H). HRMS calcd. For $C_{30}H_{38}N_4O_7$ (MH^+) *m/z* = 567.2819, found *m/z* = 567.2824.

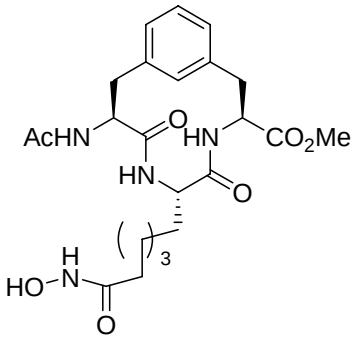

HDAC inhibitor 1. Compound **20** (5.0 mg, 8.8×10^{-3} mmol) was dissolved in MeOH (10 mL), and 10% $Pd/BaSO_4$ (10 mg) was added. The pressure in the Parr shaker was maintained at 10 psi after 3 vacuum/ H_2 cycles. The reaction was shaken for 3 h at rt. The catalyst was removed by filtration on a celite column and filtrate was concentrated to give a white solid. The hydroxamic acid **1** was purified by HPLC to afford a white powder 2.6 mg (60%). Preparative HPLC conditions: maintain 10% B for 5 min, then do a gradient from 10% B to 90% B over 12 min, keep 90% B for 4 min, do a gradient from 90% B to 10% B in 1 min on a Varian Polaris semipreparative C_{18} reverse phase analytical column at 20.0 mL/min. Retention time was 10.07 min. A solvent: H_2O; B solvent: CH_3CN. Analytical HPLC conditions: maintain 10% B for 5 min, then a gradient from 10% B to 90% B over 12 min, keep 90% B for 4 min, do a gradient from 90% B to 10% B in 1 min on a Varian Polaris analytical C_{18} reverse phase analytical column at 2.0 mL/min. Retention time was 9.38 min. A solvent: H_2O; B solvent: CH_3CN. ^1H NMR ($CDCl_3$/DMSO-d_6): δ 7.02-7.25 (m, 5H), 4.16-4.77 (m, 4H), 3.43-3.87 (m, 8H), 3.76-3.09 (m, 4H), 1.74-2.11 (m, 6H), 1.08-1.65 (m, 16H). HRMS calcd. For $C_{23}H_{32}N_4O_7$ (MH^+) *m/z* = 477.2349, found *m/z* = 477.2333.

Computational Study. The structure of **1** was built by MacroModel v. 6.0 on a Silicon Graphics Iris Indigo XZ4000, and minimized with the AMBER force field until it

converged to a maximum derivative of 0.05 kcal mol^{-1} $Å^{-1}$. Docking calculations were performed with Sybyl 7.1. The crystal structure of the HDLP-SAHA complex (1C3S)[60] was obtained from the Protein Data Bank, and crystallographic water molecules were left in the complex as they were. The cyclic peptide mimic **2** was superimposed with the ligand, SAHA, which was extracted from the X-ray structure. The superimposition directed **1** into the active site of HDLP with the right geometry. The aliphatic chain and hydroxamic acid of SAHA were fused with **1** along the Cα-Cβ bond of the Ala residue to produce compound **2**, which was docked into the active site of HDLP manually. AMBER_FF99 atom types and Gasteiger-Huckel charges were assigned to each atom of ligand **1**. Hydrogen was added to the complex. Fixing amide side chain, proline, atom types and charges of the ligand **2**, side chain bumping, set the minimization at an optimum starting point. A 6.0 Å radius sphere was set as the active site which was centered on ligand **1**. The sphere was defined as the "hot zone". The energy of a "yellow zone" of residues within 12.0 Å of the "hot zone" was calculated, but the geometry was fixed. The minimization happened with the region of the "hot zone", and the rest of the complex was not affected during the minimization. The setting of the hot zone not only dramatically decreased the time needed for the minimization, but also eliminated the interaction between the active site and the rest of the complex, which could cause unnecessary the conformational changes of the rest of the protein. The minimization was run under AMBER_FF99 force field using POWELL method until it converged to a maximum derivative of 0.10 kcal mol^{-1} $Å^{-1}$. All the other parameters used in minimization were default. The dockings using **3** capped with Boc group at the amine end demonstrated that the bumping between the Boc and the side chains of the

recognition region of the active site prevented the effective binding of **1** to HDLP. The ligand **1** binds to the pockets on the recognition region by the aromatic ring and 12-membered ring of the cyclic peptide mimic. However, the bulk Boc causes the repulsion between the mimic and side chains of the surface region of the active site. The ligand **1** capped with acetyl on the amine end gave a stronger binding with HDLP.

Chapter 3
In vitro assay of the synthesized HDAC inhibitor

3.1 The principles of HDAC assays

The discovery of new, potent HDIs is largely dependent on an effective assay system that is both sensitive and low-cost. Two main classes of assay systems for the *in vitro* determination of HDAC inhibitor activity are isotopic and non-isotopic assays, according to whether acetate-radiolabeled histones are used as substates.

The isotopic assay employs acetate-radiolabeled histones[145] or radiolabeled peptides[146] as substrate. Both of these two substrate types have their shortcomings in the HDAC assay. Acetate-radiolabeled histones can be obtained from cultured cells treated with ^{3}H-acetyl-CoA,[146] or from chicken reticulocytes, which depends on the sacrifice of animals. However, the degree of acetylation of prelabeled histones changes in different preparations, which makes it difficult to standardize the substrate. The ^{3}H-acetylated peptide substrate can be prepared by solid phase peptide synthesis under more controlled conditions.[147] However, postlabeling HPLC purification is required. The general isotopic HDAC assay includes following steps: incubation of HDAC with radiolabeled substrate, separation of product with organic solvents, and determination of released radiolabeled acetic acid by liquid scintillation counting. The use of radiolabeled substrate limits the application of the isotopic assay because it is costly in time, apparatus, and radioactive waste disposal.

MAL (*N*-(4-methyl-7-coumarinyl)-*N*-α-(*tert*-butyloxy-carbonyl)-*N*-Ω-acetylly sineamide) is the first non-isotopic substrate used in an HDAC assay.[148] Although this substrate has a lower K_m value (0.68 μM) compared to its natural counterpart (20 μM),[148] the bulky fluorescent group on the artificial substrate restricts HDAC to be effective only at a certain distance from the fluorophore. The need to monitor the deacetylated product by HPLC and fluorescence detection limits the use of this assay in high-throughout screening. The small change in the structure of the substrate before and after deacetylation makes it impossible to directly monitor the HDAC assay by spectroscopic methods. Enzymatic and chemical modifications are required to quantify the acetate released from the substrate.[149, 150]

The synthetic histone-like substrate containing non-fluorescent 4-methyl-coumarine-7-amide allows monitoring of the assay by fluorescence. The assay is highly sensitive and does not require expensive radioactive histones. After the acetate is catalytically released from the substrate, the deacetylated product is recognized as a substrate of trypsin, which cleaves a fluorophore, AMC (7-amino-4-methylcoumarin). The acetylated substrate is stable towards trypsin during the HDAC assay.[151] AMC is excited at 390 nm, and emits fluorescence at 460 nm. The fluorescence signal is linear under the assay conditions, so the fluorescence measurement of AMC is directly related to the concentration of the cleaved acetate. The use of the endopeptidase LysC to cleave AMC during the assay allows modification of substrates and assay conditions.

3.2. HDAC inhibitor in vitro inhibition assay

3.2.1. Enzyme kinetics

In general enzyme-catalyzed reactions, the reactant and product concentrations are much larger than the enzyme concentration. The enzyme converts the reactant to the product through a series of stages. After forming complexes between enzyme and substrates, several complexes will form before the formation of product and regeneration of enzyme.

The kinetics of the above reactions can be expressed by the Michaelis-Menten equation (Equation 4-1). The symbols used in the Michaelis-Menton equation are listed as follows, v is the reaction rate, V_{max} is maximum reaction rate, S is substrate concentration, and K_m is the Michaelis-Menton constant.

$$v = \frac{V_{\max} \cdot [S]}{K_m + [S]} \qquad 4.1$$

The Michaelis-Menton equation is applied to express the kinetics of reversible inhibitors. Reversible inhibitors binding to enzymes and releasing from the enzymes are fast compared to the enzyme turnover. The inhibition constant (K_i) is much larger than the enzyme concentration [E], so the concentration of complex between enzymes and inhibitors [EI] is much smaller than the concentration of inhibitors [I].

Tight binding inhibitors are another class of inhibitors that can not be described by Michaelis-Menton equation. The K_i value of a tight binding inhibitors is less than 1000-fold greater than the enzyme concentration.[152] Tight binding inhibitors bind to the

targeted enzymes with high affinity. The formation of enzyme inhibitor complexes dramatically reduces the concentration of free inhibitors.

The K_i value of a tight binding enzyme inhibitor can be obtained from enzyme inhibition assay. The following equation describes the fractional velocity of an enzymatic reaction as a function of inhibitor concentration at fixed concentrations of enzyme and substrate, where v is the rate of the enzyme reaction, $[E]_t$ and $[I]_t$ are the concentrations of enzyme and inhibitor, and K_i' is the apparent inhibition constant.

$$v = \frac{k_{cat}[S]([E]_t - [I]_t - K_i' + \sqrt{([E]_t - [I]_t - K_i')^2 + 4[E]_t K_i'})}{2(K_m + [S])} \qquad 4.2^{152}$$

The following equation is used to obtain the value of K_i for a competitive inhibitor.

$$K_i' = K_i(1 + [S]/K_m) \qquad 4.3^{152}$$

The value of IC_{50} can be obtained from the following equation.

$$IC_{50} = K_i(1 + \frac{[S]}{K_m}) + \frac{[E_t]}{2} \qquad 4.4^{152}$$

Values of k_{cat}, K_m, and k_{cat}/K_m can be obtained by fitting the data to Equation 4.5.

$$v = \frac{k_{cat}[E][S]}{K_m + [S]} \qquad 4.5^{151}$$

3.2.2. HDAC inhibitor in vitro inhibition assay

Compound **1** was assayed against Hela Nuclear extract rich with HDAC activity to determine its efficiency to inhibit HDAC. The enzyme used in the assay is HeLa cell nuclear extract (human cervical cancer cell line), which is rich in HDAC activity. The substrate is a synthetic peptide containing an acetylated lysine side chain. The apparent K_m of the HDAC activity in the HeLa nuclear extract (KI-140) for the substrate is ~50 μM. The substrate concentration must be near or below the K_m to avoid substrate competitive effects. The substrate and the enzyme are incubated in the presence of different concentrations of the inhibitor. Deacetylation of the substrate followed by mixing with the developer provided generates a fluorophore, which was measured by a Cytofluor^R Series 4000 fluorescence multi-well plate reader with excitation set at 360 nm and emission detection set at 460 nm. The percent inhibition was determined by comparison of the fluorescence signal of inhibited wells with those of control cells. The concentration of the inhibitor results in 50% inhibition (IC_{50}) was determined by plotting the percent inhibition verse log [I] (Figure 3-1).

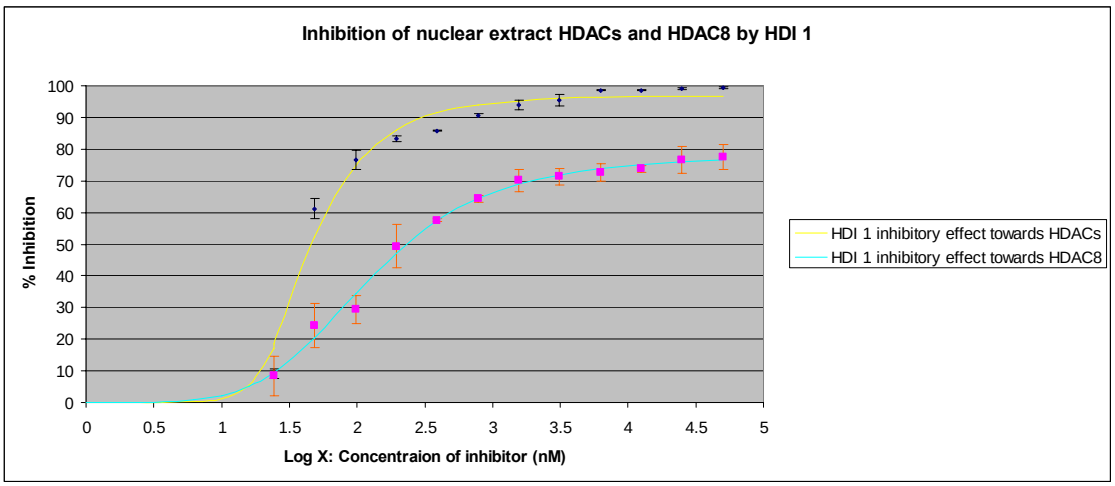

Figure 3-1. Dose response curve of HDI **1**. Yellow: the inhibition against HeLa nuclear extract (IC_{50}=46 ± 15 nM, ■ and ♦); red: the inhibition against HDAC8 (IC_{50} = 208 ± 20 nM, ▲ and *).

The results are summarized in Table 3-1. The calculated values of IC_{50} were obtained by fitting experimental data to a dose response curve (95% confidence level) by TableCurve (version 3 for win32).The IC_{50} of **1** against HeLa nuclear extract is 46 ± 15 nM. The high efficiency of the designed and synthesized HDAC inhibitor **1** proves the hydrophobicity and the size of the surface recognition element plays an important role in the formation of inhibitor-enzyme complex. To assay the compound **1** against a specific HDAC enzyme, human HDAC8 was tested in an enzyme assay. The IC_{50} value of HDI **1** against HDAC8 enzyme activity was 208 ± 20 nM (Table 3-1).

Table 3-1. In Vitro HDAC inhibition by HDI **1**, TSA, and SAHA.

Compound	HeLa nuclear extracts, IC_{50} (nM)	human HDAC8, IC_{50} (nM)
1	46 ± 15	208 ± 20
TSA	41 ± 5 [lit. (2.1)[79]]	40[153]
SAHA	110[63]	270[63]

3.3 Conclusions

A non-isotopic assay was performed to determine the efficiency of a newly designed and synthesized HDAC inhibitor. HDI **1** exhibited a much higher HDAC inhibitory activity against both HeLa nuclear extracts and HDAC8 than SAHA with IC_{50} values in the nanomolar level. Because the HeLa nuclear extracts are a mixture of several HDAC enzymes, the assay against other HDAC isozymes is needed to test the selectivity of HDI **1**. The high efficiency of HDI **1** demonstrates that modification of the recognition region plays an important role in the design of a new class HDIs. Future studies of HDIs containing the cyclic peptide mimic might lead to the discovery of lead compounds from a new generation of HDAC inhibitors.

3.4 Experimental

General. The assay of HDAC activity was performed using an HDAC fluorescent activity assay/drug discovery kit (AK-500, BIOMOL Research Laboratories). Fluorescence readings were carried out on a Cytofluor^R Series 4000 fluorescence multi-well plate reader (Perspective Biosystems). The HDAC inhibitor only dissolves in DMSO, and forms gel-like solution in the mixture of water and DMSO. The buffer for all experiments was 50 mM Tris/Cl, pH 8.0, 137 mM NaCl, 2.7 M KCl, 1 mM $MgCl_2$. Substrate was 50 mM in DMSO. Trichostatin A was 0.2 mM in DMSO

IC_{50} measurement of the HDAC inhibitor.

Preparing the assay solutions.

To minimize the cycles of thaw/freeze, aliquots of the HDAC assay substrate, HeLa nuclear extract, HDAC assay buffer, and Trichostatin A were charged into separate tubes and stored at -70ºC. The HDAC assay substrate, HeLa nuclear extract, HDAC assay buffer, and Trichostatin A were thawed and kept on ice. HeLa nuclear extract was diluted 30-fold using HDAC assay buffer. Each assay needed 15 µL of nuclear extracts containing 0.5 µL of the undiluted extract. The HDAC assay substrate was diluted to 100 µM by diluting 1 part substrate into 500 parts using assay buffer. Since 25 µL was used per well in the assay, and the final volume of the HDAC reaction was 50 µL, the final concentration of the substrate was 50 µM. The K_m value of the HeLa nuclear extract for the substrate used in the assay was 50 µM. Using the substrate concentration near the K_m value avoided substrate competitive effects. It was necessary to aliquot the substrate and thaw only enough amount for one day's experiment since the substrate formed a precipitate after it was diluted and stored on ice for 2 h. The HDAC inhibitor was dissolved in DMSO, which did not show HDAC inhibitory activity in the control assay. Since only 10 µL was used per well, and the final volume of the HDAC reaction was 50 µL, the inhibitor concentrations were 5-fold of their final concentration. All of these solutions were prepared for assay and stored on ice until use. The developer solution was prepared after the substrate solution was added to the well and the reactions were initiated. The assay developer solution was diluted 20-fold using the assay buffer, then the trichostatin A solution was diluted 100-fold in the diluted developer just prepared (e.g. 10 µL in 1 mL; final trichostatin A concentration in the developer was 2 µM; the final concentration after addition to HDAC substrate reaction was 1 µM). The

concentration of trichostatin A was enough to inhibit the HDAC activity completely when the assay developer was added at the end of the reaction.

Performing the HDAC assay

Assay buffer or HDAC inhibitor was added to the 96 wells microplate provided in the assay kit. The diluted HeLa nuclear extract was add to all wells except to the blank well. There were two control wells: the control well 1 used to determine the initial activity of HeLa extract, the control well 2 demonstrated that the amount of DMSO (10 µl) did not interfere with the HDAC assay. Both of these control wells produced almost the same readings. The diluted assay substrate and the samples in the microplate were warmed to 25 ºC. HDAC reactions were initiated by the addition of the diluted substrate to each well and mixing thoroughly. The HDAC reactions proceeded for 30 min and then were stopped by the addition of the developer solution. The stopped reactions were incubated at 25 °C for 10-15 min. Fluorescent signals were read in a microplate reader, exciting at 360 nm and detecting at 460 nm.

Sample	Assay buffer (µL)	HeLa extract (µL)	Inhibitor (µL)	Substrate (µL)
Blank	25	0	0	25
Control 1	10	15	0	25
Control 2	0	15	10 µl DMSO	25
Sample	0	15	10	25

Part 2
Studies towards a stabilized helix-turn-helix peptide

Chapter 4
Homeodomain mimics

4.1 Design of HTH-turn mimic

DNA is composed of nucleic acid chains that combine to form a double helix. The sequence of bases contains genetic information, that is the prerequisite for all life. The genetic code is deciphered and then used for protein synthesis. The deciphering of genetic information is achieved by protein interactions with DNA to create mRNA, called transcription.

Proteins that regulate the transcription of DNA recognize specific DNA sequences through discrete DNA-binding domains within their polypeptide chains. In general, these domains are relatively small, consisting of less than 100 amino acid residues. X-ray and NMR studies revealed that three major classes of structural DNA binding motifs make up 80% of the structural motifs in DNA recognition. The first recognized structural DNA binding motif was the helix-turn-helix (HTH) motif of the cAMP receptor protein from *E. coli*.[154] Two other major classes of structural motifs are the zinc finger and leucine zipper

proteins. Many prokaryotic DNA-binding domains contain a HTH motif that recognizes and binds specific regulatory regions of DNA.[155] The HTH is a well-characterized DNA-binding motif. The first successful use of X-ray techniques to determine the structure of a DNA-bound protein was on the λ repressor bound to its operator, by Anderson *et al*.[154]

The HTH motif is found in many organisms from prokaryotes (transcription repression and activation) to eukaryotes (homeodomain transcription activation). The HTH motif contains a highly unusual turn.[156] This turn is an atypical γ-turn because it does not contain a hydrogen bond between the *i* and *i*+2 residues. Instead the NH and the *N*-terminus and the C=O at the *C*-terminus are found hydrogen bonded to the two attached α-helixes that cross at a nearly 90° angle.[156] It is also unusual to find a turn between two helixes. Since these helixes are not coplanar, the turn is a minimal yet essential element of protein tertiary structure. The small size of the turn and its significance for tertiary rather than secondary structure make the HTH a very attractive target to mimic. In addition, DNA-binding peptide mimics may represent an entry to a new class of pharmaceuticals that bind DNA rather than enzymes.[156]

The *Antennapedia* homeodomain, found in the eukaryotic *Drosophila*, is 68 amino acid residues long. It contains four alpha helixes. Helix 2 (residue 28-38) and 3 (residue 42-52) adopt a HTH motif from residues 28 to 52. This motif is similar to those found in prokaryotic repressor proteins. The helix-turn-helix motif consists of two α helixes conjoined by a short turn of three amino acid residues. The small tripeptide sequence induces the protein to form its tertiary structure.[157] The hydrophobic residues of the turn form a pocket, which plays an important role in stabilizing the motif. In addition,

the second helix binds perpendicularly to the first helix, forming a criss-cross and interacting with each other through hydrophobic interactions.[99]

The HTH motif contained within the structure of homeodomains is a tertiary structure. The turn of the HTH motif is the key to formation of the HTH tertiary conformation by connecting two α-helixes that have secondary structure. The turn of the HTH motif is composed of three amino acid residues that can stabilize the tertiary structure of HTH motif with the hydrophobic properties of their side chains.[158] Comparison of HTH-turn with β- and γ-turns indicates that HTH-turns are a family of peptides with a unique structure.[156] The difference includes the dihedral angles and stabilizing forces. The γ-turn is composed of three residues. The hydrogen-bonding between the CO group of the first residue and the NH group of the third group forms a seven-membered ring.[156] The β-turn is a four amino acid residue turn. That is stabilized by a hydrogen bond between the first and fourth residues.[159] The crystal structure of the Cro/O_R1 complex is the basis for the definition of HTH-turn because of its well-defined and simple structure.[100, 160]

The definition of the HTH-turn is based on pseudo-torsion angles between the Cα of four residues of the backbone.[100] The pseudo-torsions in the turn are 235º-136º-255º-241º bracketed by two helical pseudo-torsions of 40-60º. (Etzkorn, F. A.; Pyla, P.; Niehaus, B. unpublished results)

The HTH-turn mimic was designed to increase the hydrophobic interaction between helix 2 and helix 3 by introducing a phenyl group into the turn. The HTH-turn maintains and stabilizes the tertiary conformation, so it is a good candidate for the mimic design. The HTH-turn mimic has no DNA binding and recognition capabilities, which

make it insensitive to structural alterations. However, short peptides are not conformationally stable outside of the protein.[99] For example, if three amino acids were joined together, they would likely form a relatively straight chain peptide. This would not be satisfactory for a HTH study because the two α helixes cross horizontally from the turn and could not obtain the desired tertiary structure because of their flexibility. In order to compensate for this, a different hydrophobic side chain could be employed to close the peptide into a ring, maintaining the 'v' shape. Alkenes, cycloalkanes, and phenyl substituents are a few examples of possible hydrophobic side groups that control the conformation of the peptide chain when isolated from the native protein. A mimic of the HTH-turn designed and synthesized to rigidly constrain the tripeptide by side chain bonding would be theoretically stable enough to explore the interaction between DNA and proteins.[99]

HTH mimics could be produced to act as DNA inhibitors, lowering medication dosages, decreasing possible toxicity, and relieving side effects because the conditions would be treated by manipulating genetic transcription rather than by stopping it enzymatically.[99]

The principles used to design the turn peptidomimetics were: (1) conformational constraint via side chain covalent bonds and (2) introduction of additional hydrophobic contacts in the core of the HTH motif. A wide variety of covalent bonds, from disulfides and amides to carbon-carbon bonds, could constrain the conformation. The new bonds must not interfere with the existing sterics or electrostatics of the motif. Mullen and Bartlett designed a template for the exterior region of the turn of the HTH motif.[156] Our template was designed to introduce the hydrophobic core into the HTH motif,

maintaining the native backbone of the HTH peptide sequence. We chose to make a hydrocarbon-bridged turn mimic because the carbon-carbon bond would be stable and would suit the steric constraints in the core of the tight turn. Although the mimic is rigidified relative to the natural turn motif, the 12-membered ring is somewhat flexible. This flexibility is desirable when the conformation of the natural motif can not be matched exactly or its conformation would be changed by binding with other structural motifs in the DNA-protein binding complex.[99]

Two HTH-turn mimics **4** and **5**, were designed based on the principles stated above (Figure 4-1). Residue 39 of the Antp homeodomain was changed from cysteine to serine to prevent oxidative dimerization of the protein as was done in the crystal structure.[161]

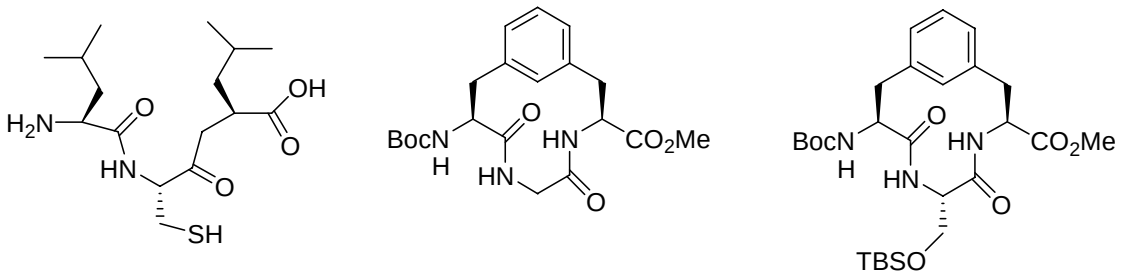

32 HTH turn from homeodomain **4** **33**

Figure 4-1. HTH-turn **32** derived from *Antennapedia* homeodomain peptide and turn mimics, containing Gly and Ser in the position of Cys in the native peptide, respectively.

4.2 Scaling up the synthesis of Gly HTH-turn mimic

The synthesis of the Gly HTH-turn mimic was accomplished by Travins.[99] This work was repeated to produce enough of the Gly HTH-turn mimic **4** to facilitate the incorporation of the mimic into the *Antennapedia* homeodomain peptide.

Ester **34** was produced from benzyl carbamate and glyoxylic acid, in 76% yield in two steps (Scheme 5-1). Protected phosphonate **36** was obtained through a phosphonylation reaction with a 90% yield.[162] Phosphonoglycinate **39** was prepared from phosphonoglycinate **36** by switching the protecting group on the amine as well as the protecting group on the carboxylic acid. The transformation from Cbz to Boc was carried out in one step without separating the dissociated amine.[163] The di-*t*-butyl dicarbonate (Boc_2O) reacts with the free amine immediately after the protected amine was freed by catalytic hydrogenation,[162] affording compound **37** with a high yield (86%). The incomplete transformation from Cbz to Boc due to the low solubility of **36** in methanol was solved by melting the phosphonoglycinate **36** by medium heating before adding methanol. The decomposition of the phosphono group of compound **37** was observed during the methyl ester hydrolysis. Saponification by dropwise addition of the solution of sodium hydroxide into the ice-bath cooled reaction produced acid **38** with a fair yield (75%). Reesterification of acid **38** produced the TMSE ester **39** in 70% yield by DCC coupling (Scheme 4-1).

Scheme 4-1. Synthesis of the orthogonally protected phosphonoglycinates **36** and **39**.

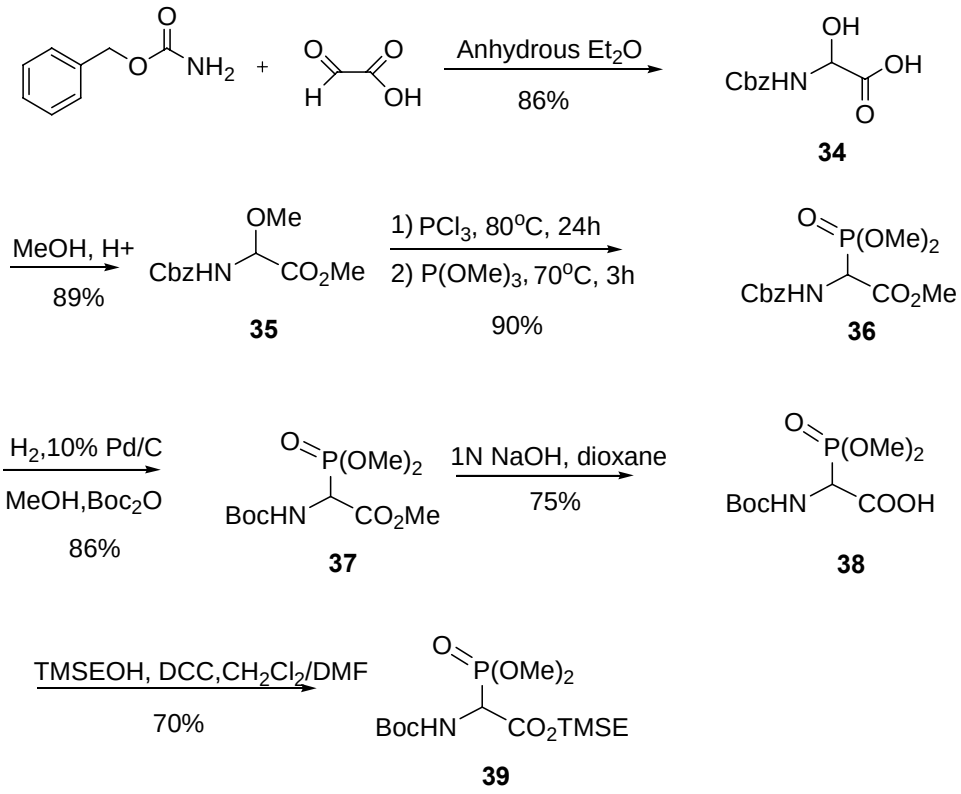

The Horner-Wittig condensation between benzene-1,3-dialdehyde and phosphonoglycinate **36** with tetramethylguanidine (TMG) as the base produced the mono-coupled product **40** with an 85% yield.[162, 164] The use of a ten-fold excess of benzene-1, 3-dialdehyde assured the formation of mono-adduct. The separation of **40** from benzene-1,3-dialdehyde was difficult due to the close polarity of these two compounds. Using a five-fold excess of benzene-1,3-dialdehyde gave the same yield of **40** and decreased the effort necessary to separate **40** from the excess benzene-1,3-dialdehyde. Compound **40** was still obtained with a high yield even when a significantly lower excess, a two-fold equivalent of benzene-1,3-dialdehyde, was used in the reaction (Table 4-1). This is a significant improvement over the published procedure. A second Horner-Wittig coupling was observed when a 1:1 ratio of benzene-1,3-dialdehyde and

phosphonoglycinate **36** was used. The first Horner-Wittig condensation was complete in 30 min, while the second coupling needed 24 h to complete due to the steric hindrance coming from the substituents on the alkene formed in the first Horner-Wittig reaction. The second Horner-Wittig coupling between aldehyde **40** and phosphonoglycinate **39** produced bis-alkene **41** (Scheme 4-2).

Scheme 4-2. Synthesis of bis-alkene **41**.

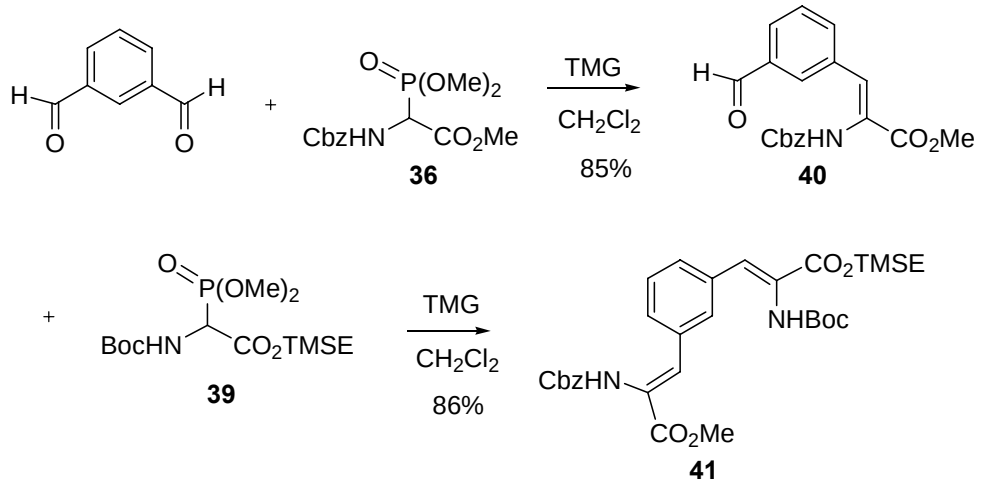

Table 4-1. Ratio optimization of the reactants for the first Horner-Wittig coupling to **40**.

Entry	Aldehyde: 36 (mol: mol)	Yield
1	10:1	0.83g (81%) [94%][99]
2	6.25:1	3.41g (83%)
3	3.72:1	7g (85.5%)
4	2:1	3.5g (85%)

TMG (tetramethyl guanidine) was chosen as the base to increase the stereoselectivity for the Horner-Wittig coupling, making the (Z)-alkene predominant in the products.[165] It was not necessary to separate the diastereoisomers because the catalyst

used in the hydrogenation step had high selectivity and reduced all the isomers into the L-configration.[166] After the enantioselective hydrogenation, the (Z)-alkene enriched isomers always produced a high enantiomeric ratio (98-99% er).[99]

The hydrogenation reaction produced the fully protected bisamino ester **13**. The ester **13** is a key intermediate in the project. The catalyst Rh(EtDUPHOS) must be handled carefully during the hydrogenation step.[167] The catalyst Rh(EtDUPHOS) was sensitive to air and water, and it could be deactivated with a small amount of air. The catalyst is more sensitive than was described in the literature.[167] The strictly controlled degassed atmosphere ensured a high yield and high stereoselectivity for **13**. Substrate to catalyst ratios was 2,000, which means only 0.05% catalyst was needed fort the reaction. The solution was stirred in a Parr reactor under 50 psi H_2 for 24 h, producing a completely reduced bisamino ester **13** in high yield.

Scheme 4-3. Asymmetric hydrogenation with Rh(EtDUPHOS).

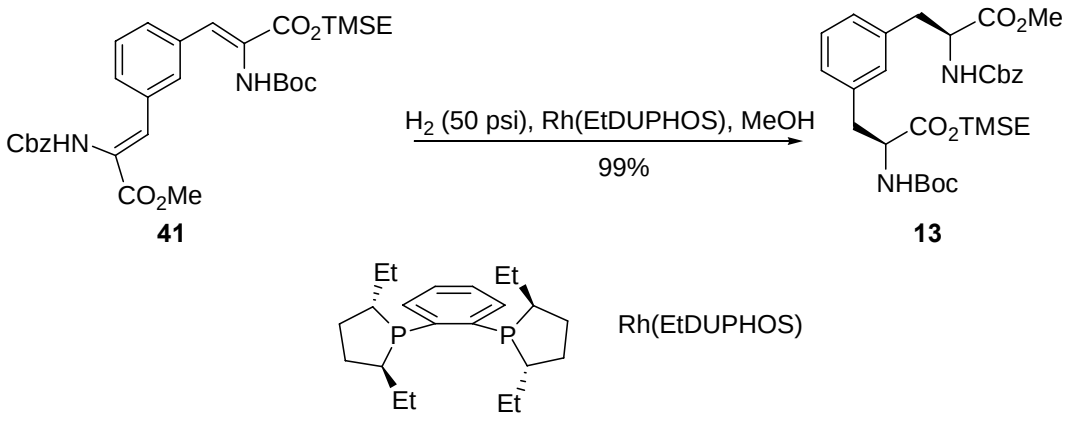

The absolute stereochemistry was proven by Travins through the degradation of **13** to the optically pure derivative Boc-Asp-OMe **43**, which had the same optical rotation as a commercially available standard.[99]

The TMSE group of **13** was removed by tetrabutylammonium fluoride (TBAF) in DMF containing a trace of water, which helped to avoid racemization.[99] The EDC coupling between **42** and the tosylate salt of benzyl glycinate produced linear peptide **43** (Scheme 4-4). EDC showed the same coupling ability as DCC, and formed a water soluble byproduct, while DCU, the byproduct formed in DCC coupling, was difficult to remove during the purification.[168, 169]

Scheme 4-4. Synthesis of the linear precursor **43**.

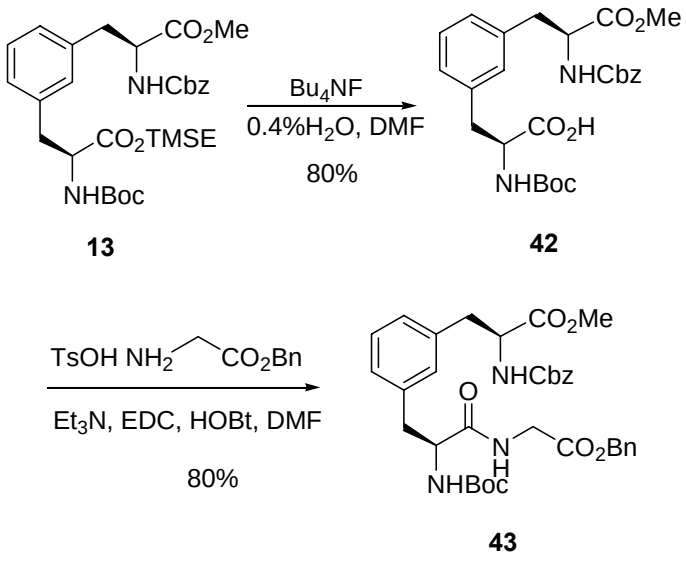

Simultaneous hydrogenolysis of the Cbz and Bn protecting groups followed by cyclization with diphenylphosphoryl azide (DPPA) in dilute DMF solution afforded cyclic peptide **4**. The cyclization step (Scheme 4-5) was always the key step in the whole

synthesis of the HTH-turn mimics. The yield of initial attempts to form cyclized product was always between 30-60%. The low yield of cyclization would limit the application of the HTH-turn mimic in peptide synthesis. DPPA proved to be the most effective coupling regent in cyclization.[99] DPPA is a powerful coupling reagent for the synthesis of macrocyclic lactams.[170] The mechanism of the reaction involves the formation of the carboxylic acid azide produced from interchanging the azido group from DPPA to the carboxylic acid.[9] The azide method is a reliable method for racemization-free fragment condensation in the peptide synthesis. Oxazolones, which result in racemization during coupling, cannot be observed during the DPPA coupling.[171]

The conditions for cyclization were optimized by the author to drive the cyclization to completion. The most effective cyclization was carried out in dilute DMF (1.5 μM) under N_2 for 5 d at 0 ºC, and for 2 d at rt. The reaction bottle was covered with aluminum foil and the reaction was kept from disturbance. A yield of 85% was the most successful cyclization ever achieved. The Gly HTH-turn mimic was synthesized in eight steps with a 33 % overall yield, producing Gly HTH-turn mimic **4** 1.5 g overall.

Scheme 4-5. Synthesis of Gly HTH-turn mimic **4**.

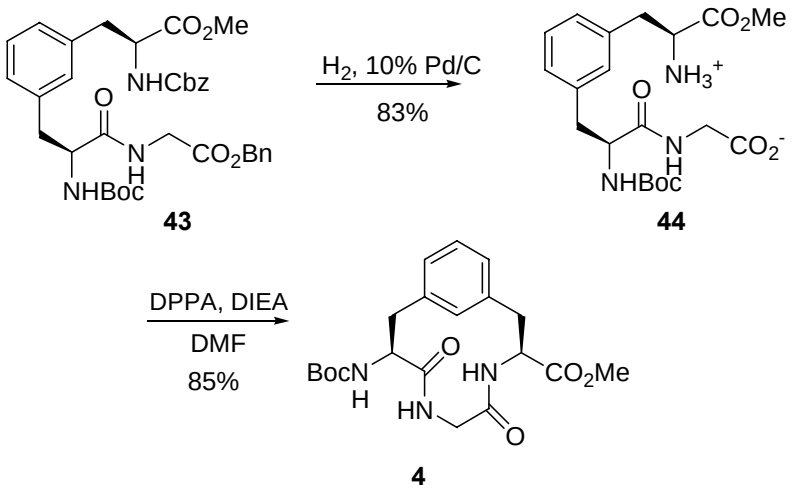

4.3 Synthesis of Ser HTH-turn mimic

Although the synthesis of the Gly HTH-turn mimic was successfully achieved in high yield, the cyclic peptide demonstrated a poor solubility towards all of the popular solvents except DMSO. We decided to incorporate the Ser side chain containing a polar functional group into the new HTH-turn mimic to increase the solubility of the cyclic peptide. Ser has the same length side chain as Cys that is one component of the HTH-turn derived from the *Antennapedia* homeodomain peptide. Retro-synthetic analysis revealed the intermediates for the synthesis of the Ser HTH-turn mimic, a bis-amino acid **13** and Ser(TBS)-OBn **47** (Figure 4-2). The synthesis of the Ser HTH-turn mimic was achieved by the author through the same synthetic strategy established by Travins.[99]

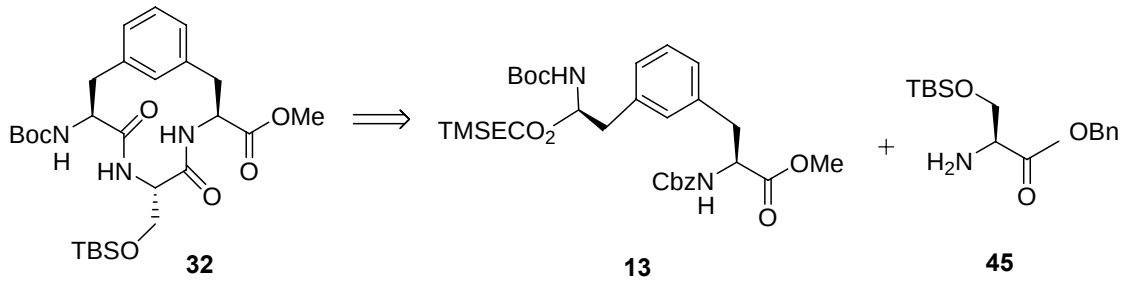

Figure 4-2. Retrosynthesis of the cyclic Ser HTH-turn mimic **32**.

The synthesis of segment **13** was accomplished through sequential Horner-Wittig reactions and stereoselective hydrogenation.[99] Several attempts were made to synthesize the other segment **45**. The hydroxyl on the side chain of serine was protected with the TBS group by the treatment of L-serine with dimethyl-*tert*-butylsilyl chloride (TBS-Cl) and imidazole to afford Ser(TBS)-OH **46**.[172] Treatment of **46** with Fmoc-OSu, followed

by benzyl esterification produced Fmoc-Ser(TBS)OBn. However, Fmoc cleavage using piperidine produced many by-products with a poor yield (<10%) (Scheme 4-6).

Scheme 4-6. Fmoc strategy to synthesize Ser(TBS)-OBn **45**.

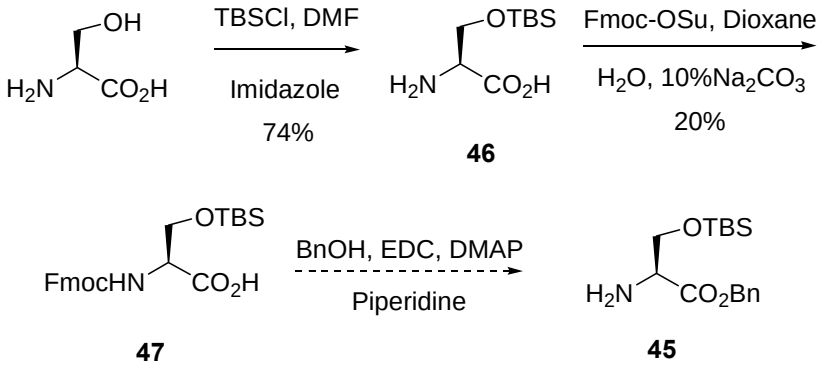

Although *O*-alkylation using alkyl halides on unprotected amino acids afforded a 50-70% yield of ester,[173] *O*-alkylation of Ser(TBS)-OH **46** failed to produce **45** due to the instability of the TBS group, which could be cleaved under acidic or basic conditions (Scheme 4-7).

Scheme 4-7. *O*-alkylation on unprotected Serine.

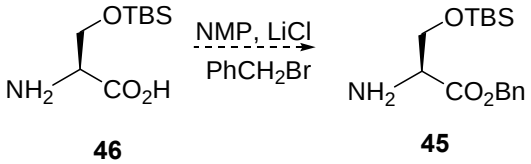

The synthesis of Ser(TBS)OBn **67** was accomplished by treatment of Ser-OBn with TBDMS-Cl and imidazole in DMF for 24h (Scheme 4-8).[174] Amine **45** would be coupled with another segment to form the linear precursor of Ser HTH-turn mimic.

Scheme 4-8. Formation of Ser(TBS)-OBn **45**.

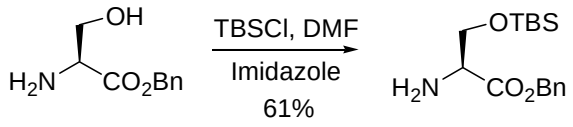

45

The EDC coupling between **42** and **45** produced the linear peptide **48** (Scheme 4-9). The Cbz amine protecting group and the Bn carboxylic acid protecting group were cleaved simultaneously by catalytic hydrogenation, producing a macrocyclic precursor **48**. The reaction was clean in high yield. However, the yield of the cyclization step was relatively low (35%), which was possibly due to the relatively bulky TBS group on the side chain of serine. The cyclization was achieved by diphenylphosphorylazide (DPPA) coupling to afford Ser HTH-turn mimic **32** (Scheme 4-9). The synthesis of the Ser HTH-turn mimic was accomplished in eight steps with a 14% overall yield.

Scheme 4-9. Synthesis of serine HTH-turn mimic **32**.

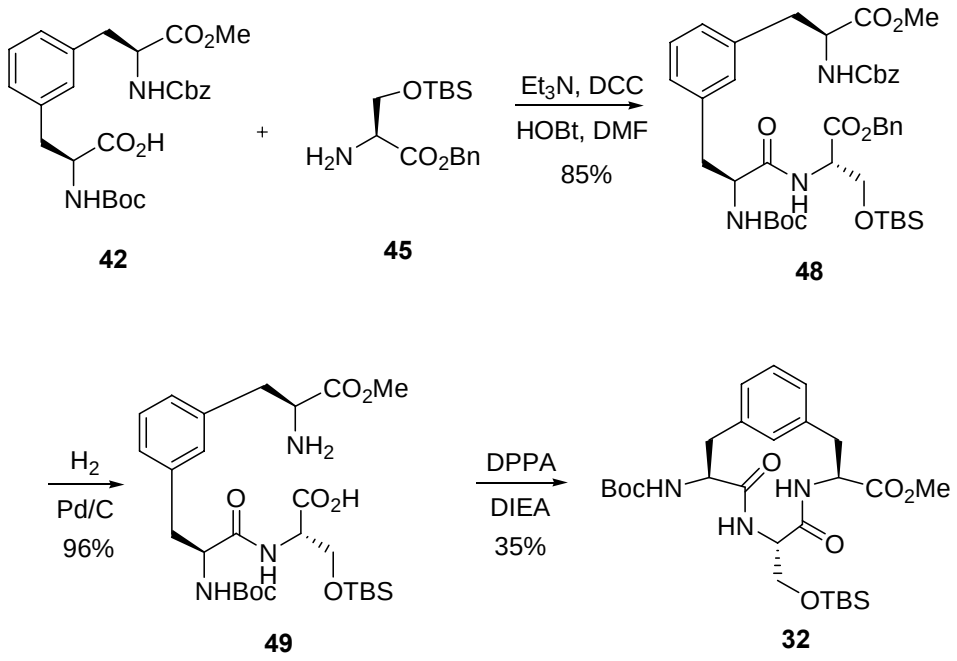

42 **45** **48**

49 **32**

4.4 Conclusions

Homeodomains are a family of HTH DNA-binding motifs, which are found in many eukaryotic transcription factors. HTH-turns are a new class of turns that are different from β- and γ-turns. HTH-turns play an important role in stabilizing the HTH tertiary structure. The small size and significance in stabilizing the tertiary structure of the HTH-turn motif make it an attractive target to mimic. The phenyl ring was introduced into the HTH-turn via side chain covalent bonds to increase hydrophobic contacts in the HTH motif. Two HTH-turn mimics, the Ser HTH-turn mimic and the Gly HTH-turn mimic were designed and successfully synthesized. These two HTH-turn mimics are ready to be incorporated into the *Antennapedia* (27-55) sequence, which contains a HTH-turn between two α-helixes. The Gly HTH-turn mimic and the Ser HTH-turn mimic were synthesized in eight steps with a 33% yield and a 14% yield, respectively. Two sequential Horner-Wittig couplings and enantioselective hydrogenation using Rh(EtDUPHOS) were the key steps for the synthesis of both HTH-turn mimics. The high efficiency of enantioselective hydrogenation allows us to make L-configration bis-amino acids without starting from an optically pure amino acid. The cyclization step was optimized to drive the reaction to completion without forming a dimer and/or a polymer. The scale up produced grams of the Gly HTH-turn mimic allowed us to construct a peptidomimetics containing a *Antennapedia* homeodomain (27-55) sequence.

4.5 Experimental

General Experiment. Unless specified otherwise, all chemicals were used as received. THF was freshly distilled under nitrogen from sodium/benzophenone ketyl immediately prior to use. Dichloromethane was freshly distilled under nitrogen from calcium hydride. DMF and MeOH were used from SureSeal^{TM} bottles. DIEA was distilled from CaH_2 under nitrogen. Brine (NaCl), $NaHCO_3$ and NH_4Cl refer to saturated aqueous solutions. ^1H NMR were recorded at 500, or 400 MHz. ^{13}C NMR were determined at 125, or 75 MHz. Flash column chromatography was performed using 230-400 mesh, EM Science silica gel. Melting points were uncorrected.

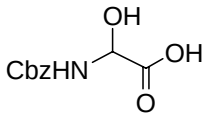

2-(Benzyloxycarbonylamino)-2-hydroxyacetic Acid (34). Benzyl carbamate (2.0 g, 13 mmol) and glyoxylic acid monohydrate (1.34 g, 14.6 mmol) were dissolved in anhydrous Et_2O (50 mL) and the solution was stirred for 24 h at rt. The resulting suspension was filtered and rinsed with anhydrous ether to produce 2.5 g (86%) of **56** as a white powder. m.p. 193-195 ºC, (lit 196-198 ºC). ^1H NMR (DMSO-d_6): δ12.74 (br, s, 1H), 8.07 (d, 1H, *J* = 8.2Hz), 7.31 (m, 5H), 6.18 (br, s, 1H), 5.16 (d, 1H, *J* = 8.8Hz), 5.00 (s, 2H).

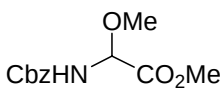

Methyl 2-(benzyloxycarbonylamino)-2-methoxyacetate (35). Cbz-Hydroxyglycine **34** (6.00 g, 26.6 mmol) was dissolved in dry methanol (150 mL) and cooled to 4 ºC. Concentrated H_2SO_4 (1.7 mL) was added dropwise and the solution was

stirred for 48 h at rt. The reaction mixture was poured into ice-cooled, saturated $NaHCO_3$ and extracted with ethyl acetate (3 × 30 mL). The organic extract was washed with water (30 mL), brine (50 mL) and dried over anhydrous $MgSO_4$. Concentration followed by precipitation (EtOAc/Hexane) yielded 5.98 g (89%) as a white powder. m.p. 75-76 ºC, (lit 76-78 ºC.) ^{1}H NMR ($CDCl_3$): δ7.4 (s, 5H), 5.95 (d, 1H, J = 9.1Hz), 5.35 (d, 1H, J = 9.1Hz), 5.15 (s, 2H), 3.79 (s, 3H), 3.45 (s, 3H).

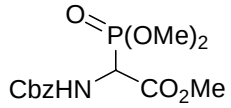

Methyl 2-(benzyloxycarbonylamino)-2-(dimethoxyphosphoryl) acetate (36). Under nitrogen in a round-bottom flask equipped with reflux condenser, a suspension of Cbz-methoxyglycine methyl ester **35** (5.98 g, 23.6 mmol) in toluene (25 mL) was heated to 70 ºC with stirring to dissolve the solid. Phosphorus trichloride (freshly distilled) (1.96 mL, 23.6 mmol) was added and the reaction was stirred at 70 ºC for 24 h. Trimethylphosphite (2.08 mL, 23.6 mmol) was added and the reaction was stirred at 70 ºC for 3 h. The solvent was evaporated and the residue was dissolved in EtOAc (50 mL). The organic solution was washed with ice-cooled, saturated $NaHCO_3$ (3 × 10 mL), water (10 mL), brine (25 mL), and then dried over anhydrous $MgSO_4$. The solvent was removed and recrystallization of the residue from EtOAc/Hexane produced 7.03 g (90%) of a white powder. m.p. 78 ºC (lit 80 ºC). ^{1}H NMR ($CDCl_3$): δ 7.35 (br, s, 5H), 5.63 (d, 1H, J = 6.8Hz), 4.92 (dd, 1H, J = 9.0, 22.0Hz), 3.82 (s, 3H), 3.80 (s, 3H).

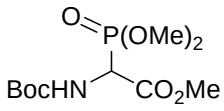

Methyl 2-(*tert*-butoxycarbonylamino)-2-(dimethoxyphosphoryl) acetate (37). Phosphonoglycinate **36.** (2.00 g, 6.04 mmol) and di-*tert*-butyl dicarbonate were dissolved in methanol (15 mL) in a Parr shaker hydrogenation bottle and degassed with N_2 for 15 min. Palladium on carbon (10%, 100 mg) was added and the solution was shaken for 3 h at rt under 40 psi of H_2. The solvent was concentrated and the residue was dissolved in EtOAc (30 mL). The organic solution was washed with saturated $NaCO_3$ (3 × 10 mL), water (10 mL), brine (20 mL), and then dried on $MgSO_4$. The solvent was concentrated and the product was precipitated by the addition of hexane yielding 1.55 g (86%) of a white solid. ^{1}H NMR ($CDCl_3$): δ 5.34 (d, 1H, *J* = 7.7Hz), 4.85 (dd, 1H, *J* = 9.0, 22.2Hz), 3.82 (d, 3H, *J* = 3Hz), 3.81(s, 3H), 3.79 (d, 3H, *J* = 3.6Hz), 1.43 (s, 9H).

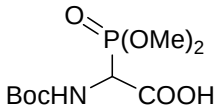

2-(*tert*-butoxycarbonylamino)-2-(dimethoxyphosphoryl)-acetic acid (38). A solution of **37** (1.00 g, 3.36 mmol) in dioxane was cooled to 0 ºC. NaOH (1N, 3.36 mL) was added dropwise over 15 min and the reaction was stirred until the starting material disappeared. The solution was acidified to pH 1 with 20% HCl and extracted with EtOAc (3 × 10 mL). The combined EtOAc layers were washed with water (10 mL), brine (20 mL) and then dried over $MgSO_4$. Concentration followed by recrystallization (EtOAc/Hexane) yielded 0.71 g (75%) of a white powder. m.p.153-155 ºC. ^{1}H NMR ($CDCl_3$): δ 9.21 (br s, 2H), 5.57 (d, 1H, *J* = 9Hz), 4.94 (dd, 1H, *J* = 9.0, 22.6Hz), 3.38 (d, 3H, *J* = 11.1Hz), 3.84 (d, 3H, *J* = 11.6Hz), 1.45 (s,9H).

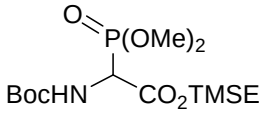

Trimethylsilylethyl 2-(*tert*-butoxycarbonylamino)-2-(dimethoxy phosphoryl) acetate (39). The acid **38** (0.45 g, 1.6 mmol) and thimethylsilylethanol (0.3 mL, 2 mmol) were dissolved in CH_2Cl_2 (30 mL) and cooled to 4 ºC. DCC (0.40 g, 1.9 mmol) was added and the reaction was stirred for 18 h. The urea was removed by filtration and the solution was concentrated. The residue was dissolved in ethyl acetate (20 mL), washed with citric acid (2 × 10 mL), water (10 mL), brine (20 mL), and then dried over $MgSO_4$. The solution was concentrated and the product was precipitated by the addition of hexane yielding 0.42 g (70%) of a white solid. ^{1}H NMR ($CDCl_3$): δ 5.31 (br d,1H, J = 8.4Hz), 4.81 (dd, 1H, J = 9.0, 22.0Hz), 4.28 (m, 2H), 3.82 (d, 3H, J = 3.1Hz), 3.78 (d, 3h, J = 3.1Hz), 1.43 (s, 9H), 1.05(m, 2H), 0.03 (s, 9H). ^{13}C NMR (CDCl3): δ 166.98, 148.6, 90.2, 65.3, 54.2, 52.3, 28.7, 17.9, -1.2.

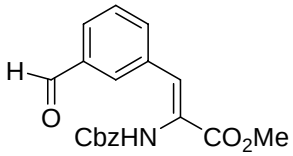

Methyl (Z)-2-(benzyloxycarbonylamino)-3-(formylphenyl)-2-(propenoate) (40). Compound **36** (4.0 g, 12 mmol) was dissolved in CH_2Cl_2 (30 mL), then tetramethylguanidine (1.88 mL, 15.0 mmol) was added. The reaction was stirred for 30 min then isophthalaldehyde (2.0 g, 6.0 mmol) was added. The reaction was judged to be complete by monitoring the disappearance of starting materials by TLC (1:1 hexane:EtOAc) after 20 min. The solution was diluted with 20 mL CH_2Cl_2 and washed with 10% citric acid (2 × 10 mL), $NaCO_3$ (20 mL), water (20 mL), brine (40 mL), and then dried on $MgSO_4$. Concentration followed by chromatography (90:10

Hexane/EtOAc-excess isophthalaldehyde; 85:15 Hexane/EtOAc-product) gave 3.41g (83%) of a light yellow oil that solidified by the addition of hexane and cooling to 0 ºC. ^{1}H NMR ($CDCl_3$): δ 9.89 (s, 1H), 7.94 (s, 1H), 7.80 (d, 1H, *J* = 7.7Hz), 7.72 (d, 1H, *J* = 7.7Hz), 7.47 (t, 1H, *J* = 7.7Hz), 7.37 (s, 1H), 7.32 (br s, 5H), 6.67 (s, 1H), 5.08 (s, 2H), 3.84 (s, 3H). ^{13}C NMR ($CDCl_3$): δ 192.2, 165.9, 153.7, 137.1, 135.0, 134.8, 131.2, 130.3, 129.5, 128.7, 128.0, 127.5, 125.9, 67.1, 52.0.

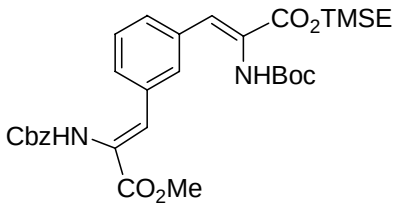

Methyl (*Z*)-2-(benzyloxycarbonylamino)-3-(3-((*Z*)-2-(*tert*-butoxycarbonyl-amino)-3-(2-trimethylsilyl)ethoxy-3-oxo-1-propenyl)phenyl)-2-propenoate (41). To the solution of **39** (4.45 g, 11.6 mmol) and tetramethylguanidine (2.0 mL, 16 mmol) in CH_2Cl_2 (10 mL), monoaldehyde **40** (3.82 g, 11.3 mmol) that was dissolved in CH_2Cl_2 (10 mL) was added, and then the reaction was stirred at rt for 20 h. The solution was diluted with CH_2Cl_2 (100 mL) and washed with 10% citric acid (2 × 30 mL), $NaCO_3$ (30 mL), water (40 mL), brine (50 mL), dried over $MgSO_4$, and concentrated *in vacuo*. The residue was purified by chromatography giving 5.81 g (86 %) of a colorless oil that was solidified to a glass-like crystal at 0 ºC. ^{1}H NMR ($CDCl_3$): δ 7.63 (s, 1H), 7.47 (d, 2H, *J* = 6Hz), 7.33-7.26 (m, 7H), 7.18 (s, 1H), 6.37 (br s, 1H), 6.23 (br s, 1H), 5.06 (s, 2H), 4.29 (t, 2H, *J* = 8.7Hz), 3.76 (s, 3H), 1.32 (s, 9H), 1.04 (t, 2H, *J* = 8.5Hz), 0.04 (s, 9H). ^{13}C NMR (CDCl3): δ 166.1, 165.5, 154.7, 153.1, 136.3, 134.2, 133.3, 131.2, 130.5, 129.4, 128.4, 128.3, 126.4, 125.0, 124.2, 80.3, 67.1, 63.5, 52.0, 27.6, 16.5, -1.9.

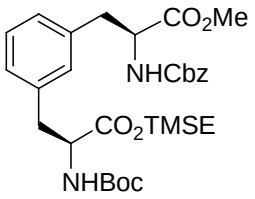

Methyl (*S*)-2-(benzyloxycarbonylamino)-3-(3-((*S*)-2-(*tert*-butoxy carbonylamino)-3-(2-trimethylsilyl)ethoxy-3-oxopropenyl)phenyl)-2-propenoate (13). Compound **41** (5.0 g, 8.4 mmol) was dissolved in MeOH (20 mL) and then the solution was flushed with N_2 for 30 min. [(COD) Rh-((S,S-Et-EtDUPHOS))]$^+$Otf$^-$ (52 mg, 0.072 mmol) was dissolved in the degassed MeOH and then transferred to a Parr shaker which contained the solution of **41**. The pressure was maintained at 60 psi after it was degassed and refilled with H_2 four times. The reaction was stirred at constant pressure at rt for 20 h. The solution was concentrated *in vacuo* followed by passage through a short silica column to remove the catalyst with EtOAc/ Hexane (1:1), giving 5g (99%) **13** as a colorless oil. ^{1}H NMR ($CDCl_3$): δ 7.32 (m, 5H), 7.19 (t, 1H, *J* = 7.5Hz), 7.00 (d, 1H, *J* = 11.4Hz), 6.98 (d, 1H, *J* = 11.4Hz), 6.86 (s, 1H), 5.28 (br d, 1H, *J* = 7.9Hz), 5.08 (s, 2H), 4.99 (br d, 1H, *J* = 7.91Hz), 4.63 (m, 1H), 4.17 (m, 2H), 3.71 (s, 3H), 3.07-2.95 (m, 4H), 1.39 (s, 9H), 0.93 (m, 2H), 0.02 (s, 9H). ^{13}C NMR ($CDCl_3$): δ 171.96, 155.72, 155.15, 137.63, 136.38, 136.41, 130.99, 129.23, 129.01, 128.66, 128.61, 128.28, 127.45, 80.33, 67.46, 64.23, 55.32, 55.03, 52.82, 38.67, 28.79, 17.89.

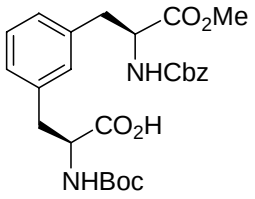

3-(3-(((*S*)-2-(benzyloxycarbonylamino)-3-methoxy-3-oxopropyl)phenyl)-(*S*)-2-(*tert*butoxycarbonylamino)propanoic acid (42). Bis-amino ester **13** was dissolved in DMF (20 mL) and was cooled to 0 ºC in an ice bath. Water (16

drops, 0.4% by vol) was added. $Bu_4N^+F^-$ (1 M in THF, 4.36 mL, 4.36 mmol) was added to the solution and the solution became yellow. The reaction was allowed to warm to rt and stirred for 16 h. DMF was removed *in vacuo* and the residue was redissolved in EtOAc (50 mL). The solution was acidified to pH 2 with HCl (2 N, 20 mL). The aqueous layer was extracted with EtOAc (3 × 30 mL). The extracts were combined and dried over Na_2SO_4, followed by concentration, giving 0.74 g (80%) **42** as a light-yellow oil. ^{1}H NMR ($CDCl_3$): δ 8.01 (s, 2H), 6.8-7.4 (m, 9H), 6.04 (d, 0.5H, J = 8.7Hz), 5.25 (s 2H,), 5.11 (s, 1H), 4.7 (s, 1H), 3.74 (s, 3H), 2.8-3.2 (m, 4H), 1.42 (m, 9H).

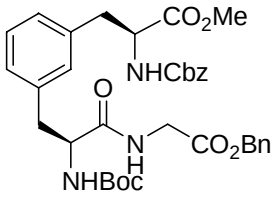

Methyl (*S*)-2-(benzyloxycarbonylamino)-3-(3-(3-((2-benzyloxy)-2-oxoethyl)amino)-(*S*)-2-(*tert*-butoxycarbonylamino)-3-oxopropyl)phenyl) propenoate (43). Acid **42** (870 mg, 1.7 mmol), glycine benzyl ester hydrotosylate (1.18 g, 3.50 mmol), triethylamine (0.48 mL, 3.5 mmol) and HOBt (0.53 g, 3.5 mmol) were dissolved in DMF (25 mL), and then cooled to 0 ºC in an ice bath. DCC (0.72 g, 3.5 mmol) was added and the reaction was stirred for 20 h at rt. DMF was removed *in vacuo*, then the residue was dissolved in CH_2Cl_2 (50 mL). The solution was cooled at 4 ºC to precipitate DCU. DCU was removed by filtration and the filtrate was concentrated. The residue was dissolved in ether (50 mL) then cooled again. The precipitate was filtered again. The filtrate was washed with 10% citric acid (2 × 30 mL), $NaCO_3$ (30 mL), water (40 mL), brine (50 mL), dried on $MgSO_4$, and concentrated *in vacuo*. The residue was purified by chromatography, giving **43** (0.73g, 80 %) as a colorless oil. ^{1}H NMR

($CDCl_3$): δ 7.26-7.32 (m, 10H), 7.15 (t, 1H, *J* = 7.5Hz), 7.06 (d, 1H, *J* = 7.9Hz), 7.04 (s, 1H), 6.96 (d, 1H, *J* =7.5Hz), 6.26 (br s, 1H), 5.42 (d, 1H, *J* = 7.8Hz), 5.21 (br s, 1H), 5.12 (s, 2H), 5.08 (br m, 1H), 5.01 (s, 2H), 4.63 (m, 1H), 4.35 (s, 1H), 3.90 (s, 2H), 3.74 (s, 3H), 2.87-3.20 (m, 4H), 1.41 (s, 9H). ^{13}C NMR ($CDCl_3$): δ 172.0, 168.4, 155.7, 155.2, 79.8, 67.4, 63.8, 54.6, 52.4, 38.3, 29.8, 28.4, 17.5,

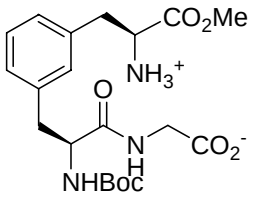

Amino acid (44). Tripeptide **43** (0.76 g, 1.2 mmol) was dissolved in MeOH (20 mL), then 10% Pd/C (0.1 g) was added. The pressure in the Parr shaker was maintained at 45 psi after 3 vacuum/ H_2 cycles. The reaction was shaken for 14 hr at rt. The catalyst was removed by filtration on a celite column and the filtrate was concentrated to give 0.335 g (83%) **44** as a colorless oil. ^1H NMR ($CDCl_3$): δ 7.9 (br s, 1H), 6.8-7.2 (m, 5H), 5.42 (d, 1H, *J* = 8.2Hz), 4.66 (s, 1H), 4.13 (br s, 1H), 3.76 (s, 3H), 3.58 (br s, 2H), 2.8-3.2 (m, 4H), 1.28 (s, 9H).

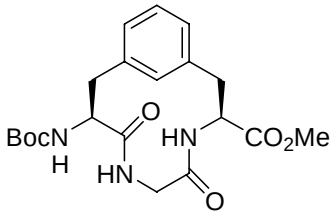

Methyl (*S*)-9-(*tert*-butoxycarbonylamino)-5,8-dioxo-(*S*)-4,7-diazabicyclo[9.3.1]pentadeca-1(15),11,13,triene-3-carboxylate (4). DPPA (0.340 mL, 1.55 mmol) and DIEA (0.54 mL, 3.0 mmol) were added to a flask containing 500 mL DMF. The amino acid **44** (0.524 g, 1.24 mmol), dissolved in 10 mL of DMF, was transferred into the flask with a syringe pump over 14 h. The reaction bottle was kept

from light without stirring under N_2 for 5 d at 0 ºC, and 2 d at rt. The solution was concentrated, and then purified by chromatography to give 0.228g (53%) Gly HTH mimic **4** as a white solid. ^{1}H NMR ($CDCl_3$/DMSO-d_6): δ 8.0 (t, 1H, *J* = 6.95Hz), 7.15 (t, 1H, *J* = 7.55Hz), 7.06 (d, 1H, *J* = 7.5Hz), 6.96 (d, 1H, *J* =7.5Hz), 6.87 (d, 1H, *J* =7.5Hz), 6.68 (s, 1H), 5.78 (d, 1H, *J* = 8.95Hz), 4.69 (m, 1H), 4.30 (m, 1H), 3.65-3.72 (m 5H), 2.92-3.05 (m, 1H,) 2.68 (dd, 1H, *J* =7.5, 12.7Hz), 2.60 (dd, 1H, *J* = 5.7Hz), 1.36 (s, 9H). ^{13}C NMR (CDCl3): δ 171.7, 169.5, 154.9, 136.2, 136.0, 133.3, 128.9, 128.63, 127.1, 79.0, 56.3, 52.9, 52.2, 43.7, 38.4, 36.7, 28.8.

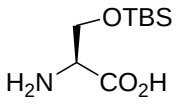

Serine- (O-TBS) (46).[172] L-serine (5.3 g, 50 mmol) was suspended in DMF (100 mL). Imidazole (6.87 g, 55.0 mmol) and TBSCl (8.36 g, 55.0 mmol) were added and the solution was stirred at rt for 20 h. DMF was evaporated and the residue was stirred with a mixture of water and hexanes (1:1) for 4 h. The precipitated white solid was filtered and washed with hexanes, giving 7.66 g **46** in a yield of 74%. ^{1}H NMR ($CDCl_3$): δ 4.00 (d, 2H, *J* = 25.4Hz), 3.61 (s, 1H), 0.92 (s, 9H), 0.12 (s, 6H).

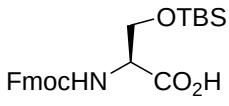

Fmoc-Ser(O-TBS) (47). Compound **47** (1.0 g, 5.0 mmol) was dissolved in 10% $NaHCO_3$ (20 mL) and cooled in an ice bath. A solution of Fmoc-OSu dissolved in dioxane was added dropwise over 20 min. The mixture was stirred for 20 h at rt. The mixture was diluted with water (50 mL) and extracted with EtOAc (20 mL). The aqueous layer was acidified to pH 1 with concentrated HCl and extracted with

EtOAc (3 × 20 ml). The extract was dried on Na_2SO_4 and evaporated to yield 0.4 g **47** as a colorless oil in a yield of 20%. ^{1}H NMR ($CDCl_3$): δ 7.76 (d, 2H, *J* = 7.55Hz), 7.60 (t, 2H, *J* = 8.25Hz), 7.40 (t, 2H, *J* = 7.55Hz), 7.31 (t, 2H, *J* = 7.55Hz), 5.76 (d, 1H, *J* = 9.45Hz), 4.46 (t, 2H, *J* = 3.9Hz), 4.40 (dd, 1H, *J* = 7.3, 13.95Hz), 4.14 (br s, 1H), 4.40 (dd, 1H, *J* = 3.9, 6.4Hz), 0.89 (s, 9H), 0.08 (s, 6H).

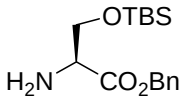

Serine(TBS)-OBn 45.[174] Ser-OBn (1.00 g, 2.72 mmol) was suspended in DMF (10 mL). Imidazole (0.65 g, 9.5 mmol) and TBSCl (0.47 g, 3.1 mmol) were added and then the solution was stirred at rt for 24 h. The mixture was diluted in 100 mL ether and washed with water (3 × 50 mL). The solution was dried on Na_2SO_4 and concentrated. Chromatography on silica gel gave **45** (2.91 g) as a light yellow oil in a yield of 61%. ^{1}H NMR ($CDCl_3$): δ 7.35 (s, 5H), 5.16 (s, 2H), 3.94 (dd, 2H, *J* = 4.15, 5.5Hz), 3.55 (t, 1H, *J* = 3.4Hz), 1.78 (s, 2H), 0.85 (s, 9H), 0.13 (s, 6H).

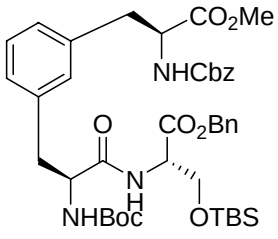

Tripeptide 48. Acid **42** (442 mg, 0.890 mmol), amine **45** (612 mg, 1.77 mmol), DIEA (288 mg, 1.77 mmol) and HOBt (270 mg, 1.77 mmol) were dissolved in DMF (10 mL), and then cooled down to 0 ºC in an ice bath. EDC (338 mg, 1.77 mmol) was added and the reaction was stirred for 24 h at rt. The mixture was diluted with EtOAc (50 mL) and then washed with 10% citric acid (2 × 10 mL), $NaCO_3$ (10 mL), water (10 mL), brine (20 mL), dried on $MgSO_4$, and concentrated *in vacuo*. Chromatography on

silica gel gave **48** (719 mg, 85%) as a colorless oil. ^{1}H NMR ($CDCl_3$): δ 7.30-7.38 (m, 10H), 7.15 (t, 1H, *J* = 7.8Hz), 7.06 (d, 1H, *J* = 7.35Hz), 7.04 (s, 1H), 6.94 (d, 1H, *J* = 6.4Hz), 6.55 (d, 0.5H, *J* = 6.65Hz), 6.30 (d, 0.5H, *J* = 8.25Hz), 5.40 (d, 1H, *J* = 8.0Hz), 5.13 (s, 2H), 5.07 (s, 2H), 4.61-4.70 (m, 4H), 4.36 (d, 1H, *J* = 6.85), 3.96 (m, 1H), 3.71 (s, 3H), 2.9-3.10 (m, 4H), 1.39 (s, 9H), 0.82 (s, 9H), 0.05 (s, 6H). ^{13}C NMR ($CDCl_3$): δ 177.7, 177.0, 176.6, 175.6, 161.3, 143.0, 142.2, 141.1, 140.7, 136.6, 85.8, 69.1, 61.1, 60.7, 59.8, 58.1, 43.4, 33.9, 31.4, 23.6, 19.6, 0.0.

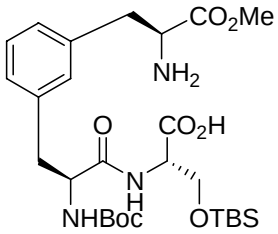

Amino acid 49. Compound **48** (719 mg, 0.870 mmol) was dissolved in MeOH (20 mL), and 10% Pd/C (100 mg) was added. The pressure in the Parr shaker was maintained at 30 psi after 3 vacuum/ H_2 cycles. The reaction was shaken for 14 h at rt. The catalyst was removed by filtration and the filtrate was concentrated to give 490 mg (92%) **49** as a colorless oil. ^{1}H NMR ($CDCl_3$): δ 7.22 (t, s, 1H, *J* = 7.55Hz), 7.14 (t, s, 1H, *J* = 8.45Hz), 7.02 (d, s, 1H, *J* = 7.55Hz), 6.53 (d, 0.5H, *J* = 7.6Hz), 6.44 (br s, 0.5H), 5.41 (d, 1H, *J* = 7.8Hz), 4.34-4.60 (m, 4H), 3.96-4.28 (m, 3H), 3.73 (s, 3H), 3.22-3.48 (m, 2H), 2.92-3.12 (m, 2H), 1.42 (s, 9H), 0.82 (s, 9H), 0.003 (s, 6H).

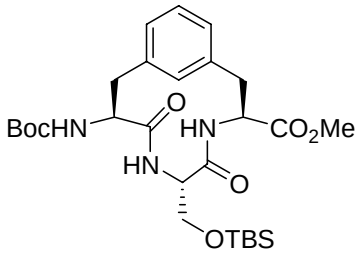

Serine HTH-turn mimic 32. DPPA (655 mg, 2.37 mmol) and DIEA (510 mg, 3.95 mmol) were added to a flask that contained 500 mL DMF. The amino acid **49** (490 mg, 0.79 mmol) dissolved in 10 mL of DMF (anhydrous) was transferred into the flask with a syringe pump over 6 h. The reaction was stirred under N_2 for 7 d at 0 ºC. The solution was concentrated followed by chromatography to give 165 mg (35%) of Serine HTH-turn mimic **55** as a white solid. ^{1}H NMR ($CDCl_3$/DMSO-d_6): δ 6.93-7.35 (m, 4H), 4.64 (s, 2H), 3.41-4.15 (m, 7H), 2.92-3.12 (m, 4H), 1.49 (s, 9H), 0.87 (m, 2H), 0.05 (m, 9H). ^{13}C NMR ($CDCl_3$): δ 177.1, 176.6, 175.2, 160.1, 142.2, 141.5, 137.8. 135.4, 134.1, 133.1, 132.9, 84.2, 67.1, 61.6, 59.5, 57.9, 43.5, 40.0, 31.4, 32.7., 2.2.,0.0. HRMS calcd. For $C_{27}H_{43}O_7N_7Si$ (MH^+) *m/z*=550.2949, found *m/z*=550.2950.

Chapter 5
Solid-phase synthesis of HTH peptides

5.1 Design of the peptide sequence containing HTH-turn mimics

Two major questions in protein chemistry still need to be solved. Firstly, how does an amino acid sequence determine the three-dimensional structure of a protein? Secondly, how do proteins regulate the gene expression by forming DNA-protein complexes? One method to investigate the first problem is to study the structural and functional properties of mimic proteins. Forming complexes between mimic proteins and targeted DNA is a powerful tool to study the biological characteristics of proteins adopting a specific structure. The mimic proteins containing unnatural amino acids are relatively small and easy to handle, characterize, and produce quantitative measurements.

The Homeobox genes were the first discovered genes to be regulated by proteins, encoding a family of proteins.[175] The encoded 60 amino acid residues of proteins are termed as the homeodomain. Homeodomain proteins bind to nucleotide sequences in DNA and regulate the expression of genes. The homeodomain is found in many eukaryotic transcription factors. Homeodomain proteins play a fundamental role in diverse developmental processes, including the specification of body plan, pattern formation, and the determination of cell fate.[176, 177] The malfunction of these genes may result in genetic disorders such as aniridia, cone-rod retinal dystrophy, and Waardenburg syndrome.[176, 177] The homeodomain has been identified in a broad spectrum of organisms,

ranging from yeast to *Drosophila* to human.[178]

All homeodomains consist of three α-helixes.[179] The second and third helixes of the homeodomain form a helix-turn-helix DNA binding motif, whereas the position of the first helix is specific to the homeodomain subfamily.[179] The first helix may help to stabilize the tertiary structure of the homeodomain. The second helix of this motif binds to DNA via a number of hydrogen bonds and hydrophobic interactions, which occur between specific side chains of peptides and the exposed bases and thymine methyl groups within the major groove. The third helix, called the recognition helix, is positioned roughly perpendicular to the other two and fits into the major groove of the DNA.[180] The *N*-terminal regions of the homeodomain are the primary regions of the protein that interact with DNA. The most consistent part of a homeodomain is the recognition helix that is structurally conserved when in contact with DNA.[181] In order to fit the requirement of the DNA binding proteins, some changes have to made in the amino acid sequence of the recognition helix and the conformation of the homeodomain.

The smaller size of the HTH relative to general tertiary structures such as β-sheet barrels and α-helix bundles makes it a good target to mimic. The consistent structure of HTH in both prokaryotes and eukaryotes also makes it a good target to mimic.[182, 183] The design of HTH mimics included the design of HTH-turn mimic, whose structure may assist the formation of a tertiary structure between two helixes and does not affect the properties of the binding DNA.[158] The mimics of the HTH-turn and HTH motif were designed by F. Etzkorn with the assistance of MacroModel software (an easily operated modeling system for designing and studying organic and bioorganic molecules and their complexes).[184]

5.2 Synthesis of Fmoc protected Gly HTH-turn mimic

The scaled up synthesis of Gly HTH-turn mimic made it possible to incorporate the cyclic peptide mimic into the HTH peptide sequence. Building Boc protected Gly HTH-turn mimic into the sequence of protein *Antennapedia* was attempted both in solution phase and in solid phase using Merrifield chemistry by J. M. Travins and subsequently by G. T. Foulds, but no target molecule was obtained. Merrifield chemistry uses TFA to cleave the Boc protecting group in each sequence elongation step, and also needs HF to remove the side chain protecting groups and cleave the peptide sequence from the solid phase.[185] Both of these reagents might be harsh on the cyclized HTH-turn mimics. Fmoc chemistry is carried out under milder basic conditions for *N*-terminus deprotection, which is easy to operate and produce better results. To use Fmoc chemistry, the Boc protecting group had to be switched to the Fmoc protecting group, and the carboxylic acid of the HTH mimic peptide needs to be liberated.

The methyl ester was cleaved with 1N NaOH in a mixture of THF/MeOH to give acid **50** (Scheme 5-1). The Boc protecting group was cleaved by TFA to afford **51** and the *N*-terminus was reprotected by the Fmoc protecting group using Fmoc-OSu. Many examples demonstrated that the Fmoc protection could happen only on the amine of a free amino acid without being attached to the acid using Fmoc-OSu,[101, 186, 187] or FmocOPfp.[188] All of these successful cases were carried out on relatively small molecules. In our case, only the mimic with two consecutive Lys residues in the sequence was observed during the reaction between **51** and Fmoc-Lys(Boc)-OH with HBTU coupling. It was hypothesized that a mixed anhydride formed by the attack of the free carboxylate by Fmoc-Lys(Boc)-OBt. (J. M. Travins' unpublished results). The substance

obtained from the reaction was insoluble in all standard peptide synthesis solvents (CH_2Cl_2, DMF, N-methylpyrrolidinone, DMSO),[158] which prohibited obtaining any analytical data from this substance or incorporating it into the peptide sequence.

Scheme 5-1. Synthesis of Fmoc protected Gly HTH-turn mimic using Fmoc-OSu.

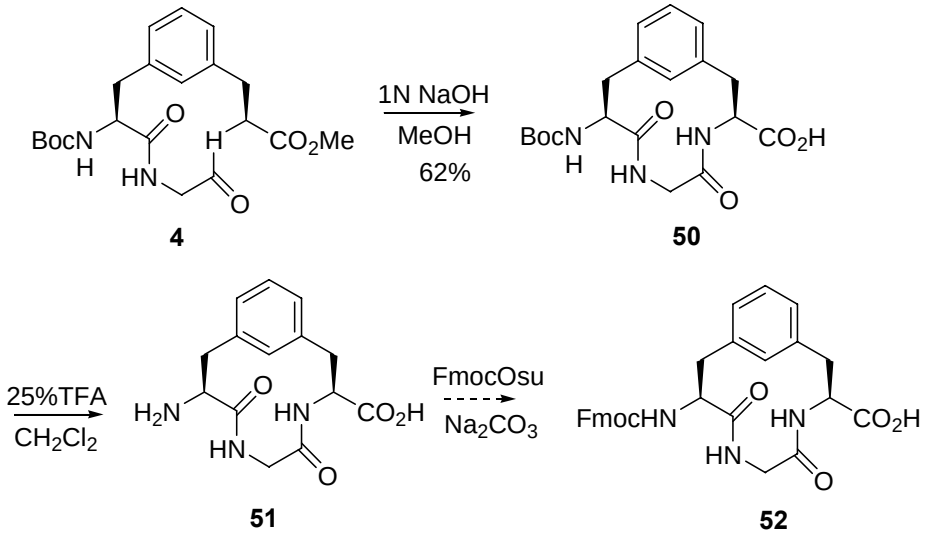

We tried to introduce an Fmoc group into the cyclic peptide by forming an *O,N-bis*-trimethylsilyl intermediate **53**.[189] The intermediate was formed *in situ* by mixing the amino acid with trimethylsilylchloride and a base in an aprotic solvent (Scheme 5-2). The model reaction using proline as a substrate afforded Fmoc protected proline **55** with a high yield (75%) (Scheme 5-3).

Scheme 5-2. Attempts to synthesize Fmoc protected Gly HTH-turn mimic **52** through the formation of temporarily protected intermediate with TMS.

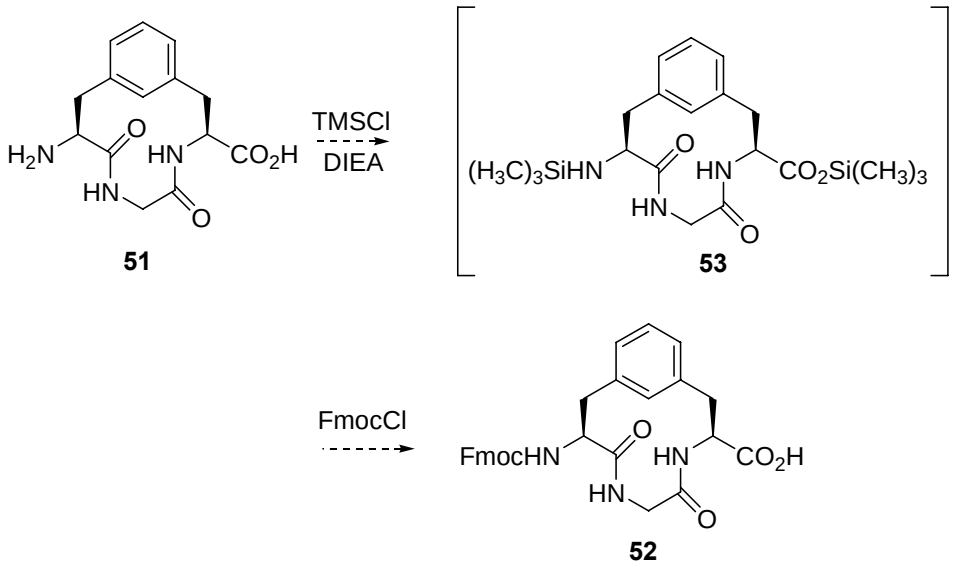

However, no desired product was obtained by treatment of **51** with trimethylsilylchloride at 0 ºC, or at room temperature, whereas the model reaction gave an excellent result at 0 ºC. The formation of the intermediate **75** was difficult without heating (Scheme 5-2).[189] The amide bonds in the Gly HTH-turn mimic might be unstable towards high temperature due to the ring strain in the 12-membered ring and be decomposed under refluxing conditions. The formation of a dimer peptide also competed with the formation of the *O,N-bis*-trimethylsilyl intermediate.[189]

Scheme 5-3. Synthesis of Fmoc-Pro **55** by temporary protection with TMS.

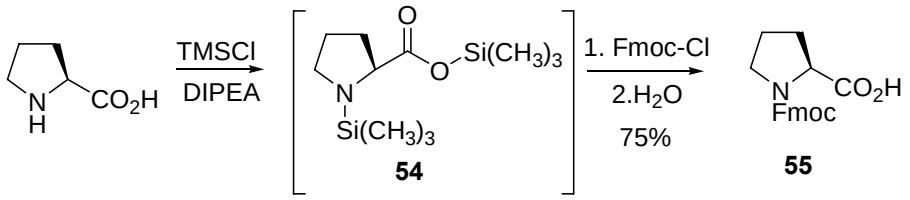

To avoid double Fmoc protection on amino acid **51**, Boc was switched to Fmoc followed by saponification to liberate the carboxylic acid. Fmoc-Cl and Fmoc-OSu are two major Fmoc providing reagents, and the reaction could be carried out either in the organic phase or in the aqueous phase employing different bases, including Et_3N,[187, 190, 191] DIEA,[192, 193] NMM,[194] NaOH, Na_2CO_3,[186] $NaHCO_3$,[195] and pyridine.[196] In our case, the reaction proceeded in the organic phase using DIEA with the best results.

The cleavage of Boc can be performed by treatment with TFA[188, 192-194] or HCl.[197] The TFA cleavage shows poor selectivity in the presence of benzyl protecting groups, which leads to side reactions and decreases yields.[134] Triethylsilane was found to be the most effective carbocation scavenger acting as a hydride donor under acidic conditions when Boc and *t*-butyl ester groups need to be removed in the presence of Cbz, Fmoc, and benzyl groups.[134, 135]

Fmoc-OSu was found to be less active than Fmoc-Cl. The reaction carried out in the aqueous solution using Fmoc-OSu produced an unidentifable mixture. The basicity of Na_2CO_3 and $NaHCO_3$ employed in the aqueous phase reaction could partially deprotect methyl ester during the reaction. The introduction of Fmoc into the cyclic peptide mimic was accomplished using Fmoc-Cl and DIEA in CH_2Cl_2. This was the first time that the Fmoc group was introduced into the HTH-turn mimic successfully (Scheme 5-4).

Scheme 5-4. Synthesis of Fmoc protected Gly HTH-turn mimic **57**.

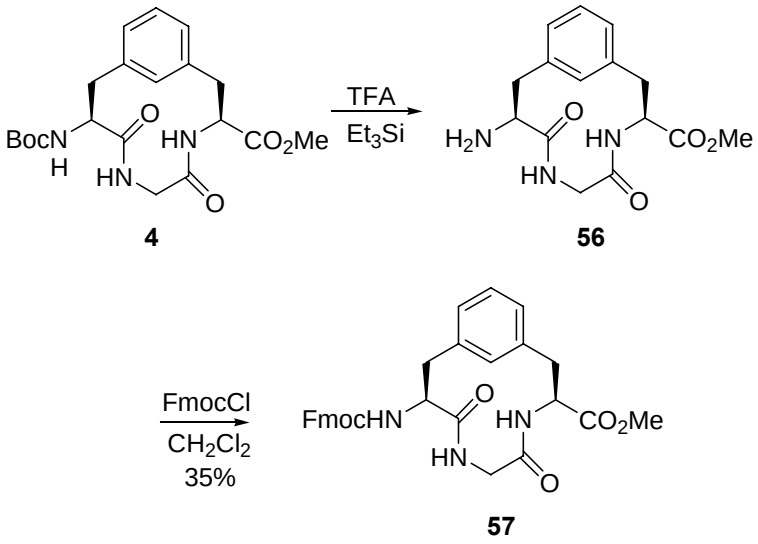

Fmoc is unstable under basic conditions, but it shows stability in a diluted basic solution at 0 ºC for 30 min.[167, 186] The model reaction, using phenylalanine as a substrate, demonstrated that the substrate part lost the Fmoc group (30-40%) during a 30-min saponification at 0 ºC (Scheme 5-5).

Scheme 5-5. Test stability of Fmoc under 0.2 N LiOH using phenylalanine as a substrate.

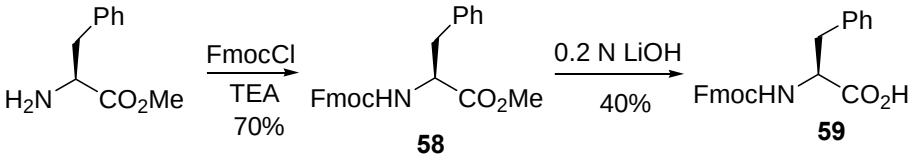

Although the model reaction showed that the Fmoc group could partly survive the condition of methyl saponification, the treatment of **57** with 0.2 N LiOH afforded a

substance that had a same molecular weight as **52** in a low yield (<5%), and this substance only dissolved in TFA.

Scheme 5-6. Saponification of the methyl ester in the presence of Fmoc.

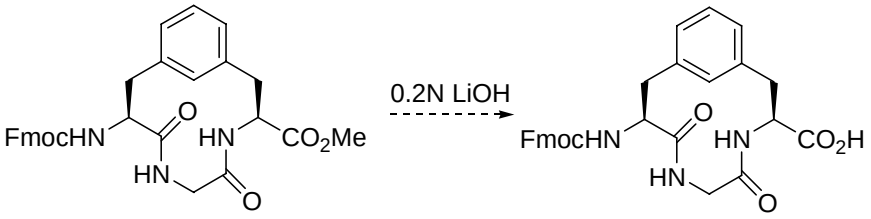

57 **52**

Considering the incompatibility between Fmoc and methyl ester, different protecting group strategies were proposed. The methyl ester was switched to the TMSE ester **60** in the first strategy to avoid Fmoc exposure to basic solutions by methyl deprotection and TMSE reesterification. Several cases have shown the TMSE group was stable towards TFA,[198-200] however, the treatment of **60** with TFA cleaved both Boc and TMSE. Our experience that Fmoc could be cleaved by TBAF in a model reaction by N. Dai forced us to abandon the TMSE strategy (Scheme 5-7).

Scheme 5-7. The TMSE strategy to make Fmoc Gly mimic acid **52**.

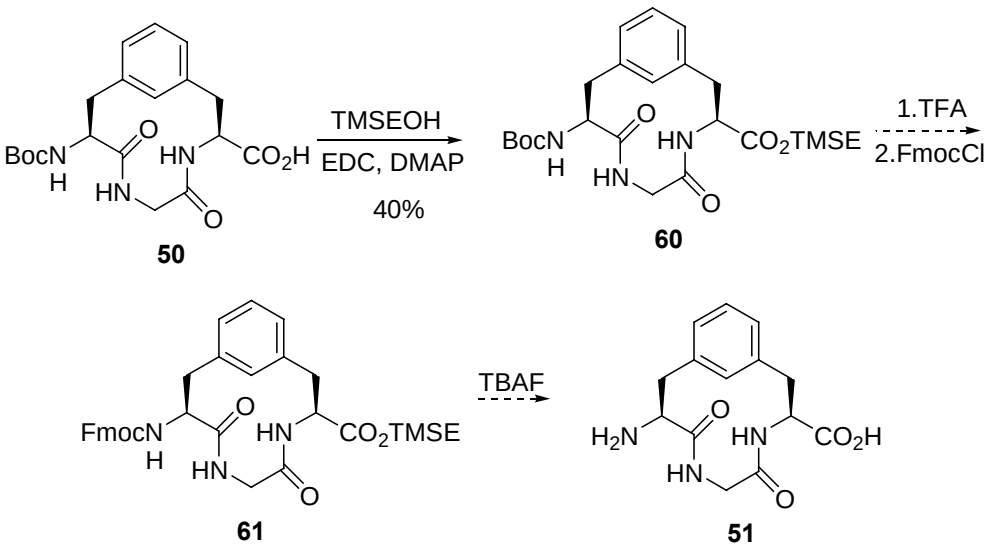

50 **60** **61** **51**

The allyl protecting group was chosen to protect the carboxylic acid of the HTH-turn mimic peptide **72** in the second strategy since the allyl cleavage could be carried out under neutrally catalytic conditions. The allylation of **72** followed by switching Boc to Fmoc produced **63**. Neutral dimedone was chosen as an allylamine scavenger instead of morpholine due to the lability of Fmoc under basic conditions. The yield of the allyl cleavage to afford **52** was low and the product was difficult to interpret. It was suspected the hydrophobicity of the HTH-turn mimic peptide allowed the formation of a complex between palladium and the 12-membered cyclic peptide (Scheme 5-8).

Scheme 5-8. The Allyl strategy to make Fmoc Gly mimic acid **52**.

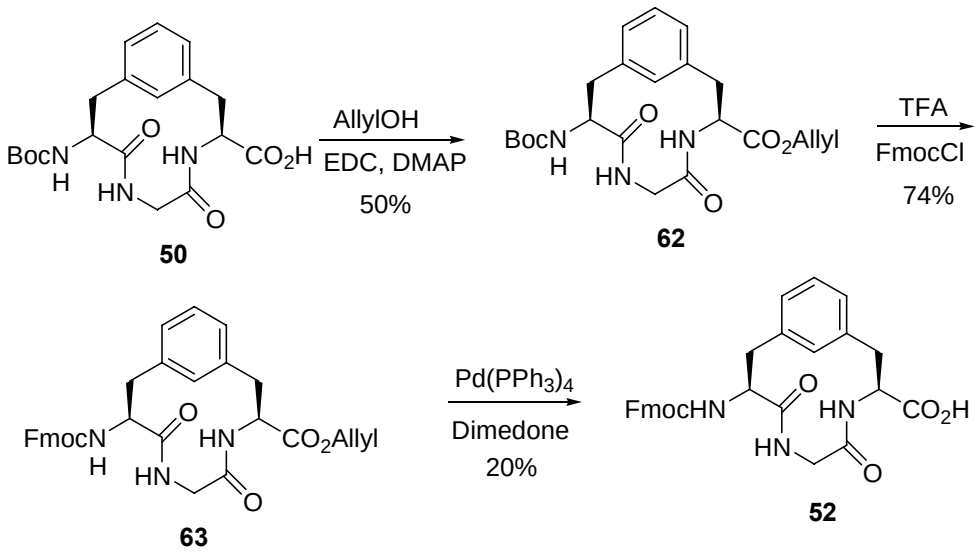

Both of these alternative synthetic routes failed to produce enough Fmoc protected Gly mimic **52** for the peptide synthesis. All the compounds including the HTH-turn cyclic mimic had a poor solubility. The unique structural properties of the HTH-turn mimics resulted in difficulty of modifications of the cyclic peptides. The more protecting

groups were involved in the synthesis, the less **52** was obtained. Switching from Boc to Fmoc directly would produce the best the results. However, the transformation carried out by TFA cleavage, followed by Fmoc protection produced an insoluble substance. Several hypotheses were made to explain the formation of this insoluble substance. TFA might decompose the mimic peptide in the Boc cleavage or form trifluoroacetamide **64** with the resulted amine. Another hypothesis made was that the insoluble substance might be a dimer or a polymer **65** since the substance did not dissolve in any popular solvent. J. M. Travins previously showed that Fmoc-mimic-Fmoc (carbonate) was made during Fmoc protection with very poor solubility (unpublished results). The possible side reactions during the TFA cleavage are summarized in Scheme 5-9.

Scheme 5-9. Possible side reactions that may occur during the TFA cleavage.

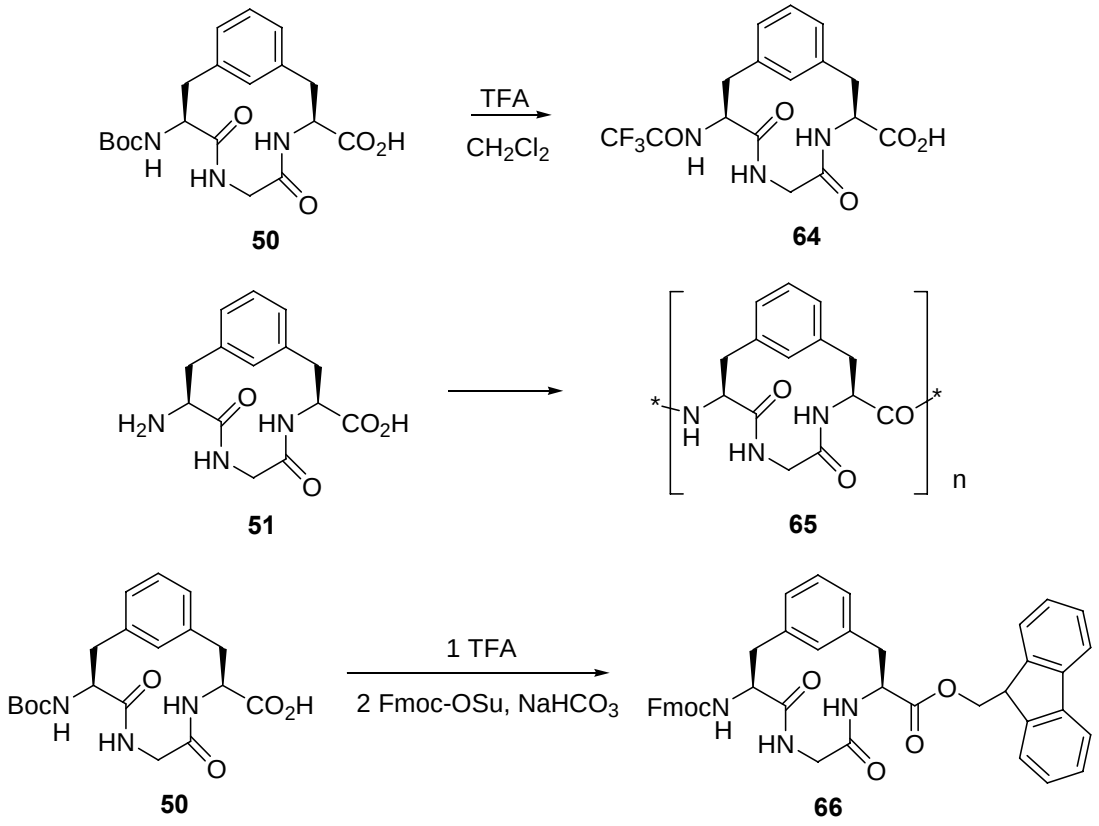

The use of HCl to remove the Boc protecting group circumvented the harsh conditions produced by TFA.[115] The Fmoc protected mimic **52** was successfully synthesized by reacting with Fmoc-Cl after the Boc group was removed by HCl (Scheme 5-10). Fmoc protected Gly mimic **52** did not dissolve in ethyl acetate, dichloromethane, or chloroform. It only dissolved in DMSO, forming a gel-like solution in 30 min. The poor solubility of Fmoc protected Gly mimic **52** made it difficult to purify by flash chromatography. However, this characteristic was employed to purify mimic **52**. Fmoc protected Gly mimic **52** was precipitated out of the solution as white solid after 1M HCl was added. The precipitate was then washed with hexane, ethyl acetate, and water to remove all the soluble impurities.

Scheme 5-10. Cleavage of Boc using HCl facilitated the synthesis of Fmoc mimic acid.

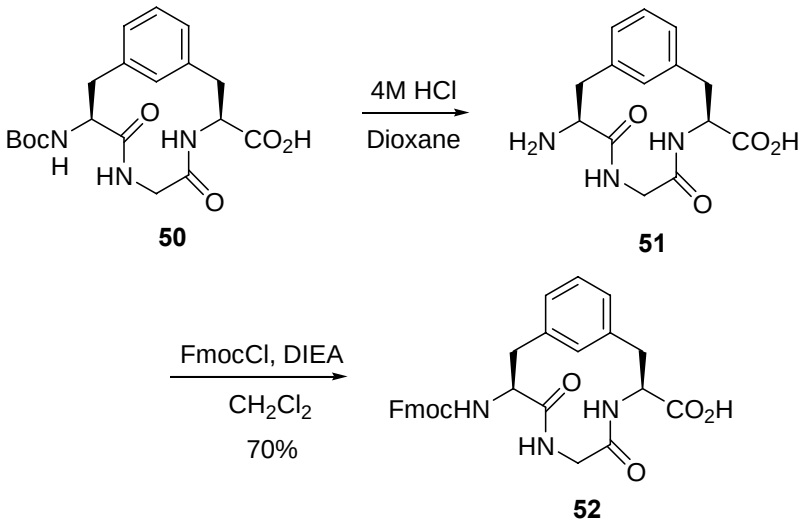

5.3 Synthesis of Fmoc protected Ser HTH-turn mimic

The synthesis of Fmoc protected Ser HTH-turn mimic **69** was also accomplished. The methyl ester was cleaved with LiOH, followed by the Boc protecting group removal by 4M HCl. Without purification, the resulting amino acid **68** reacted with Fmoc-Cl to produce Ser mimic acid **69**. The low yield of **69** might the result of the instability of TBS under both acidic and basic conditions. Fmoc protected Ser mimic **69** exhibited the same solubility properties as Fmoc protected Gly HTH-turn mimic **52**.

Scheme 5-11. Synthesis of Fmoc Ser mimic acid **69**.

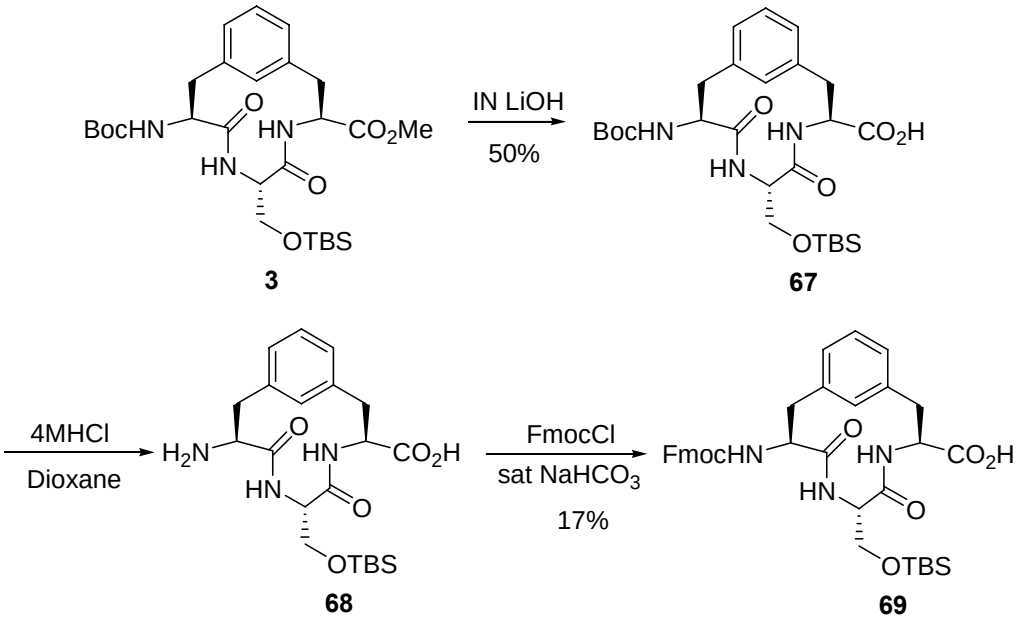

5.4 Solid-phase synthesis of HTH peptide

5.4.1 Sequential elongation synthesis of HTH peptide

The successful synthesis of Fmoc protected Gly mimic **74** on a gram amounts allowed us to incorporate the mimic peptide into the HTH sequence. The synthesis of the HTH sequence containing the mimic peptide had been attempted several times using sequential elongation and segment condensation (J. M. Travins and G. T. Foulds).[158] All of the peptide reactions were carried out on solid phase using Fmoc chemistry.

Incorporation of Gly HTH-turn mimic peptide into the sequence of *Antennapedia* protein was attempted either in solution phase or on solid phase using Boc chemistry, but no target molecule was obtained. The Boc chemistry strategy requires TFA to cleave Boc in each elongation step and employes HF to remove the side chain protecting groups and cleave the peptide sequence from the solid phase. The peptide sequence containing the Gly HTH-turn mimic peptide has not yet been obtained. Several different coupling systems were attempted to incorporate Gly HTH-turn mimic into the *Antennapedia* homeodomain peptide using sequential elongation as described below.

a) The Fmoc peptide synthesis was performed on MBHA resin using HBTU/HOBT/DIEA (3 eq relative to FmocAA) in NMP for 20 min at rt. This procedure was repeated if the Kaiser tests gave a positive result. Coupling the first amino acid to MBHA resin was more difficult than other coupling steps due to steric and bead surface effects. The first coupling was conducted 2 × 1 h. Amino acids with a long functionalized side chain, such as Arg and Trp, always needed to be doubly coupled. All the natural amino acids coupled into the sequence smoothly until the introduction of Fmoc protected

Gly mimic **74** into the sequence. The coupling of Fmoc mimic acid was carried out for 3 hr. The Kaiser test gave a light blue color after the coupling. Capping with DIEA/Ac_2O/CH_2Cl_2 produced a negative Kaiser test. A mass peak corresponding to the sequence of Ac-M-TERQIKIFQNRRMK-NH_2 was observed in the FAB+ mass spectrum (m+1=2349.2). However, the Kaiser test only gave a very light blue color after the resin was treated with piperidine/ NMP to remove the Fmoc group attached to the mimic peptide. Only very light blue color was observed by Kaiser tests during the following Fmoc deprotection. No blue color was observed after the last a few amino acid coupling. The target mass peak was not observed in the MALDI-TOF mass spectra after the cleavage and workup.

b) The Fmoc peptide synthesis was performed on MBHA resin using HATU/HOAT/DIEA (3 eq relative to FmocAA) in NMP for 10 min at rt. HATU gave a better coupling result that HBTU.[139] The amino acids that were difficult to achieve with HBTU could be achieved in less time with HATU coupling. The shorter coupling time produced better results. The coupling of Gly HTH-turn mimic was carried out twice for 30 min each. After the Fmoc group attached to Gly HTH mimic peptide was cleaved, the Kaiser test gave a darker blue color than that observed in the HBTU coupling. The blue color became weaker as more amino acids were coupled onto the sequence. Only very light blue was observed after the last Fmoc was cleaved from the sequence. Yet, no target mass peak was observed in the MALDI-TOF mass spectrum after the cleavage and workup.

c) Sequential elongation carried out with HATU coupling in the "magic mixture", which prevents the formation of the secondary structure and aggregates.[201] A growing

peptide chain attached to resin can form secondary structures, or aggregate with other peptide chains or with the matrix to which the peptide sequence attached. The formation of the secondary structure or aggragates causes low reaction rates and low coupling yields. Aggregates results from the hydrogen bond and hydrophobic forces between the intra- and interchain association. A dipolar aprotic solvent, such as DMF, DMSO or NMP can decrease the occurrence of aggregates.[202] Washing resin with solutions of chaotropic salts, such as 0.8M $NaClO_4$, LiCl or 4M KSCN in DMF before coupling, or addition of these salts to the coupling reactions can overcome the formation of aggregates. Using magic mixture can also supress the formation of aggregates. A mixture of DCM/DMF/NMP (1:1:1) with 1% Triton X100 and 2M ethylenecarbonate at 55º C was used as the solvent system for acetylation and coupling and 20% piperidine in DCM/DMF/NMP (1:1:1) with 1% Triton X100 was used for Fmoc-cleavage. Using a chaotropic salt and magic mixture during the coupling process gave better Kaiser tests after the mimic peptide attached to the peptide sequence. The darker blue color, though not a dark blue, was a good sign that coupling was more efficient. However, no target peak showed up in the MALDI-TOF mass spectrum after the cleavage and workup.

Although better results were obtained using HATU[139] as the coupling reagent in the magic mixture, the most efficient method to incorporate the mimic peptide into the peptide chain is still a problem that requires further investigation. Fmoc amino acid fluorides have been reported as excellent coupling reagents in both solution phase and solid phase peptide synthesis.[203] The acyl fluoride also shows an amazing ability in the coupling of sterically hindered amino acids.[204] Thr is the amino acid that the mimic peptide attaches to in the peptide sequence. It is sterically hindered and always causes the

formation of aggregates.[202] The Fmoc mimic acid will be transformed to the acyl fluoride using cyanuric fluoride[205] before coupling to the peptide sequence in order to overcome the problem of coupling efficiency.

5.4.2 Fragment condensation for the synthesis of HTH mimic peptide

Since the HTH peptide synthesis through sequential elongation failed to afford the Gly HTH-turn mimic incorporated peptide, the peptide sequence was cut into three pieces around the site of HTH-turn mimic. Synthetic HTH-turn mimic may not be stable towards the environment of the peptide synthesis. Incorporation of the hydrophobic HTH-turn mimic into the peptide sequence may lead to the formation of aggregates, which resulted in the low yield of coupling. Therefore, incorporation of the HTH-turn mimic into the peptide sequence at a later stage may eliminate these side effects. The peptide sequence was divided into three parts according to principles listed above (Figure 5-1). Three pieces were fragment **1** (amino acid 27-41), Gly HTH mimic (42-44), and fragment **2** (45-55).

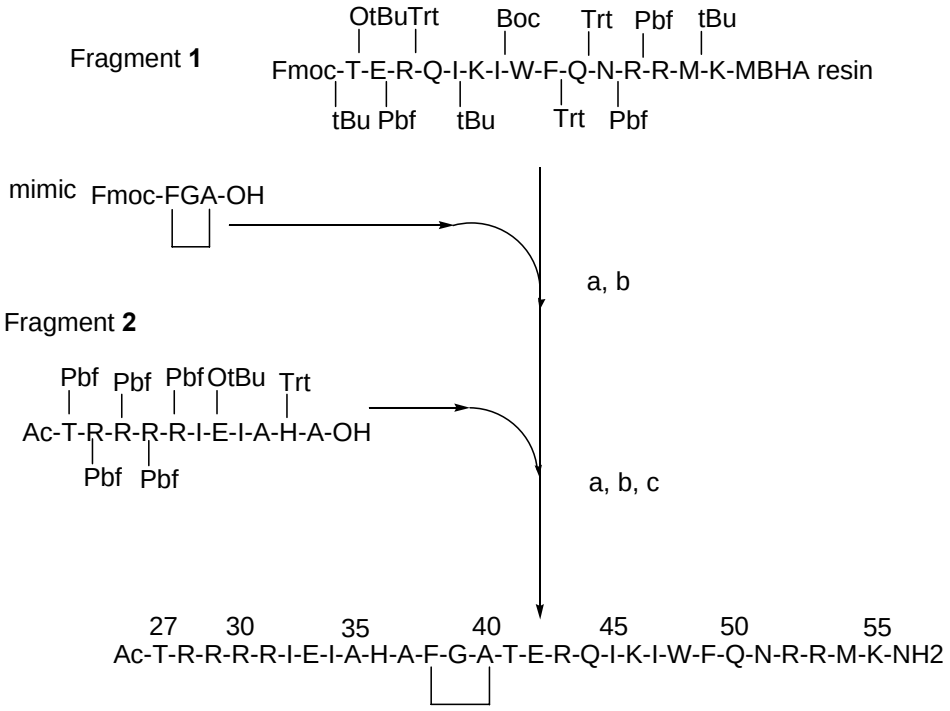

Figure 5-1. Fragment condensation strategy for the synthesis of mimic peptide: a) deprotection, 20% piperidine/NMP; b) coupling, HATU/HOAT/DIEA/magic mixture; c) cleavage and final deprotection, TFA/H_2O/thioanisole/ triisopropylsilane (94:2.5:2.5:1).

Fragment **1** was synthesized on Rink resin by Fmoc chemistry. Fully protected fragment **2** was obtained by anchoring amino acids onto 2-chlorotrityl chloride resin,[126, 127] which can be cleaved under mild acidic conditions. The cleavage was achieved by repetitive treatment of the resin with a 1% solution of TFA in CH_2Cl_2. The mass peak (m+1=2784.4) corresponding to fragment **2** was observed in a FAB+ mass spectrum. Incorporation of Gly HTH mimic into fragment **1** was accomplished by HATU coupling in magic solution with high efficiency judged by the Kaiser tests. Although the Kaiser tests indicated that fragment **2** was coupled into the peptide sequence with high efficiency, the peptide cleaved from the resin failed to give the right sequence containing the Gly HTH mimic. The major peak in the MALDI-TOF mass spectrum was a 1568 Da,

the molecular mass region of fragment **1**. However, no mass peak can be interpreted to be in agreement with any possible combination of the amino acids in the peptide sequence. Kaiser tests were suspected to give false signals due to possible formation of aggregates after the incorporation of Gly HTH-turn mimic into the sequence. The observed low mass peak may be in accordance with the fragment pieces resulting from the decomposition of the peptide sequence. More effective methods are needed to supress aggregation. HTH-turn mimics containing side chains at the position of glycine, such as Ser, will not only increase the solubility of the synthetic HTH-turn mimics, but also interfere the formation of aggregates.

5.5 Conclusions

The successful introduction of the Fmoc protecting group into the HTH-turn mimics allowed us to apply Fmoc chemistry for the incorporation of HTH-turn mimics into the *Antennapedia* peptide. The synthesis of Fmoc protected Gly HTH-turn and Ser HTH-turn mimics were accomplished by employing 4M HCl to cleave the Boc protecting group. The attempts to incorporate the Gly HTH-turn mimic into the HTH peptide proved to be challenging either by sequential elongation or by fragment condensation. The synthesis of an 18mer peptide ending with the Gly HTH-turn mimic at *N*-terminus illustrated the Fmoc chemistry was a suitable method to couple the turn mimics into the HTH peptides. However, the sequential elongation after the Gly HTH-turn mimic was incorporated into the HTH peptide produced weak signals by Kaiser tests. The peptides obtained from the sequential elongation had poor solubility, which made MS and HPLC analysis difficult. The peptides obtained from segment condensation between fragment **1**

and an 18mer containing the Gly HTH-turn mimic was also difficult to interpret due to the poor solubility. Introducing the side chain containing amino acids into HTH-turn mimics may help to increase the solubility of the mimics and the peptide sequences incorporating these mimics.

5.6 Experimental

General Experiment. Unless specified otherwise, all chemicals were used as received. THF was freshly distilled under nitrogen from sodium/benzophenone ketyl immediately prior to use. Dichloromethane was freshly distilled under nitrogen from calcium hydride. DMF and MeOH were used from SureSeal^{TM} bottles. DIEA was distilled from CaH_2 under nitrogen. Brine (NaCl), $NaHCO_3$ and NH_4Cl refer to saturated aqueous solutions. ^1H NMR were recorded at 500, or 400 MHz. ^{13}C NMR were determined at 125, or 75 MHz. Flash column chromatography was performed using 230-400 mesh. MALDI-TOF mass spectra was performed on a Kratos Analytical Kompact SEQ time-of mass spectrometer. Pulses of 3-nanosecond duration of 337.1-nanometer radiation from a nitrogen laser were directed at the solid sample-matrix mixture. Samples were dissolved in DMSO and 0.5 *t*L of solution was placed on the stainless steel target plates. An equal volume of saturated solution of the 9-nitroanthracene matrix in DMSO was added, and the mixture was evaporated to dryness. The dried sample on the target plate was subjected to irradiation from a nitrogen laser (227 nm), and the resulting ions formed were accelerated through a potential difference of 20 kV and detected at the end of 1.8-meter flight tube by a discrete dynode electron multiplier detector. Minimal laser power was used to achieve sufficient sensitivity, while avoiding degradation of the signal in

terms of resolution and noise. Spectra were recorded and processed using the Krato "Lauchpad" MALDI software.

Kaiser Test. The "Kaiser Test" is a colorimetric test for the presence of amino groups. It is used to make sure that each coupling step in peptide synthesis goes to completion. It is based on the reaction of ninhydrin with amino groups to form a blue adduct. Therefore, an incomplete coupling cycle will lead to a positive Kaiser test, demonstrated by the development of a blue color, while coupling to completion will yield a negative (yellow) test.

Prepare the following solutions:

Solution A. Dissolve 8 g phenol in 2 mL absolute ethanol. Warming of the solution will be required to completely dissolve the phenol. (Note: It is easiest to weigh out phenol when it is still cold. Still, the large crystals make it difficult to weigh out exactly 8 g. Try to get close and adjust the volume of ethanol accordingly.)

Solution B. Dissolve 13 mg KCN in 20 mL water. (Transfer the KCN into a tared vial in the hood, then carry to the balance with the cap on.) Check in the hood before preparing this solution as there might already be some available. Dilute 20 μL of aqueous KCN solution with 980 μL pyridine.

Solution C. Dissolve 1.0 g ninhydrin in 20 mL absolute ethanol.

The test procedure is as follows: Set a heating block to 100 °C. Remove a small amount of resin from the reactor and place in a microcentrifuge tube. Add two drops each of three solutions. Mix by tapping the tube. Place in the heat block for two minutes.

Colorless or faint blue color: complete coupling, proceed with synthesis. Dark blue solution but beads are colorless: nearly complete coupling, extend coupling or cap unreacted chains. Solution is light and beads are dark blue: coupling incomplete, recouple. Solution is intense blue and all beads are blue: failed coupling, check amino acid, reagents, then recouple.

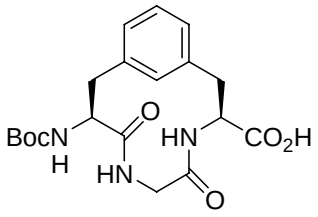

(*S*)-9-(*tert*-butoxycarbonylamino)-5,8-dioxo- (*S*)-4,7-diazabicyclo [9.3.1] pentadeca- 1(15), 11,13,triene-3- carboxylic acid (50).[99] Cyclized peptide methyl ester **4** (30 mg, 0.074 mmol) was dissolved in a mixture of MeOH/ THF (20 mL, 1:1). The solution was heated to help the solid dissolve. The reaction was cooled to 0 ºC and NaOH (1N, 0.08 mL) was added dropwise. The reaction was followed by TLC (120:5:1 CHCl3/MeOH/AcOH, ninhydrin stain) and reached completion in 1 h. Ice cooled 2N HCl was added to the solution to produce precipitation. The solution was concentrated followed by filtration to give 18 mg (62 %) **72** as a white solid. $[\alpha]_D^{20}$= +82.8 (c=2, DMSO). ^{1}H NMR ($CDCl_3$/DMSO-d_6): δ 8.67 (br s, 1H), 8.0 (t, 1H, *J* = 6.95Hz), 7.14 (t, 1H, *J* = 6.3Hz), 6.96 (d, 1H, *J* = 9.4Hz), 6.86 (t, 1H, *J* = 7.0Hz), 6.68 (d, 1H, *J* = 7.0Hz), 6.66 (s, 1H), 6.37 (d, 1H, *J* = 7.8Hz), 4.38 (m, 1H), 4.00 (m, 1H), 3.85 (s, 2H), 2.95-3.03 (m, 2H), 2.68 (m, 2H), 1.40 (s, 9H). ^{13}C NMR ($CDCl_3$/DMSO-d_6): δ 173.0, 171.8, 168.8, 155.2, 133.0, 130.1, 129.1, 128.4, 128.2, 127.7, 79.4, 56.1, 52.2, 38.6, 36.7, 31.8, 28.8.

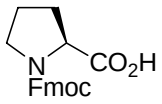

Fmoc- Proline (54).[189] L-Proline (1.00 g, 8.69 mmol) was suspended in CH_2Cl_2 (25 mL) and stirred vigorously. Then TMS-Cl (1.50 mL, 17.4 mmol)was added. The reaction was refluxed for 1 h and cooled in an ice bath. DIEA (3.03 mL, 17.4 mmol) and Fmoc-Cl (1.80 g, 1.96mmol) were then added. The solution was stirred for 20 min at 0 ºC and warmed to rt for 1.5 h. The solution was concentrated and redissolved in 100 mL ether and 100 ml 2.5% $NaHCO_3$. The ether layer was washed with water (2 × 20 mL). The combined aqueous layer was acidified to pH 2 with 1N HCl and extracted with EtOAc (3 × 50 mL), then dried over Na_2SO_4. Recrystallization with EtOAc/Hexane gave 2.2 g (75%) of a white solid. m.p.108-110 ºC (lit 114-145 ºC). ^{1}H NMR ($CDCl_3$): δ 7.76 (m, 2H), 7.59 (m, 2H), 7.40 (m, 2H), 7.31 (m, 2H), 4.66 (s, 1H), 7.31 (m, 2H), 4.06-4.69 (m, 4H), 1.87-2.39 (m, 4H).

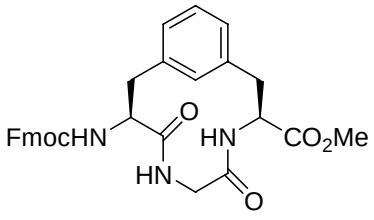

Fmoc Gly HTH-turn mimic 57. Gly mimic **4** (68 mg, 0.16 mmol) and triethylsilane (49 mg, 0.42mmol) were dissolved in CH_2Cl_2 (10 mL), and a cloudy solution was formed. The solution was cooled to 0 ºC in an ice bath, and TFA (3.5 mL) was added to the solution. The reaction was stirred for 30 min and allowed to warm to rt. The solution was concentrated *in vacuo*. The residue was treated with diethyl ether (3 × 5 mL), affording **56** as a white powder. The crude product **56** was dissolved in 10 mL of CH_2Cl_2 and cooled to 0 ºC, followed by addition of Fmoc-Cl (44 mg, 0.17 mmol) and DIEA (0.12 mL, 0.68 mmol). After stirring at rt for 13 h, the reaction was diluted

with 50 mL of CH_2Cl_2 and washed with $NaHCO_3$ (15 mL), citric acid (15 mL), and brine (20 mL). The organic layer was dried over Na_2SO_4, filtered, concentrated *in vacuo*, and purified by flash column chromatography to produce 30 mg (35%) of a white solid. ^{1}H NMR ($CDCl_3$): δ 7.76 (m, 2H), 7.59 (m, 2H), 7.40 (m, 2H), 7.31 (m, 2H), 7.17 (m, 2H), 7.03 (d, 1H, *J* = 6.2Hz), 6.93 (d, 1H, *J* = 7.3Hz), 6.49 (s, 1H), 6.05 (s, 1H), 5.55 (s, 1H), 4.41 (m, 2H), 4.21 (s, 1H), 3.68-4.02 (m, 8H), 3.13- 3.24 (m, 2H), 2.84- 2.96 (m, 2H).

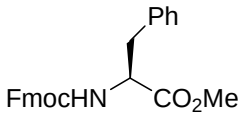

Fmoc-PheOMe 58. To a solution of phenylalanine methyl (0.23 g, 1.0 mmol) ester dissolved in CH_2Cl_2 (10 mL) was added Fmoc-Cl (0.31 g, 1.2 mmol) and TEA (0.24 mL, 1.7 mmol). After stirring at rt for 4 h, the reaction was diluted with 75 mL of CH_2Cl_2 and washed with $NaHCO_3$ (15 mL), citric acid (15 mL), and brine(20 mL). The organic layer was dried over Na_2SO_4, filtered, concentrated *in vacuo*, and purified by flash column chromatography to produce 0.29 g (70%) of a white solid. ^{1}H NMR ($CDCl_3$): δ 7.78 (m, 2H), 7.62 (m, 2H), 7.42 (m, 2H), 7.34 (m, 2H), 7.11- 7.30 (m, 5H), 5.58 (s, 1H), 4.76 (s, 1H), 4.41 (s, 1H), 4.10 (m, 2H), 3.70 (s, 3H), 3.05 (m, 2H).

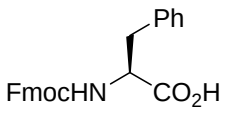

Fmoc-Phe-OH 59. Fmoc-phenylalanine methyl ester **58** (290 mg, 0.70 mmol) was dissolved in MeOH (10 mL) and cooled to 0 ºC in an ice bath. LiOH (0.2N, 7mL) was added dropwise to the mixture. The solution was stirred for 1 h at rt. MeOH was removed *in vacuo* and the residue was washed with ether. The aqueous solution was

acidified with 1N HCl and extracted with EtOAc (3 × 30mL). The EtOAc extract was washed with water (10mL), brine (10 mL), and dried over Na_2SO_4. The solvent was evaporated to produce 110 mg (40%) of a colorless oil. ^{1}H NMR ($CDCl_3$): δ 7.78 (m, 2H), 7.63 (m, 2H), 7.42 (m, 2H), 7.34 (m, 2H), 7.15- 7.30 (m, 5H), 5.58 (s, 1H), 4.72 (s, 1H), 4.41 (s, 1H), 4.10 (m, 2H), 3.05 (m, 2H).

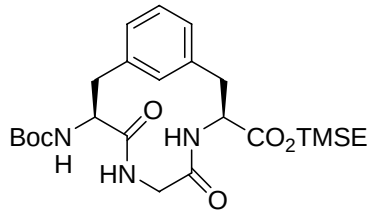

TMSE ester 60. Mimic acid **50** (30 mg, 0.076 mmol) was dissolved in CH_2Cl_2 (10 mL). The solution was cooled down to 0°C in an ice bath, followed by addition of TMSE alcohol (50mg, 0.36 mmol), EDC (29 mg, 0.090 mmol), and DMAP (1mg, 0.007 mmol). The reaction was stirred at r.t for 14 h. The solution was concentrated and then the residue was dissolved in EtOAc (20 mL). The solution was washed with 10% citric acid (2 × 10 mL), $NaHCO_3$ (10 mL), water (10 mL), brine (20 mL), dried over $MgSO_4$, and concentrated *in vacuo*. The residue was purified by chromatography to produce 15 mg (40%) of a white powder. ^{1}H NMR ($CDCl_3$): δ 6.85-7.26 (m, 5H), 4.74 (s, 1H), 4.27 (m, 3H), 3.22 (s, 2H), 2.87 (s, 2H), 1.46 (s, 9H), 1.08 (m, 2H), 0.07 (s, 9H). HRMS calcd. For $C_{24}H_{38}O_3N_6Si$ (MH^+) *m/z* = 492.6695, found *m/z* = 492.6677.

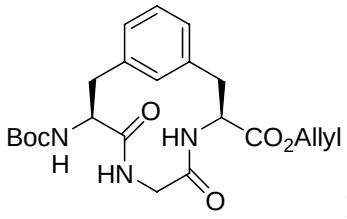

Boc mimic allyl ester 62. Mimic acid **50** (80 mg, 0.02 mmol) was dissolved in THF (10 mL). The solution was cooled to 0 °C in an ice bath, followed by addition of allyl alcohol (12 mg, 0.20 mmol), EDC (58 mg, 0.030 mmol) and DMAP (2.4 mg, 0.0020 mmol). The reaction was stirred at r.t for 16 h. The solution was concentrated and then residue was dissolved in EtOAc (20 mL). The solution was washed with NH_4Cl (2 × 10 mL), $NaHCO_3$ (10 mL), water (10 mL), brine (20 mL), dried on $MgSO_4$, and concentrated *in vacuo*. The residue was purified by chromatography, producing 44 mg (50 %) of a colorless oil. ^1H NMR ($CDCl_3$): δ 7.95 (s, 1H), 6.73-7.11 (m, 4H), 5.88 (m, 1H), 5.20-5.32 (m, 2H), 4.55-4.68 (m, 2H), 3.64 (s, 1H), 3.23 (m, 2H), 2.97 (m, 2H), 1.33 (s, 9H). ^{13}C NMR ($CDCl_3$): δ 171.6, 170.6, 169.0, 155.2, 135.9, 133.2, 131.9, 128.5, 128.2, 127.3, 119.0, 79.1, 65.8, 43.7, 38.6, 36.6, 28.6.

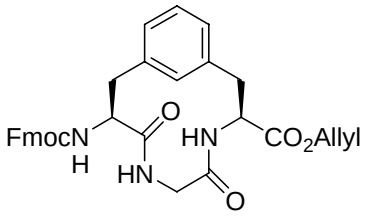

Fmoc mimic allyl ester 63. Boc mimic allyl ester **62** (60 mg, 0.13 mmol) was dissolved in CH_2Cl_2 (10 mL), and a cloudy solution was formed. The solution was cooled to 0 °C in an ice bath, and TFA (5.0 mL) was added to the solution. The reaction was allowed to warm to rt and stirred for 30 min. The solution was concentrated *in vacuo*. The excess TFA was removed with diethyl ether (3 × 5 mL), producing a white powder. Without further purification, the crude product was dissolved

in 10 mL of CH_2Cl_2 and cooled to 0 °C in an ice bath, followed by addition of Fmoc-Cl (67mg, 0.26 mmol) and DIEA (51 mg, 0.40 mmol). After stirring at rt for 18 h, the reaction was diluted with 50 mL of CH_2Cl_2 and washed with $NaHCO_3$ (15 mL), citric acid (15 mL), and brine (20 mL). The organic layer was dried over Na_2SO_4, filtered, concentrated, and purified by flash column chromatography to give 55 mg (74%) of a white solid. ^1H NMR ($CDCl_3$): δ 6.81-8.16 (m, 13H), 5.90-6.36 (m, 1H), 5.25-5.36 (2H), 3.71-5.00 (m, 9H,) 2.76-3.40 (m, 4H). HRMS calcd. For $C_{32}H_{32}O_3N_6$ (MH^+) *m/z* = 554.2291, found *m/z* = 554.2304.

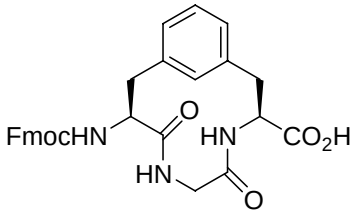

Fmoc mimic acid 52. $Pd(PPh_3)_4$ (4.0 mg, 0.036 mmol) was added under N_2 at rt to a solution of **63** (10 mg, 0.018 mmol) in THF (10 mL), followed by the addition of dimedone (25 mg, 0.18 mmol). The THF was removed *in vacuo* after 30 min. The residue was acidified to pH 2 with 2N HCl, and the solution was extracted with EtOAc (3 × 20 mL). The organic layer was dried over Na_2SO_4, filtered, concentrated, and purified by flash column chromatography to produce 3 mg (20%) of a yellow oil. The substance obtained showed a poor solubility toward general NMR solvents, such as $CDCl_3$ and DMSO. HRMS calcd. For $C_{29}H_{28}O_3N_6$ (MH^+) *m/z* = 514.1978, found *m/z* = 514.1954.

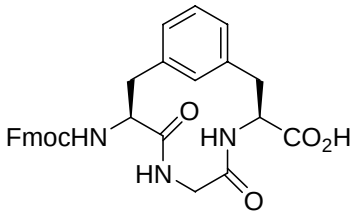

Fmoc mimic acid 52. Boc mimic acid **50** (72 mg, 0.18 mmol) was dissolved in 4N HCl in dioxane (6 mL). The reaction was cooled to 0 ºC in an ice bath. The reaction was followed by TLC (60:10:3:4, EtOAc/Pyridine/AcOH/H_2O, ninhydrin stain) and completed in 1 h. The solution was concentrated *in vacuo* and no further purification was attempted. The crude product **73** was dissolved in 10 mL of CH_2Cl_2 and cooled to 0 ºC, followed by the addition of Fmoc-Cl (46 mg, 0.18 mmol) and DIEA (67 mg, 0.45 mmol). After stirring at rt for 12h, the reaction was concentrated by evaporation. The residue was diluted with 10 mL of EtOAc and acidified to pH 1 with 1N HCl. The precipitate was collected by filtration and washed with water, hexane, and EtOAc, affording a white solid (64 mg) 70%. ^{1}H NMR ($CDCl_3$/DMSO-d_6): δ 13.76 (s, 1H), 8.75 (s, 1H), 8,52 (s, 1H), 7.89 (m, 2H), 7.75 (m, 2H), 6.66-7.73 (m, 12H), 3.84-4.52 (m, 7H), 2.70-3.03 (m, 4H). ^{13}C NMR ($CDCl_3$): δ 172.9, 171.3, 168.8, 155.9, 144.5, 141.4, 137.0, 132.8, 128.9, 128.3, 127.7, 125.5, 120.8, 65.9, 60.3, 56.6, 52.3, 47.3, 43.7, 36.8. HRMS calcd. For $C_{29}H_{28}O_3N_6$ (MH^+) *m/z* = 514.1978, found *m/z* = 514.1964.

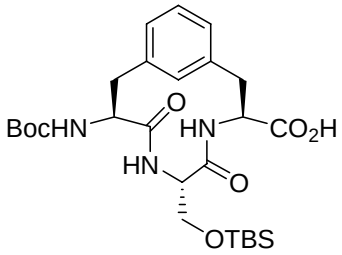

Seine HTH-turn mimic acid 67. Cyclized peptide **33** (50 mg, 0.090 mmol) was dissolved in a mixture of MeOH/THF (20 mL, 1:1). The solution

was heated to help the solid dissolve. The reaction was cooled to 0 ºC and NaOH (1N, 0.12 mL) was added dropwise. The reaction was followed by TLC (120:5:1 CHCl3/MeOH/AcOH, ninhydrin stain) and completed in 1 h. Ice cooled 2N HCl was added to the solution to produce precipitation. The solution was concentrated followed by filtration to give 25 mg (50 %) of **67** as a white solid. ^{1}H NMR ($CDCl_3$/DMSO-d_6): δ 6.40-7.30 (m, 4H), 4.40 (d, 2H), 2.35-4.00 (m, 8H), 1.37 (s, 9H), 0.83 (s, 2H), 0.04 (m, 9H). ^{13}C NMR ($CDCl_3$/DMSO-d_6): δ 178.0, 176.2, 174.6, 160.0, 142.6, 141.2, 137.3. 133.6, 130.4, 83.4, 67.3, 61.3, 58.9, 57.7, 44.4, 40.0, 36.0, 33.8, 31.1, 23.4,0.0. HRMS calcd. For $C_{26}H_{42}O_7N_3Si$ (MH^+) *m/z* = 536.2792, found *m/z* = 536.2774.

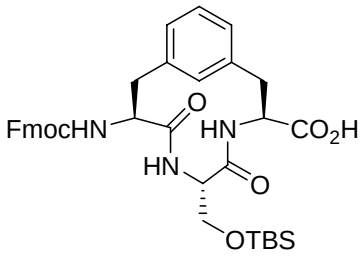

Serine mimic acid 69. Serine HTH-turn mimic acid **67** (25 mg, 0.045 mmol) was dissolved in 4M HCl in dioxane (5 mL), the solution was stirred for 1 h. The solution was concentrated under pressure. The residue was treated with diethyl ether (3 × 5 mL) to produce a white powder **68** (HRMS calcd. For $C_{21}H_{33}O_5N_3Si$ (MH^+) *m/z* = 437.2346, found *m/z* = 437.2368). The amino acid **68** was treated by Fmoc-Cl (23 mg, 0.09 mmol) and DIEA (33mg, 0.26 mmol). The reaction was stirred for 14 h, followed by concentration. The residue was diluted with 10 mL of EtOAc and acidified to pH 1 with 1N HCl. The organic layer was dried over Na_2SO_4, filtered, concentrated *in vacuo*, and purified by flash column chromatography to give 10 mg (17%) of a white powder. ^{1}H NMR ($CDCl_3$/DMSO-d_6): δ 6.85-8.24 (m, 14H), 3.66-4.67 (m, 6H), 2.64-

3.05 (m, 4H), 0.78 (s, 9H), 0.04 (s, 6H). ^{13}C NMR ($CDCl_3$): δ 173.0, 171.0, 169.7, 155.6, 144.5, 141.3, 137.7, 136.1, 132.3, 128.2, 127.6, 125.9, 120.7, 66.2, 62.3, 60.6, 55.0, 47.2, 30.6, 26.3, 19.4, 18.4, -4.8. HRMS calcd. HRMS calcd. For $C_{36}H_{44}O_7N_3Si$ (MH^+) *m/z* = 658.2949, found *m/z* = 658.2972.

Chapter 6
Achievements of the research and future work

A new histone deacetylase (HDAC) inhibitor **1** was designed, synthesized, and assayed. The design of the new HDAC inhibitor **1** was based on the cyclic HTH-turn turn mimic, to which a hydroxamic acid motif was fused through an aliphatic chain. The results of the computational analysis demonstrated HDAC inhibitor **1** could bind to the active site with a conformationally preference. The synthesis of the HDI employed stereoselective hydrogenation and macrocyclization. The fluorescent HDAC assay demonstrated HDAC inhibitor **1** provided significant inhibitory activity against HDACs with an IC_{50} value of 46 ± 15 nM. HDAC inhibitor **1** also inhibited the activity of a specific HDAC, HDAC8 with an IC_{50} value of 208 ± 20 nM. The high HDAC inhibitory activity of **1** demonstrates the specific hydrophobic interactions between the HDIs and the rim region of HDACs play an important role during the formation of the HDAC-inhibitor complexes. A new class of HDIs containing the cyclic turn mimic as the rim recognition component will be synthesized and assayed.

Two HTH-turn mimics, Gly HTH-turn mimic and Ser HTH-turn mimic were synthesized by stereoselective hydrogenation and macrocyclization starting from unnatural amino acids in yields of 33% and 12%, respectively. The synthesis of Fmoc protected Gly HTH-turn mimic and Ser HTH-turn mimic were accomplished by employing 4M HCl to deprotect the Boc protecting group. The synthesis of Fmoc protected HTH-turn mimics allowed us to attempt incorporation of mimic compounds

into HTH peptides using Fmoc chemistry on solid phase. The incorporation of the turn mimics into the peptides produced poor results either by sequential elongation or by segment condensation. This may result from the poor reactivity of the turn mimics on solid phase. The HTH-turn mimics will be transformed into acyl fluorides to solve the problem. Incorporating sidechain containing amino acids into the cyclic HTH-turn mimics will be attempted to increase the solubility of the modified HTH peptides.

References

1. Egger, G.; Liang, G.; Aparicio, A.; Jones, P. A., Epigenetics in human disease and prospects for epigenetic therapy *Nature* **2004,** 429, 457-463
2. Luger, K.; Mader, A. W.; Richmond, R. K.; Sargent, D. R.; Richmond, T. J., Crystal structure of the nucleosome core particle at 2.8 Å resolution. *Nature* **1997,** 389, 251-260.
3. Wolffe, A. P.; Guschin, D., Review: chromatin structural features and targets that regulate transcription. *J. Struct. Biol.* **2000,** 129, 102-122.
4. Lusser, A., Acetylated, methylated, remodeled: chromatin states for gene regulation *Curr. Opin. Plant Biol.* **2002,** 5, 437-443
5. Li, G.; Chandrasekharan, M. B.; Wolffe, A. P.; Hall, T. C., Chromatin structure and phaseolin gene regulation. *Plant Mol. Biol.* **2001,** 46, 121-129.
6. Jenuwein, T.; Allis, C. D., Translating the histone code. *Science* **2001,** 293, 1074-1080.
7. Shiio, Y.; Eisenman, R. N., Histone sumoylation is associated with transcriptional repression. *Proc. Natl. Acad. Sci. USA* **2003,** 100, 13225-13230.
8. Strahl, B. D.; Allis, C. D., The language of covalent histone modifications. *Nature* **2000,** 403, 41-45.
9. Monneret, C., Histone deacetylase inhibitors. *Eur. J. Med. Chem.* **2005,** 40, 1–13.
10. Ruijter, A. J. M. d.; Gennip, A. H. v.; Caron, H. N.; Kemp, S.; Kuilenburg, A. B. P. v., Histone deacetylases (HDACs): characterization of the classical HDAC family. *Biochem J.* **2003,** 370, 737–749.
11. Roth, S. Y.; Denu, J. M.; Allis, C. D., Histone acetyltransferases. *Annu. Rev. Biochem.* **2001,** 120, 81-120
12. Carrozza, M. J.; Utley, R. T.; Workman, J. L.; Cote, J., The diverse functions of histone acetyltransferase complexes. *Trends in Genetics* **2003,** 19, 321-328.
13. Chen, H.; Tini, M.; Evans, R. M., HATs on and beyond chromatin. *Curr. Opin. Cell. Biol.* **2001,** 13, 218-224.
14. Mei, S.; Ho, A. D.; Majlknecht, U., Role of histone deacetylase inhibitors in the treatment of cancer (Review). *Int. J. Oncol.* **2004,** 25, 1509-1519.
15. Sterner, D. E.; Berger, S. L., Acetylation of histones and transcription-related factors. *Microbiol. Mol. Biol. Rev.* **2000,** 64, 435–459.
16. Marks, P.; Rifkind, R. A.; Richon, V. M.; Breslow, R.; Miller, T.; Kelly, W. K., Histone deacetylases and cancer: causes and therapies. *Nat. Rev. Cancer* **2001,** 1, 194–202.
17. Galasinski, S. C.; Resing, K. A.; Goodrich, J. A.; Ahn, N. G., Phosphatase inhibition leads to histone deacetylase 1/2 phosphorylation and disruption of co-repressor interactions. *J. Biol. Chem.* **2002,** 277, 19618-19626.
18. Pflum, M. K.; Tong, J. K.; Lane, W. S.; Schreiber, S. L., Histone deacetylase 1 phosphorylation promotes enzymatic activity and complex formation. *J. Biol. Chem.* **2001,** 276, 47733-47741.
19. Juan, L. J.; Shia, W. J.; Chen, M. H., Histone deacetylases specifically down-regulate p53- dependent gene activation. *J. Biol. Chem.* **2000,** 275, 20436-20443.

20. Boyes, J.; Byfield, P.; Nakatani, Y.; Ogryzko, V., Regulation of activity of the transcription factor GATA-1 by acetylation. *Nature* **1998,** 396, 594-598.
21. Luo, J.; Li, M.; Tang, Y.; Laszkowska, M.; Roeder, R. G.; Gu, W., Acetylation of p53 augments its site-specific DNA binding both in vitro and in vivo. *Proc. Natl. Acad. Sci. USA* **2004,** 101, 2259-2264.
22. Taunton, J.; Hassig, C. A.; Schreiber, S. L., A mammalian histone deacetylase related to the yeast transcriptional regulator Rpd3p. *Science* **1996,** 272, 408-411.
23. Gray, S. G.; Ekstrom, T. J., The human histone deacetylase family. *Exp. Cell Res.* **2001,** 262, 75-83.
24. Verdin, E.; Dequiedt, F.; Kasler, H. G., Class II histone deacetylases: versatile regulators. *Trends in Genetics* **2003,** 19, 286-293.
25. Johnstone, R. W., Histone-deacetylase inhibitors: novel drugs for the treatment of cancer. *Nature Rev. Drug Discovery* **2002,** 1, 287-299
26. Khochbin, S.; Wolffe, A. P., The origin and utility of histone deacetylases. *FEBS Lett.* **1997,** 419, 157-160.
27. Hassig, C. A.; Fleischer, T. C.; Billin, A. N.; Schreiber, S. L.; Ayer, D. E., Histone deacetylase activity is required for full transcriptional repression by mSin3A. *Cell* **1997,** 89, 341-347.
28. Vidal, M.; Gaber, R. F., RPD3 encodes a second factor required to achieve maximum positive and negative transcriptional states in Saccharomyces cerevisiae. *Mol. Cell. Biol.* **1991,** 11, 6317-6327.
29. Jackson, J. C.; Lopes, J. M., The yeast UME6 gene is required for both negative and positive transcriptional regulation of phospholipid biosynthetic gene expression. *Nucleic Acids Res.* **1996,** 24, 1322-1329.
30. Rossi, V.; Hartings, H.; Motto, M., Identification and characterisation of an RPD3 homologue from maize (Zea mays L.) that is able to complement an rpd3 null mutant of Saccharomyces cerevisiae. *Mol. Gen. Genet.* **1998,** 258, 288-296.
31. Wade, P. A., Transcriptional control at regulatory checkpoints by histone deacetylases: molecular connections between cancer and chromatin. *Hum. Mol. Gen.* **2001,** 10, 693-698.
32. You, A.; Tong, J. K.; Grozinger, C. M.; Schreiber, S. L., CoREST is an integral component of the CoREST-human histone deacetylase complex. *Proc. Natl. Acad. Sci. USA* **2001,** 98, 1454-1458.
33. Humphrey, G. W.; Wang, Y.; Russanova, V. R.; Hirai, T.; Qin, J.; Nakatani, Y.; Howard, B. H., Stable histone deacetylase complexes distinguished by the presence of SANT domain proteins CoREST/kiaa0071 and Mta-L1. *J. Biol. Chem.* **2001,** 276, 6817-6824.
34. Heinzel, T.; Lavinsky, R. M.; Mullen, T. M.; Soderstrom, M.; Laherty, C. D.; Torchia, J.; Yang, W. M.; Brard, G.; Ngo, S. D.; Davie, J. R., A complex containing N-CoR, mSin3 and histone deacetylase mediates transcriptional repression. *Nature* **1997,** 387, 43-48.
35. Ashburner, B. P.; Westerheide, S. D.; Baldwin, A. S. J., The p65 (RelA) subunit of NF-kappaB interacts with the histone deacetylase (HDAC) corepressors HDAC1 and HDAC2 to negatively regulate gene expression. *Mol. Cell. Biol.* **2001,** 21, 7065-7077.

36. Zhang, J.; Kalkum, M.; Chait, B. T.; Roeder, R. G., The *N*-CoR-HDAC3 nuclear receptor corepressor complex inhibits the JNK pathway through the integral subunit GPS2. *Mol. Cell* **2002,** 9, 611-623.
37. Nicolas, E.; Ait-Si-Ali, S.; Trouche, D., The histone deacetylase HDAC3 targets RbAp48 to the retinoblastoma protein. *Nucleic Acids Res.* **2001,** 29, 3131-3136.
38. Gregoretti, I.; Lee, Y.-M.; Goodson, H. V., Molecular evolution of the histone deacetylase family: functional implications of phylogenetic analysis. *J. Mol. Biol.* **2004,** 338, 17-31.
39. Gantt, S. L.; Gattis, S. G.; Fierke, C. A., Catalytic activity and inhibition of human histone deacetylase 8 is dependent on the identity of the active site metal Ion. *Biochemistry* **2006,** 45, 6170-6178.
40. Somoza, J. R.; Skene, R. J.; Katz, B. A.; Mol, C.; Ho, J. D.; Jennings, A. J.; Luong, C.; Arvai, A.; Buggy, J. J.; Chi, E., Structural snapshots of human HDAC8 provide insights into the class I histone deacetylases. *Structure* **2004,** 12, 1325-1334.
41. Grozinger, C. M.; Schreiber, S. L., Regulation of histone deacetylase 4 and 5 and transcriptional activity by 14-3-3-dependent cellular localization. *Proc. Natl. Acad. Sci. USA* **2000,** 97, 7835-7840.
42. Muslin, A. J.; Xing, H., 14-3-3 proteins: regulation of subcellular localization by molecular interference. *Cell. Signal.* **2000,** 12, 703-709.
43. Fischle, W., Enzymatic activity associated with class II HDACs is dependent on a multiprotein complex containing HDAC3 and SMRT/N-CoR. *Mol. Cell* **2000,** 9, 45-57.
44. Verdel, A., Identification of a new family of higher eukaryotic histone deacetylases. Coordinate expression of differentiation-dependent chromatin modifiers. *J. Biol. Chem.* **1999,** 274, 2440-2445.
45. Tong, J. J.; Liu, J.; Bertos, N. R.; Yang, X.-J., Identification of HDAC10, a novel class II human histone deacetylase containing a leucine-rich domain. *Nucleic Acids Res.* **2002,** 30, 1114-1123.
46. Guardiola, A. R.; Yao, T. P., Molecular cloning and characterization of a novel histone deacetylase HDAC10. *J. Biol. Chem.* **2002,** 277, 3350-3356.
47. Furumai, R.; Komatsu, Y.; Nishino, N.; Khochbin, S.; Yoshida, M.; Horinouchi, S., Potent histone deacetylase inhibitors built from trichostatin A and cyclic tetrapeptide antibiotics including trapoxin. *Proc. Natl. Acad. Sci. USA* **2001,** 98, 87-92.
48. Fischer, D. D.; Cai, R.; Bhatia, U.; Asselbergs, F. A.; Song, C.; Terry, R.; Trogani, N.; Widmer, R.; Atadja, P.; Cohen, D., Isolation and characterization of a novel class II histone deacetylase, HDAC10. *J. Biol. Chem.* **2002,** 277, 6656-6666.
49. McLaughlin, F.; Thangue, N. B. L., Histone deacetylase inhibitors open new doors in cancer therapy. *Biochem. Pharmacol.* **2004,** 68, 1139-1144.
50. Johnstone, R. W.; Licht, J. D., Histone deacetylase inhibitors in cancer therapy: is transcription the primary target? *Cancer Cell* **2003,** 4, 13-18.
51. Drummond, D. C.; Noble, C. O.; Kirpotin, D. B., Clinical development of histone deacetylase inhibitors as anticancer agents. *Annu. Rev. Pharmaco.l Toxicol.* **2005,** 45, 495-528.
52. Marks, P. A.; Richon, V. M.; Breslow, R.; Rifkind, R. A., Histone deacetylase inhibitors as new cancer drugs. *Curr. Opin. Oncol.* **2001,** 13, 477-483.
53. Gibbons, R. J., Histone modifying and chromatin remodelling enzymes in cancer and dysplastic syndromes. *Hum. Mol. Genet.* **2005,** 14, 85-92.

54. Gayther, S. A.; Batley, S. J.; Linger, L.; Bannister, A.; Thorpe, K.; Chin, S. F.; Daigo, Y.; Russell, P.; Wilson, A.; Sowter, H. M.; Delhanty, J. D.; Ponder, B. A.; Kouzarides, T.; Caldas, C., Mutations truncating the EP300 acetylase in human cancers. *Nat. Genet.* **2000,** 24, 300-303.
55. Borrow, J.; Jr, V. P. S.; Andresen, J. M.; Becher, R.; Behm, F. G.; Chaganti, R. S. K.; Civin, C. I.; Disteche, C.; Dubé, I.; Frischauf, A. M.; Horsman, D.; Mitelman, F.; Volinia, S.; Watmore, A. E.; Housman, D. E., The translocation t(8;16)(p11;p13) of acute myeloid leukaemia fuses a putative acetyltransferase to the CREB-binding protein. *Nature Genetics* **1996,** 14, 33 - 41.
56. Rowley, J. D.; Reshmi, S.; Sobulo, O.; Musvee, T.; Anastasi, J.; Raimondi, S.; Schneider, N. R.; C., B. J.; Cantu, E. S.; Schlegelberger, B.; Behm, F.; Doggett, N. A.; Borrow, J.; Zeleznik-Le, N., All patients with the T(11;16)(q23;p13.3) that involves MLL and CBP have treatment-related hematologic disorders. *Nat. Genet.* **1996,** 14, 33-41.
57. Cress, W. D.; Seto, E., Histone deacetylases, transcriptional control, and cancer. *J. Cell. Physiol.* **2000,** 184, 1-16.
58. He, L. Z.; Guidez, F.; Tribioli, C.; Peruzzi, D.; Ruthardt, M.; Zelent, A.; Pandolfi, P. P., Distinct interactions of PML-RARalpha and PLZF-RARalpha with co-repressors determine differential responses to RA in APL. *Nat. Genet.* **1998,** 18, 126-135.
59. Minucci, S.; Nervi, C.; Lo, C. F.; Pelicci, P. G., Histone deacetylases: a common molecular target for differentiation treatment of acute myeloid leukemias? *Oncogene* **2001,** 20, 3110-3115.
60. Finnin, M. S.; Donigian, J. R.; Cohen, A.; Richon, V. M.; Rifkind, R. A.; Marks, P. A.; Breslow, R.; Pavletich, N. P., Structures of a histone deacetylase homologue bound to the TSA and SAHA inhibitors. *Nature* **1999,** 401, 188 - 193.
61. Vannini, A.; Volpari, C.; Filocamo, G.; Casavola, E. C.; Brunetti, M.; Renzoni, D.; Chakravarty, P.; Paolini, C.; Francesco, R. D.; Steinku, P. G.; Marco, S. D., Crystal structure of a eukaryotic zinc-dependent histone deacetylase, human HDAC8, complexed with a hydroxamic acid inhibitor. *Proc. Natl. Acad. Sci. USA* **2004,** 201, 15064–15069.
62. Christianson, D. W.; Lipscomb, W. N., Carboxypeptidase A. *Acc. Chem. Res.* **1989,** 22, 62.
63. Kapustin, G. V.; Fejer, G.; Gronlund, J. L.; McCafferty, D. G.; Seto, E.; Etzkorn, F. A., Phosphorus-based SAHA analogues as histone deacetylase inhibitors. *Org. Lett.* **2003,** 5, 3053.
64. Bartlett, P. A.; Marlowe, C. K., Phosphonamidates as transition-state analog inhibitors of thermolysin *Biochemistry* **1983,** 22, 4618-4624.
65. Corminboeuf, C. m.; Hu, P.; Tuckerman, M. E.; Zhang, Y., Unexpected deacetylation mechanism suggested by a density functional theory QM/MM study of histone-deacetylase-like protein. *J. Am. Chem. Soc.* **2006,** 128, 4530-4531.
66. Wang, D.-F.; Wiest, O.; Helquist, P.; Lan-Hargest, H.-Y.; Wiech, N. L., On the function of the 14 Å long internal cavity of histone deacetylase-like protein: implications for the design of histone deacetylase inhibitors. *J. Med. Chem.* **2004,** 47, 3409-3417.
67. Dashwood, R. H.; Myzak, M. C.; Ho, E., Dietary HDAC inhibitors: time to rethink weak ligands in cancer chemoprevention. *Carcinogenesis* **2006,** 27 344-349.
68. Krämer, O. H.; Göttlicher, M.; Heinzel, T., Histone deacetylase as a therapeutic target. *Trends Endocrinol. Metabol.* **2001,** 12, 294-300.

69. Sambucetti, L. C.; Fischer, D. D.; Zabludoff, S.; Kwon, P. O.; Chamberlin, H.; Trogani, N.; Xu, H.; Cohen, D., Histone deacetylase inhibition selectively alters the activity and expression of cell cycle proteins leading to specific chromatin acetylation and antiproliferative effects. *J. Biol. Chem.* **1999,** 274, 34940-34947.
70. Minucci, S.; Pelicci, P. G., Histone deacetylase inhibitors and the promise of epigenetic (and more) treatments for cancer. *Nature Rev. Cancer* **2006,** 6, 38-51.
71. Kelly, W. K.; O'Connor, O. A.; Marks, P., A., Histone deacetylase inhibitors: from target to clinical trials. *Expert Opin. Investig. Drugs* **2002,** 11, 1695-1713.
72. Marks, P. A., Histone deacetylase inhibitors: inducers of differentiation or apoptosis of transformed cells. *J. Natl. Cancer Inst.* **2000,** 92, 1210-1216.
73. Deroanne, C. F.; Bonjean, K.; Servotte, S.; Devy, L.; Colige, A.; Clausse, N.; Blacher, S.; Verdin, E.; Foidart, J. M.; Nusgens, B. V.; Castronovo, V., Histone deacetylases inhibitors as anti-angiogenic agents altering vascular endothelial growth factor signaling. *Oncogene* **2002,** 21, 427-436.
74. Miller, T. A.; Witter, D. J.; Belvedere, S., Histone Deacetylase Inhibitors. *J. Med. Chem.* **2003,** 46, 5097-5116.
75. Yoshida, M.; Kijima, M.; Akita, M.; Beppu, T., Potent and specific inhibition of mammalian histone deacetylase both in vivo and in vitro by trichostatin A. *J. Biol. Chem.* . **1990,** 265, 17174.
76. Richon, V. M.; Emiliani, S.; Verdin, E.; Webb, Y.; Breslow, R.; Rifkind, R. A.; Marks, P. A., A class of hybrid polar inducers of transformed cell differentiation inhibits histone deacetylases. *Proc. Natl. Acad. Sci. USA* **1998,** 95, 3003-7.
77. Ohtani, M.; Matsuura, T.; Shirahase, K.; Sugita, K., (2*E*)-5-[3-[(Phenylsulfonyl)amino]phenyl]-pent-2-en-4-ynohydroxamic acid and its derivatives as novel and potent inhibitors of ras transformation. *J. Med. Chem.* **1996,** 39, 2871-2873.
78. Su, G. H.; Sohn, T. A.; Ryu, B.; Kern, S. E. A., A novel histone deacetylase inhibitor identified by high-throughput transcriptional screening of a compound library. *Cancer Res.* **2000,** 60, 3137-3142.
79. Ueda, H.; Nakajima, H.; Hori, Y.; Fujita, T.; Nishimura, M.; Goto, T.; Okuhara, M., FR901228, a novel antitumor bicyclic depsipeptide produced by Chromobacterium violaceum no. 968. *J. Antibiot.* **1994,** 47, 301-310.
80. Marshall, J. L.; Rizvi, N.; Kauh, J.; Dahut, W.; Figuera, M., A phase I trial of depsipeptide (FR901228) in patients with advanced cancer. *J. Exp. Ther. Oncol.* **2002,** 2, 325-332.
81. Furumai, R.; Matsuyama, A.; Kobashi, N.; Lee, K. H.; Nishiyama, M., FK228 (depsipeptide) as a natural prodrug that inhibits class I histone deacetylases. *Cancer Res.* **2002,** 62, 4916-4921.
82. Phiel, C. J.; Zhang, F.; Huang, E. Y.; Guenther, M. G.; Lazar, M. A.; Klein, P. S., Histone deacetylase is a direct target of valproic acid, a potent anticonvulsant, mood stabilizer, and teratogen. *J. Biol. Chem.* **2001,** 276, 36734-36741.
83. Boivin, A. J.; Momparler, L. F.; Hurtubise, A.; Momparler, R. L., Antineoplastic action of 5-aza-2-deoxycytidine and phenylbutyrate on human lung carcinoma cells. *Anticancer Drugs* **2002,** 13, 869-874.
84. Suzuki, T.; Ando, T.; Tsuchiya, K.; Fukazawa, N.; Saito, A., Synthesis and histone deacetylase inhibitory activity of new benzamide derivatives. *J. Med. Chem.* **1999,** 42, 3001-3003.

85. El-Beltagi, H. M.; Martens, A. C. M.; Lelieveld, P.; Haroun, E. A.; Hagenbeek, A., A. Acetyldinaline: a new oral cytostatic drug with impressive differential activity against leukemic cells and normal stem cellsspreclinical studies in a relevant rat model for human acute myelocytic leukemia. *Cancer Res.* **1993,** 53, 3008-3014.
86. Frey, R. R.; Wada, C. K.; Garland, R. B.; Curtin, M. L.; Michaelides, M. R.; Li, J.; Pease, L. J.; Glaser, K. B.; Marcotte, P. A.; Bouska, J. J., Trifluoromethyl ketones as inhibitors of histone deacetylase. *Bioorg Med Chem Lett* **2002,** 12, 3443-3447.
87. Suzuki, T.; Miyata, N., Rational design of non-hydroxamate histone deacetylase inhibitors *Mini Rev. Med. Chem.* **2006,** 6, 515-526.
88. Gennaro, E. D.; Bruzzese, F.; Caraglia, M.; Abruzzese, A.; Budillon, A., Acetylation of proteins as novel target for antitumor therapy: Review article. *Amino Acids* **2004,** 26, 435-441.
89. Van Lint, C.; Emiliani, S.; Verdin, E., The expression of a small fraction of cellular genes is changed in response to histone hyperacetylation. *Gene. Exp.* **1996,** 5, 245-253.
90. Chambers, A. E.; Banerjee, S.; Chaplin, T.; Dunne, J.; Debernardi, S.; Joel, S. P.; Young, B. D., Histone acetylation-mediated regulation of genes in leukaemic cells. *Eur. J. Cancer* **2003,** 39, 1165-1175.
91. Dokmanovic, M.; Marks, P. A., Prospects: Histone Deacetylase Inhibitors. *J. Cell. Biochem.* **2005,** 96, 293-304
92. Gu, W.; Roeder, R. G., Activation of p53 sequence-specific DNA binding by acetylation of the p53 C-terminal domain. *Cell* **1997,** 90, 595-606.
93. Munshi, N.; Merika, M.; Yie, J.; Senger, K.; Chen, G.; Thanos, D., Acetylation of HMG I(Y) by CBP turns off IFN beta expression by disrupting the enhanceosome. *Mol. Cell* **1998,** 2, 457-467.
94. el-Deiry, W. S.; Tokino, T.; Velculescu, V. E.; Levy, D. B.; Parsons, R.; Trent, J. M.; Lin, D.; Mercer, W. E.; Kinzler, K. W.; Vogelstein, B., WAF1, a potential mediator of p53 tumor suppression. *Cell* **1993,** 75, 817-825.
95. Kim, Y. B.; Lee, K. H.; Sugita, K.; Yoshida, M.; Horinouchi, S., Oxamflatin is a novel antitumor compound that inhibits mammalian histone deacetylase. *Oncogene* **1999,** 18, 2461-2470.
96. Peart, M. J.; Tainton, K. M.; Ruefli, A. A.; Dear, A. E.; Sedelies, K. A.; O'Reilly, L. A.; Waterhouse, N. J.; Trapani, J. A.; Johnston, R. W., Novel mechanisms of apoptosis induced by histone deacetylase inhibitors. *Cancer Res.* **2003,** 63, 4460-4471.
97. Nakamura, M.; Saito, H.; Ebinuma, H.; Wakabayashi, K.; Saito, Y.; Takagi, T.; Nakamoto, N.; Ishii, H., Reduction of telomerase activity in human liver cancer cells by a histone deacetylase inhibitor. *J. Cell. Physiol.* **2001,** 187, 392-401.
98. Jaboin, J.; Wild, J.; Hamidi, H.; Khanna, C.; Kim, C. J.; Robey, R.; Bates, S. E.; Thiele, C. J., MS-275, an inhibitor of histone deacetylase, has marked in vitro and in vivo antitumor activity against pediatric solid tumors. *Cancer Res.* **2002,** 62, 6108-6115.
99. Travins, J. M.; Etzkorn, F. A., Design and enantioselective synthesis of a peptidomimetic of the turn in the helix-turn-helix DNA-binding protein motif. *J. Org. Chem.* **1997,** 62, 8387-8393.
100. Etzkorn, F. A.; Travins, J. M., Stereoselective deuterium labeling of proR-protons in the NMR structure determination of a helix-turn-helix turn peptide mimic *J. Peptide Res.* **2000,** 55, 436-446.

101. Kortenaar, P. B. W. T.; Dijk, B. G. V.; Peeters, J. M.; Raaben, B. J.; Tesser, P. J. H. M. A. G. I., Rapid and efficient method for the preparation of Fmoc- amino acids starting from 9-fluorenylmethanol. *Int. J. Peptide Protein Res.* **1986,** 27, 398-400.
102. Olsen, R. K.; Ramasamy, K., Synthesis of retrohydroxamate analogs of the microbial iron-transport agent ferrichrome. *J. Org. Chem.* **1985,** 50, 2264-2271.
103. Acton, J. J.; Jones, A. B., Synthesis and derivatization of a versatile α-substituted lactam dipeptide isostere. *Tetrahedron Lett.* **1996,** 37, 4319-4322.
104. Chevallet, P.; Garrouste, P.; Malawska, B.; Martinez, J., Facile synthesis of *tert*-butyl ester of N-protected amino acids with *tert*-butyl bromide. *Tetrahedron Lett.* **1993,** 34, 7409-7412.
105. Ben-Ishai, D., Reaction of acylamino acids with paraformaldehyde. *J. Am. Chem. Soc.* **1957,** 79, 5736-5738.
106. Abell, A. D.; Taylor, J. M., Synthesis of cyclic acylated enamino ester dipeptide analogs via the bromolactonization of a keto acid phosphorane. *J. Org. Chem.* **1993,** 58, 14-15.
107. Goodman, M.; Gantzel, J. Z. P.; Benedetti, E., The stereocontrolled synthesis of orthogonally protected (*R*)--methyltryptophan. *Tetrahedron Lett.* **1998,** 39, 9587-9588.
108. Curran, W. V.; Lenhard, R. H., *N*-Azamonobactams. 2. Synthesis of some *N*-iminoacetic acid and *N*-glycyl analogs. *J. Med. Chem.* **1989,** 32, 1749-1753.
109. Carrasco, M. R.; Brown, R. T.; Serafimova, I. M.; Silva, O., Synthesis of *N*-Fmoc-*O*- (*N*'-Boc-*N*'-methyl)-aminohomoserine, an amino acid for the facile preparation of neoglycopeptides. *J. Org. Chem.* **2003,** 68, 195-197.
110. Friedrich-Bochnitsche, S.; Waldmann, H.; Kunz, H., Allyl esters as carboxy protecting groups in the synthesis of *O*-glycopeptides. *J. Org. Chem.* **1989,** 54, 751-756.
111. Phillips, S. T.; Rezac, M.; Abel, U.; Kossenjans, M.; Bartlett, P. A., "@-Tides": the 1,2-dihydro-3(6H)-pyridinone unit as a β-strand mimic. *J. Am. Chem. Soc.* **2003,** 124, 58-66.
112. Boeckman, R. K.; Perni, J. R. B., Studies directed toward the synthesis of naturally occurring acyltetramic acids. 2. Preparation of the macrocyclic subunit of ikarugamycin. *J. Org. Chem.* **1986,** 51, 5486-5489.
113. Sarabia, F.; Chammaa, S.; Lez-Herrera, F. J., A macrolactonization approach to the stevastelins. *Tetrahedron Lett.* **2002,** 43, 2961-2965.
114. Boeckman, R. K.; Potenza, J. J. C.; Enholm, E. J., Synthetic studies directed toward naturally occurring tetramic acids. 3. Synthesis of (-)-methyl ydiginate and the tetramic acid subunit for streptolydigin. *J. Org. Chem.* **1987,** 52, 469-472.
115. Stahl, G. L.; Walter, R.; Smith, C. W., General procedure for the synthesis of mono-*N*-acylated 1,6-diaminohexanes. *J. Org. Chem.* **1978,** 43, 2285-2286.
116. Chen, J.; Forsyth, C. J., Total synthesis of Apratoxin A. *J. Am. Chem. Soc.* **2003,** 125, 8734-8735.
117. Albericio, F.; Cases, M.; Alsina, J.; Triolo, S. A.; Carpino, L. A.; Kates, S. A., On the use of PyAOP, a phosphonium salt derived from HOAt, in solid-phase peptide synthesis. *Tetrahedron Lett.* **1997,** 38, 4853-4856.
118. Guibe, F., Allylic protecting groups and their use in a complex environment part II: Allylic protecting groups and their removal through catalytic palladium [pi]-allyl methodology. *Tetrahedron* **1998,** 54, 2967-3042.

119. Genet, J. P.; Blart, E.; Savignac, M.; Lemeune, S.; Lemaireaudoire, S.; Paris, J. M.; Bernard, J. M., Practical palladium-mediated deprotective method of Allyloxycarbonyl in aqueous media. *Tetrahedron* **1991,** 50, 497-503.
120. Lemaireaudoire, S.; Savignac, M.; Blart, E.; Pourcelot, G.; Genet, J. P.; Bernard, J. M., Selective deprotective method using palladium-water soluble catalysts. *Tetrahedron Lett.* **1994,** 35, 8783-8786.
121. Arnould, J. C.; Landier, F.; Pasquet, M. J., New applications of the mitsunobu reaction in the synthesis of *C*-2 *N*-methyl carbapenems. *Tetrahedron Lett.* **1992,** 33, 7133-7136.
122. Alsina, J.; Rabanal, F.; Giralt, E.; Albericio, F., Solid-phase synthesis of "head-to-tail" cyclic peptides via lysine side-chain anchoring. *Tetrahedron Lett.* **1994,** 35, 9633-9636.
123. Kates, S. A.; Sole, N. A.; Johnson, C. R.; Hudson, D.; Barany, G.; Albericio, Fernando, A novel, convenient, three-dimensional orthogonal strategy for solid-phase synthesis of cyclic peptides. *Tetrahedron Lett.* **1993,** 34, 1549-1552.
124. Li, P.; Roller, P. P., Cyclization strategies in peptide derived drug design. *Curr. Top. Med. Chem.* **2002,** 2, 325-341.
125. Kates, S. A.; Albericio, F., *Solid-phase synthesis: a practical guide*. Marcel Dekker: New York, 2000.
126. Barlos, K.; Gatos, D.; Kallitsis, J.; Papaphotiu, G.; Sotiriu, P.; Yao, W.; Schafer, W., Darstellung geschützter peptid-fragmente unter einsatz substituierter triphenylmethyl-harze. *Tetrahedron Lett.* **1989,** 30, 3943-3946.
127. Barlos, K.; Gatos, D.; Kapolos, S.; Papaphotiu, G.; Schafer, W.; Yao, W., Veresterung von partiell geschutzten peptid-fragmenten mit harzen. Einsatz von 2-chlortritylchlorid zur synthese von Leu15 -gastrin I. *Tetrahedron Lett.* **1989,** 30, 3947-3950.
128. Hu, T.; Panek, J. S., Enantioselective synthesis of the protein phosphatase inhibitor (-)-motuporin. *J. Am. Chem. Soc.* **2002,** 124, 11368-11378.
129. Murakami, N.; Wang, W.; Ohyabu, N.; Ito, T.; Tamura, S.; Aoki, S.; Kobayashi, M.; Kitagawa, I., Synthesis of amide analogs of Arenastatin A. *Tetrahedron* **2000,** 56, 9121-9128.
130. Chao, H.; Bernatowicz, M. S.; Reiss, P. D. M., G. R., Synthesis and application of bis-silylethyl-derived phosphate-protected Fmoc-phosphotyrosine derivatives for deptide synthesis. *J. Org. Chem.* **1994,** 59, 6687-6691.
131. Gao, C.; Lin, C.; Lo, C. L.; Mao, S.; Wirsching, P.; Lerner, R. A.; Janda, K. D., Making chemistry selectable by linking it to infectivity. *Proc. Natl. Acad. Sci. USA* **1997,** 94, 11777-11782.
132. Jansson, K.; Ahlfors, S.; Frejd, T.; Kihlberg, J.; Magnusson, G.; Dahmen, J.; Noori, G.; Stenvall, K., 2-(Trimethylsilyl)ethyl glycosides. 3. Synthesis, anomeric deblocking, and transformation into 1,2-trans 1-*O*-acyl sugars. *J. Org. Chem.* **1988,** 53, 5629-5647.
133. Chiosis, G.; Boneca, I. G., Selective cleavage of D-Ala-D-Lac by small molecules: re-sensitizing resistant bacteria to vancomycin. *Science* **2001,** 293, 1484-1487.
134. Mehta, A.; Jaouhari, R.; Benson, T. J.; Douglas, Kenneth T., Improved efficiency and selectivity in peptide synthesis: Use of triethylsilane as a carbocation scavenger in

deprotection of *t*-butyl esters and *t*-butoxycarbonyl-protected sites. *Tetrahedron Lett.* **1992,** 33, 5441-5444.
135. Pearson, D. A.; Blanchette, M.; Baker, M. L.; Guindon, C. A., Trialkylsilanes as scavengers for the trifluoroacetic acid deblocking of protecting groups in peptide synthesis. *Tetrahedron Lett.* **1989,** 30, 2739-2742.
136. Fields, C. G.; Fields, G. B., Minimization of tryptophan alkylation following 9-fluorenylmethoxycarbonyl solid-phase peptide synthesis. *Tetrahedron Lett.* **1993,** 34, 6661-6664.
137. Jingen Deng; Yasumasa Hamada; Takayuki Shioiri, A new synthesis of cyclotheonamide B via guanidination of ornithine. *Tetrahedron Lett.* **1996,** 37, 2261-2264.
138. Carpino, L. A.; Dean, S.; Chao, H. G.; DeSelms, R. H., [(9-Fluorenylmethyl)oxy]carbonyl (Fmoc) amino acid fluorides. Convienient new peptide coupling reagents applicable to the Fmoc/*tert*-butyl strategy for solution and solid-phase syntheses. *J. Am. Chem. Soc.* **1990,** 112, 9651-9652.
139. Carpino, L. A.; Faham, A. E.; F., A., Racemization studies during solid-phase peptide synthesis using azabenzotriazole-based coupling reagents. *Tetrahedron Lett.* **1995,** 35, 2279-2282.
140. Carpino, L. A.; El-Faham, A., Tetramethylfluoroformamidinium hexafluorophosphate: a rapid-acting peptide coupling reagent for solution and solid phase peptide synthesis. *J. Am. Chem. Soc.* **1995,** 117, 5401-5402.
141. Miyano, H.; Toyo'oka, T.; Imai, K., Further studies on the reaction of amines and proteins with 4-fluoro-7-nitrobenzo-2-oxa-1,3-diazole. *Anal. Chim. Acta.* **1985,** 170, 81-87.
142. Nikam, S. S.; Komberg, B. E.; Johnson, D. R.; Doherty, A. M., Synthesis of hydroxamic acids: $Pd/BaSO_4$ as a new catalyst for the deprotection of *O*-benzyl hydroxamates. *Tetrahedron Lett.* **1995,** 36, 197-200.
143. Stoermer, D.; Liu, Q.; Hall, M. R.; Flanary, J. M.; Thomas, A. G.; Rojas, C.; Slusher, B. S.; Tsukamoto, T., Synthesis and biological evaluation of hydroxamate-based inhibitors of glutamate carboxypeptidase II. *Bioorg. Med. Chem. Lett.* **2003,** 13, 2097-2100.
144. Hoekstra, W. J.; Greco, M. N.; Yabut, S. C.; Hulshizer, B. L.; Maryanoff, B. E., Solid-phase synthesis via N-terminal attachment to the 2-chlorotrityl resin. *Tetrahedron Lett.* **1997,** 38, 2629-2632.
145. Kolle, D.; Brosch, G.; Lechner, T.; Lusser, A.; Loidl, P., Biochemical methods for analysis of histone deacetylases. *Methods* **1998,** 15, 323-331.
146. Kijma, M.; Yoshida, M.; Sugita, K.; Horinouchi, S.; Beppu, T., Trapoxin, an antitumor cyclic tetrapeptide, is an irresversible
inhibitor of mammalian histone deacetylase. *J. Biol. Chem.* **1993,** 268, 22429-22435.
147. Darkin-Rattray, S. J.; Gurnett, A. M.; Myers, R. W.; Dulski, P. M.; Crumley, T. M.; Allocco, J. J.; Cannova, C.; Meinke, P. T.; Colletti, S. L.; Bednarek, M. A.; Singh, S. B.; Goetz, M. A.; Dombrowski, A. W.; Polishook, J. D.; Schmatz, D. M., Apicidin: a novel antiprotozoal agent that inhibits parasite histone deacetylase. *Proc. Natl. Acad. Sci. USA* **1996,** 93, 13143-13147.
148. Hoffmann, K.; Brosch, G.; Loidl, P.; Jung, M., A non-isotopic assay for histone deacetylase activity. *Nucleic Acids Res.* **1999,** 27, 2057-2058.

149. Wegener, D.; Hildmann, C.; Schwienhorst, A., Recent progress in the development of assays suited for histone deacetylase inhibitor screening. *Mol. Gen. Metab.* **2003,** 80, 138-147.
150. Wegener, D.; Wirsching, F.; Riester, D.; Schwienhorst, A., A fluorogenic histone deacetylase assay well suited for high-throughput activity screening. *Chem. Biol.* **2003,** 10, 61-68.
151. Schultz, B. E.; Misialek, S.; Wu, J.; Tang, J.; Conn, M. T.; Tahilramani, R.; Wong, L., Kinetics and comparative reactivity of human class I and class IIb histone deacetylases. *Biochemistry* **2004,** 43, 11083-11091.
152. Williams, J. W.; Morrison, J. F., The kinetics of reversible tight-binding inhibition. *Methods Enzymol.* **1979,** 63, 437-467.
153. Nishino, N.; Jose, B.; Okamura, S.; Ebisusaki, S.; Kato, T.; Sumida, Y.; Yoshida, M., Cyclic tetrapeptides bearing a sulfhydryl group potently inhibit histone deacetylases. *Org. Lett.* **2003,** 5, 5079-5082
154. Anderson, W. F.; Ohlendorf, D. H.; Takeda, Y.; Mattews, B. W., Structure of the cro repressor from bacteriophage labmbda and its interaction with DNA. *Nature* **1981,** 290, 754-758.
155. Branden, C.; Tooze, J., *Introduction to protein structure* Garland Publishig Inc.: 1991; p 13.
156. Etzkorn, F. A.; Travins, J. M.; Hart, S. A., *Rare protein turns: helix-turn-helix, gamma-turn and cis-proline mimics*. JAI Press Inc: Greenwich, CT, 1999; Vol. 2.
157. Passner, J. M.; Ryoo, H. D.; Shen, L.; Mann, R. S.; Aggarwal, A. K., Structure of aDNA-bound Ultrabithorax-Extradenticle homeodomain complex. *Nature* **1999,** 397, 714-719.
158. Travins, J. M. Turn mimics for the helix-turn-helix protein motif. Ph. D., University of Virginia, 1999.
159. Chou, P. Y.; Fasman, G. D., β-Turns in proteins. *J. Mol. Biol.* **1977,** 115, 135-175.
160. Mondragon, A.; Harrison, C., The phage 434-Cro/OR1 complex at 2.5Å resolution. *J. Mol. Biol.* **1991,** 219, 321-334.
161. Muller, M.; Affolter, M.; Leupin, W.; Otting, G.; Wuthrich, K.; J.Gehring, W., Isolation and sequence-specific DNA binding of the Antennapedia homeodomain. *The EMBO Journal* **1988,** 7, 4299-4304.
162. Schmidt, U.; Lieberknect, A.; Wild, J., Amino acids and peptides; XLlll. Dehydroamino acids; XVlll. Synthesis of dehydroamino and amino acid from N-Acyl-2-(dialkyloxyphosphinyl)-glycine esters. *Synthesis* **1984**, 53-60.
163. Bajwa, J. S., One-pot transformation of benzyl carbamates into *t*-butyl carbamates. *Tetrahedron Lett.* **1992,** 33, 2955-2956.
164. Schmidt, U.; Griesser, H.; Leiberknecht, A. L., V.; Mangold, R.; Meyer, R., Diastereoselective formation of (*Z*)-diadehydroamino acid esters *Synthesis* **1992**, 487-490.
165. Schmidt, U.; Meyer, R.; Leitenberger, V.; Griesser, H.; Leiberknecht, A., Total synthesis of the biphenomycins; III. synthesis of Biphenomyrin B. *Synthesis* **1992**, 1025-1030.

166. Burk, M. J.; Feaster, J. E.; Nugent, W. A.; Harlow, R. L., Preparation and use of C2-symmetric bis(phospholanes): production of α-amino acid derivatives via highly enantioselective hydrogenation reactions *J. A. C. S.* **1993,** 115, 10125-10138.
167. BurkeJr., T. R.; Smyth, M. S.; Otaka, A.; Roller, P. P., Synthesis of 4-phosphono(difluoromethyl)-D,L-phenylalanine and *N*-boc and *N*-Fmoc derivatives suitably protected for solid-phase synthesis of nonhydrolyzable phosphotyrosyl peptide analogues. *Tetrahedron Lett.* **1993,** 34, 4125-4128.
168. Sheehan, J.; Cruickshank, P.; Boshart, G., Notes- a convenient synthesis of water-soluble carbodiimides. *J. Org. Chem.* **1961,** 26, 2525-2528.
169. Sheehan, J. C.; Preston, J. A., Rapid synthesis of oligopeptide derivatives without isolation of intermediates. . *J. A. C. S.* **1965,** 87, 2492-2493.
170. Mertes, K. B.; Qian, L.; Sun, Z.; Deffo, T. A., Convenient synthesis of macrocyclic lactams. *Tetrahedron Lett.* **1990,** 31, 6469-6472.
171. Shioiri, T.; Ninomiya, K.; Yamada, S., Diphenylphosphory azide: a new convenient reagent for a modified curtius reaction and for the peptide synthesis. *J. Am. Chem. Soc.* **1972,** 94, 6203-6205.
172. Corey, E. J.; Venkateswarlu, A., Protection of hydroxyl groups as *tert*-butyldimethylsilyl derivatives. *J. Am. Chem. Soc.* **1972,** 94, 6190-6191.
173. Hughes, D. L.; Bergan, J. J.; Grabowski, J. J., Amino acid chemistry in dipolar aprotic solvents: dissociation constants and ambident reactivity. *J. Org. Chem.* **1986,** 51, 2579-2585.
174. Lajoie, G. A.; Luo, Y.; Evindar, G.; Fishlock, D., Synthesis of *N*-protected *N*-methyl serine and threonine. *Tetrahedron Lett.* **2001,** 42, 3807-3809.
175. Casares, F.; Mann, R. S., Control of antennal versus leg development in Drosophila. *Nature* **1998,** 392, 723 - 726.
176. Brennan, R. G.; Mattews, B. W., Helix-turn-helix DNA binding motif. *J. Biol. Chem.* **1989,** 264, 1903-1906.
177. Gehring, W.; Affolter, M.; Burglin, T., Homeodomain proteins. *Annu. Rev. Biochem.* **1994,** 63, 487-526.
178. Banerjee-Basu, S.; Ferlanti, E. S.; Ryan, J. F.; Baxevanis, A. D., The Homeodomain Resource: Sequences, Structures, and Genomic Information. *Nucleic Acids Res.* **1999,** 27, 336-337.
179. Wintjens, R.; Rooman, M., Structural classification of HTH DNA-binding domains and protein-DNA intreraction modes. *J. Mol. Biol.* **1996,** 262, 294-313.
180. Weiler, S.; Gruschus, J. M.; Tsao, D. H.; Yu, L.; Wang, L.; Nirenberg, M.; Ferretti, J. A., Site-directed mutations in the and-NK-2 homeodomain. *J. Mol. Biol.* **1998,** 273, 10994-11000.
181. Tsao, D. H. H.; Gruschus, J. M.; Wang, L.-H.; Nirenberg, M.; Ferretti, J. A., Elongaton of helix III of the NK-2 homeodomain upon binding to DNA: a secondary structure study by NMR. *Biochemstry* **1994,** 33, 15053-15060.
182. Klemm, J. D.; Rould, M. A.; Aurora, R.; Herr, W.; Pabo, C. O., Crystal structure of the Oct-1 POU domain bound to an octamer site: DNA recogniton with tethered DNA-binding modules. *Cell* **1994,** 77, 21-32.
183. Ruvkun, G.; Finney, M., Regulation of Transcription and Cell Identity by POU Domain Proteins. *Cell* **1991,** 64, 475-478.

184. Mohamadi, F.; Richards, N. G.; Guida, W. C.; Liskamp, R.; Lipton, M.; Caufield, C.; Chang, G.; Hendrickson, T.; Still, W. C., MacroModel---an integrated software system for mdeling organic and bioorganic molecules using molecular mechanics. *J. Comp. Chem.* **1990,** 11, 440-467.
185. Pennington, M. W., HF cleavage and deprotection procedures for peptides synthesized using a Boc/Bzl strategy. *Methods Mol. Biol.* **1994,** 35, 41-62.
186. Ye, B.; Akamatsu, M.; Shoelson, S. E.; Wolf, G.; Giorgetti-Peraldi, S.; Yan, X.; Roller, P. P.; Burke, T. R., L-*O*-(2-Malonyl)tyrosine: a new phosphotyrosyl mimetic for the preparation of Src homology 2 domain inhibitory peptides. *J. Med. Chem.* **1995,** 38, 4270-4275.
187. Sypniewski, M.; Penke, B.; Simon, L.; Rivier, J., (*R*)-*tert*-butoxycarbonylamino-fluorenylmethoxycarbonyl- glycine from (*S*)-benzyloxycarbonyl- serine or from papain resolution of the corresponding amide or methyl ester. *J. Org. Chem.* **2000,** 65, 6595-6600.
188. Gordeer, M. F.; Patel, D. V.; Barker, P. L.; Gordon, E. M., *N*-a-Fmoc-4-Phosphono(difluromethyl)-L-phenylalanine: A new *O*-phosphotyrosine ssosteric building block suitable for direct incorporation into peptides. *Tetrahedron Lett.* **1994,** 35, 7585-7588.
189. Bolin, D.; Sytwu, I.-I.; Humiec, F.; Meienhofer, J., Preparation of oligomer-free *N*-Fmoc and *N*-urethane amino acids. *Int. J. Peptide Protein Res.* **1989,** 33, 353-359.
190. Young, T.; Kiessling, L. L., A strategy for the synthesis of sulfated peptides. *Angew . Chem. Int. Ed.* **2002,** 41, 3449-3451.
191. West, C. W.; Estiarte, M. A.; Rich, D. H., New methods for side-chain protection of cysteine. *Org. Lett.* **2001,** 3, 1205-1208.
192. Lenzi, A.; Reginato, G.; Taddai, M., Synthesis of *N*-Boc-α-amino acids with nucleobase residues as building blocks for the preparation of chiral PNA (peptidic nucleic acids). *Tetrahedron Lett.* **1995,** 36, 1713-1716.
193. Ciapettia, P.; Soccolinib, F.; Taddei, M., Synthesis of *N*-Fmoc--amino acids carrying the four DNA nucleobases in the side chain. *Tetrahedron* **1997,** 53, 1167-1176.
194. Doi, M.; Kiritoshi, Y. N. N.; Iwata, T.; Nago, M.; Nakano, H.; Uchiyama, S.; Nakazawa, T.; Wakamiya, T.; Kobayashi, Y., Simple and efficient syntheses of Boc- and Fmoc-protected 4(*R*)- and 4(*S*)-fluoroproline solely from 4(*R*)-hydroxyproline. *Tetrahedron* **2002,** 58, 8453-8459.
195. Murray, P. J.; Starkey, I. D.; Davies, J., The enatiospecific synthesis of novel Lysine analogues incorporating a pyrrolidine containing side chain. *Tetrahedron Lett.* **1998,** 39, 6721-6724.
196. Schmidt, U.; Kroner, M.; Griesser, H., Total synthesis of the didemnins - 1. synthesis of the peptolide ring1. *Tetrahedron Lett.* **1988,** 29, 3057-3060.
197. Gosselin, F.; Lubell, W. D., Rigid dipeptide surrogates: syntheses of enantiopure quinolizidinone and pyrroloazepinone amino acids from a common diaminodicarboxylate precursor. *J. Org. Chem.* **2000,** 65, 2163-2171.
198. Fenniri, H.; Mathivanan, P.; Vidale, K. L.; Sherman, D. M.; Hallenga, K.; Wood, K. V.; Stowell, J. G., Helical rosette nanotubes: design, self-Assembly, and characterization. *J. Am. Chem. Soc.* **2001,** 123, 3854-3855.

199. Van den Broek, L. A. G. M.; Breuer, M. L.; Liskamp, R. M. J.; Ottenheijm, H. C. J., Total synthesis and absolute configuration of the natural dipeptide γ-glutamylmarasmine. *J. Org. Chem.* **1987,** 52, 1511-1517.
200. Nomura, M.; Shuto, S.; Matsuda, A., Development of an efficient intermediate, α-[2-(trimethylsilyl)ethoxy]-2-*N*- [2-(trimethylsilyl)ethoxycarbonyl]folic acid, for the synthesis of folate γ-conjugates, and its application to the synthesis of folate-nucleoside conjugates. *J. Org. Chem.* **2000,** 65, 5016-5021.
201. Besser, D.; Müller, B.; Kleinwächter, P.; Greiner, G.; Seyfarth, L.; Steinmetzer, T.; Reissmann, S., Synthesis and characterization of octapeptide somatostatin analogues with backbone cyclization: comparison of different strategies, biological activities and enzymatic stabilities. *J. Prakt. Chem.* **2000,** 342, 537-545.
202. Fields, G. B., Noble, R. L., Solid phase peptide syntheis utilizing 9-fluorenylmethoxycarbonyl amino acids. *Int. J. Peptide Res.* **1990,** 35, 161-214.
203. Ananda, K.; Gopi, H. N.; Suresh Babu, V. V., Convenient and efficient synthesis of Boc/Z/Fmocamino acids employing Nprotected amino acid fluorides. *J. Peptide Res.* **2000,** 55, 289-294.
204. Carpino, L. A.; Ionescu, D.; El-Faham, A.; Beyermann, M.; Henklein, P.; Hanay, C.; Wenschuh, H.; Bienert, M., Complex polyfluoride additives in Fmoc-amino acid fluoride coupling processes. Enhanced reactivity and avoidance of stereomutation. *Org Lett.* **2003,** 3, 975-977.
205. White, J. M.; Tunoori, A. R.; Turunen, B. J.; Georg, G. I., [Bis(2-methoxyethyl)amino]sulfur trifluoride, the deoxo-fluor reagent: application toward one-flask transformations of carboxylic acids to amides. *J. Org. Chem.* **2004,** 69, 2573-2576.

Appendix A. Control Compound of Histone deacetylase inhibitor.

Two control compounds were designed and synthesized, and assayed against HDAC's activity. The control compound **70** was synthesized from intermediate **28** by removing the protecting groups. The control compound **73** was synthesized through solution-phase peptide synthesis, starting from intermediate **10**.

Scheme A1. The synthesis of control compound **70**.

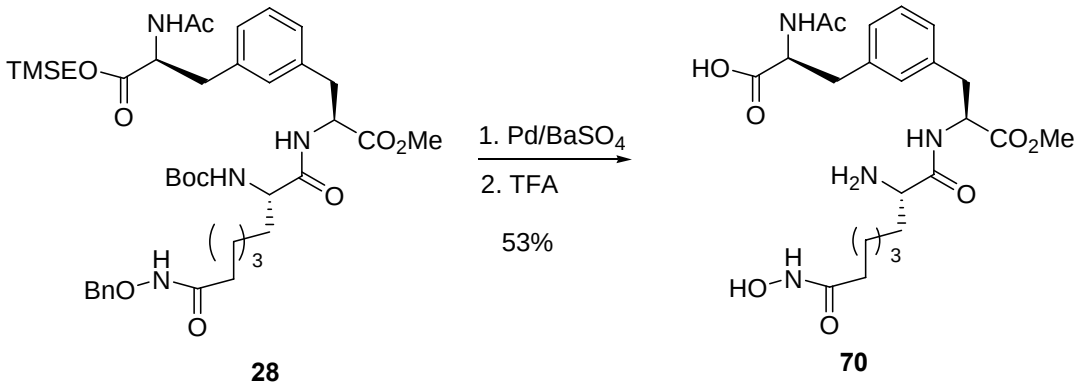

Scheme A2. The synthesis of control compound **73**.

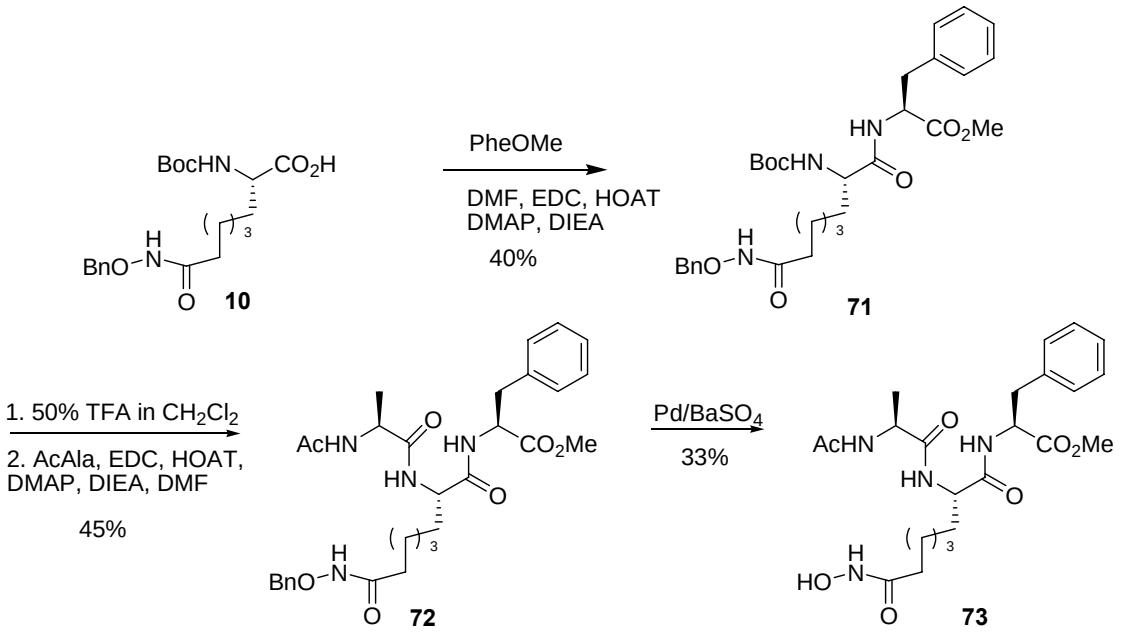

The HDAC inhibitors' inhibitory effects towards HDACs.

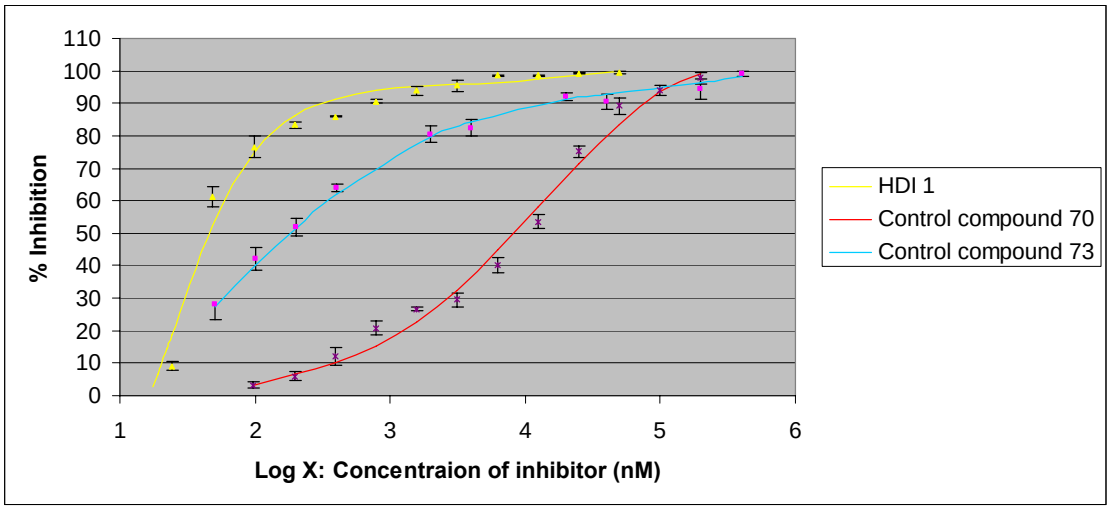

Figure A1. Dose response curve of HDIs toward HDACs. Yellow: inhibitory effect of HDI **1** against HDACs (IC_{50} = 46 ± 15 nM); blue: the inhibitory of control compound **73** against HDACs (IC_{50} = 167 ± 23 nM); red: the inhibitory of control compound **70** against HDACs (IC_{50} = 8.2 ± 1.1 μM).

The concentration of HDAC inhibitors for 50% inhibition was determined by plotting the percent inhibition versus the log [I], and fitting experimental data to a dose response curve (95% confidence level) using equation (1) in TableCurve (version 3 for win32). Where % I is the % inhibition, and [I] is the substrate concentration. For HDI **1**, a = 23.17, b = 120.07, c = 1.54, and d = 5.88 are the fitted constants; r_2 = 0.9999. For HDI **73**, a = 40.81, b = 53.64, c = 2.94, and d = -5.62 are the fitted constants; r^2 = 0.9865. For HDI **70**, a = 4.87, b = 122.57, c = 4.28, and d = -6.13; r_2 = 0.9866.

$$\%I = a + \frac{b}{\{1 + (\log[S]/c)^d\}}$$

The HDAC inhibitors' inhibitory effects towards HDAC1.

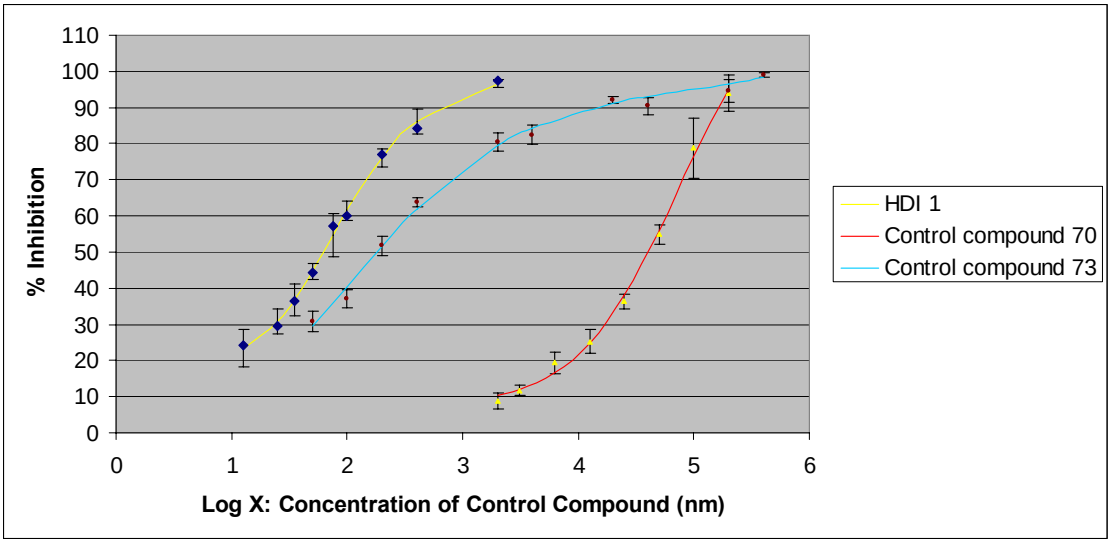

Figure A2. Dose response curve of HDIs toward HDAC1. Yellow: inhibitory effect of HDI **1** against HDAC1 (IC_{50} = 59.0 ± 4.7 nM); blue: the inhibitory of control compound **73** against HDAC1 (IC_{50} = 183 ± 18 μM); red: the inhibitory of control compound **70** against HDAC1 (IC_{50} = 40.2 ± 6.0 μM).

The concentration of compound **1** for 50% inhibition was determined by plotting the percent inhibition versus the log [M], and fitting experimental data to a dose response curve (95% confidence level) using equation (1) in TableCurve (version 3 for win32). Where % I is the % inhibition, and [S] is the substrate concentration. For HDI **1**, a = 23.10, b = 45.08, c = 4.70, and d = -26.44 are the fitted constants; r_2 = 0.9972. For HDI **73**, a = 12.07, b = 87.20, c = 2.41, and d = -3.95 are the fitted constants; r^2 = 0.9967. For HDI **70**, = 8.43, b = 131.15, c = 4.97, and d = -10.13; r_2 = 0. 9937.

$$\%I = a + \frac{b}{\{1 + (\log[S]/c)^d\}}$$

Table A1. In vitro inhibition of HDAC activity.

	HDACs (IC_{50})	HDAC1 (IC_{50})	HDAC8 (IC_{50})
HDI **1**	46 ± 15 nM	59.0 ± 4.7 nM	208 ± 20 nM
HDI **73**	8.2 ± 1.1 μM	40.2 ± 6.0 nM	NA
HDI **70**	167 ± 23 nM	183 ± 18 μM	NA
TSA	41 ± 5 nM [2.1][79]	6.0 ± 2.5 nM[47]	40[153]
SAHA	110 nM[63]	112 nM[270]	270 nM[63]

***K_i* Measurements for Pin1 Inhibitors.** Assays were performed as described for the determination of IC_{50}. The substrate concentrations were 20, 35, 50, 75, and 100 μM. The final concentrations of the HDAC inhibitor **1** were 6, 12, 24, 48, and 97 nM. All the data were fitted to Enzyme Kinetics module and calculate by SigmaPlot 9.0. The best model was selected using the goodness fit criteria AIC (Akaike Information Criterion) derived from SigmaPlot. The AIC is one extremely handy and often used method to compare models. It evaluates the overall discrepancy between observed and model-implied values (data fit), while taking into account the model's simplicity. The best fitted model has the lowest AIC value. The AIC values of HDI **1** for competitive, noncompetitive, and uncompetitive inhibition patterns were -96.933, -87.341, -77.390, respectively. The calculated Ki value by fitting the competitive model in Enzyme Kinetics module was 17.52. The following Michaelis- Menten and Lineweaver- Burk graphs were generated by Enzyme Kinetics module.

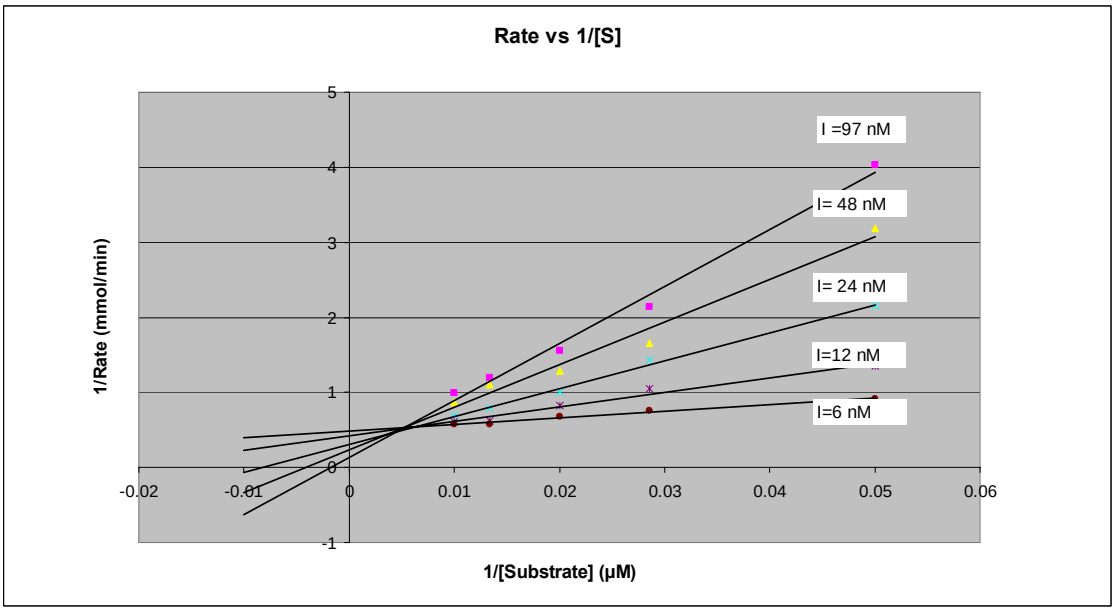

Figure A3. Michaelis-Menten chart of HDI **1**. (Created from Excel)

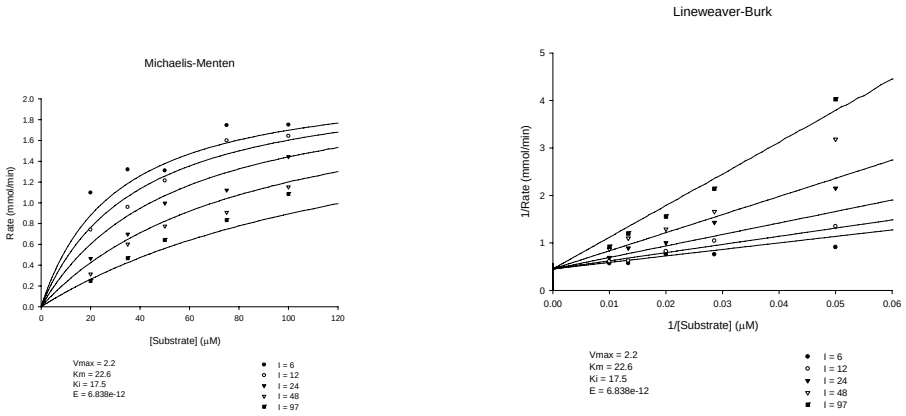

Figure A4. Michaelis-Menten chart and Lineweaver-Burk chart of HDI **1**. (Created from Enzyme Kinetics module)

Experimental

General Experiment. Unless specified otherwise, all chemicals were used as received. THF was freshly distilled under nitrogen from sodium/benzophenone ketyl immediately prior to use. Dichloromethane was freshly distilled under nitrogen from calcium hydride.

DMF and MeOH were used from SureSeal^{TM} bottles. DIEA was distilled from CaH_2 under nitrogen. Brine (NaCl), $NaHCO_3$ and NH_4Cl refer to saturated aqueous solutions. ^1H NMR were recorded at 500, or 400 MHz. ^{13}C NMR were determined at 125, or 75 MHz. Flash column chromatography was performed using 230-400 mesh.

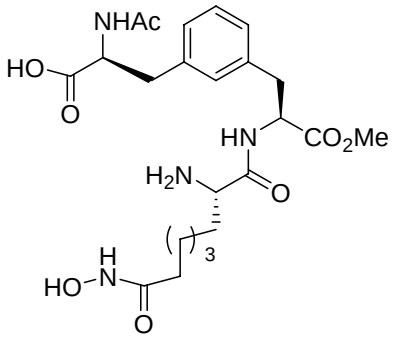

Control compound 70. Tripeptide **28** (15 mg, 0.019 mmol) was dissolved in was dissolved in MeOH (10 mL), and 5 % Pd/$BaSO_4$ (10 mg) was added. The pressure in the Parr shaker was maintained at 10 psi after 3 vacuum/H_2 cycles. The reaction was shaken 3 h at rt. The catalyst was removed by filtration on Celite, and the filtrate was concentrated to give a white solid. Without purification, the white solid was treated by a mixture of triethylsilane (22 mg, 0.19 mmol), TFA (3.0 mL), and CH_2Cl_2 (3.0 mL). The reaction mixture was stirred under N_2 for 1 h at rt. The solution was concentrated, followed by chromatography to give 5 mg (53% over two steps) as a colorless oil. Semi-preparative HPLC conditions: 10% B for 5 min, 10% B to 90% B over 12 min, 90% B for 4 min, at 20.0 mL/min. Retention time: 9.76 min. Analytical HPLC conditions: 10% B for 5 min, 10% B to 90% B over 12 min, 90% B for 4 min, at 2.0 mL/min. Retention time: 13.05 min. Purity: > 99%. ^1H NMR ($CDCl_3$/DMSO-d_6): δ 7.79 (br, s, 1H), 6.93-7.18 (m, 4H), 4.62 (m, 1H), 4.39 (m, 1H), 3.83 (t, 1H, J = 4 Hz), 3.65 (s, 3H), 3.08 (m, 2H), 2.85 (m, 2H), 2.17 (t, 2H, J = 7 Hz),

1.78 (s, 3H), 1.68 (m, 2H), 1.50 (t, 2H, J = 7 Hz), 1.29 (m, 4H). ^{13}C NMR (DMSO-$CDCl_3$): 175.0, 174.0, 171.1, 169.7, 169.6, 138.6, 137.3, 130.2, 128.7, 128.3, 127.7, 54.5, 53.8, 52.8, 52.3, 37.5, 36.6, 34.0, 31.6, 28.8, 24.8, 24.2, 23.1.

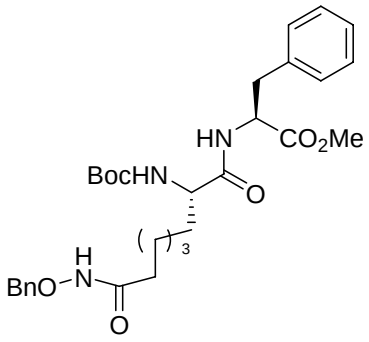

Dipeptide 71. A solution of **10** (82.0 mg, 0.208 mmol) in DMF (3 mL) was cooled in an ice bath, followed by the addition of DIEA (80.0 mg, 0.624 mmol), EDC (79.5 mg, 0.416 mmol), DMAP (2.50 mg, 0.0208 mmol), and HOAT (56.6 mg, 0.416 mmol). The resulting solution was stirred for 2 min before PheOMe (149 mg, 0.172 mmol) was added. The reaction was stirred at rt for 13 h. The reaction was diluted with EtOAc (30 mL), then washed with NH_4Cl (10 mL), water (10 mL), and Brine (10ml). The organic layer was dried over $MgSO_4$. The filtrate was concentrated *in vacuo* and purified by chromatography to give 48 mg (40 %) of a colorless oil. ^{1}H NMR ($CDCl_3$): δ 6.97-7.45 (m, 9H), 4.65-5.05 (m, 3H), 3.54-3.76 (m, 3H), 2.90- 3.28 (m, 2H), 1.08-2.42 (m, 19H). ^{13}C NMR ($CDCl_3$): δ 174.9, 172.4, 171,2, 155.8, 136.9, 136.1, 129.5, 129.3, 128.9, 128.0, 127.2, 80.2, 78.2, 55.6, 53.5, 52.4, 40.6, 29.9, 39.0, 32.3, 28.5, 24.9, 21.2.

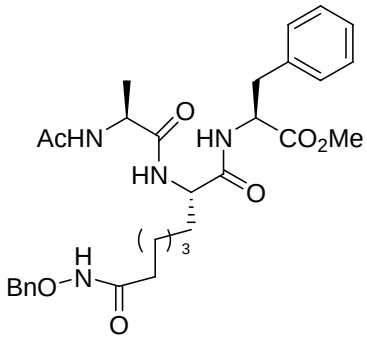

Tripeptide 72. Boc protected dipeptide **71** (41.0 mg, 0.072 mmol) was dissolved in 2.5 mL CH_2Cl_2, and then was cooled to 0 ºC by an ice bath. TFA (2.5 mL) was added to the solution. The reaction was allowed to warm to rt and stirred for 30 min. The solution was concentrated under pressure. The excess TFA was removed with diethyl ether (3 × 5 mL), producing a colorless oil. The crude product was dissolved in DMF (3 mL) and cooled to 0 ºC. AcAlaOH (29.8 mg, 0.216 mmol) were dissolved in DMF (10 mL). The solution was cooled down to 0 ºC in an ice bath, followed by the addition of DIEA (36.5 mg, 0.287 mmol), EDC (27.5 mg, 0.144 mmol), DMAP (1.75 mg, 0.0144 mmol), and HOAT (19.6 mg, 0.144 mmol). The resulting solution was stirred for 2 min before the solution of crude amine in DMF (3 mL) was added. The reaction was stirred at rt for 12 h. The reaction was quenched with EtOAc (20 mL), and was washed with NH_4Cl (10 mL), water (10 mL), and Brine (10 mL). The organic layer was dried on $MgSO_4$. The filtrate was concentrated *in vacuo*. The residue was purified by chromatography, giving a colorless oil 18.0 mg (45%). ^{1}H NMR (CD_3OD): δ 7.8-7.33 (m, 9H), 4.74 ()s, 2H), 4.64 (m, 1H), 4.10 (m, 1H), 3.67 (s, 3H), 3.10 (m, 1H), 2.94 (m, 1H), 2.13 (s, 2H), 2.00 (s, 3H), 1.90 (s, 2H), 1.10-1.53 (m, 7H), 0.89 (m, 2H). ^{13}C NMR ($CDCl_3$): δ 172.3, 171.9, 170.2, 169.9, 136.0, 129.4, 129.3, 129.0, 128.7, 127.2, 77.6, 53.5, 52.6, 48.2, 37.0, 29.9, 27.2, 23.3, 18.7, 18.4, 17.9, 17.4.

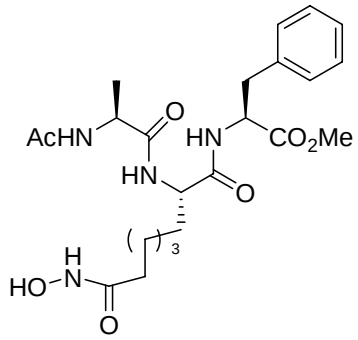

Control compound 73. Compound **72** (16.0 mg, 0.0274 mmol) was dissolved in MeOH (10 mL), and 5 % $Pd/BaSO_4$ (10 mg) was added. The pressure in the Parr shaker was maintained at 10 psi after 3 vacuum/H_2 cycles. The reaction was shaken 3 h at rt. The catalyst was removed by filtration on Celite, and the filtrate was concentrated to give a white solid. The hydroxamic acid **1** was purified by HPLC to afford 4.5 mg (33%) of a white powder. Semi-preparative HPLC conditions: 10% B for 5 min, 10% B to 90% B over 12 min, 90% B for 4 min, at 20.0 mL/min. Retention time: 11.5 min. Analytical HPLC conditions: 10% B for 5 min, 10% B to 90% B over 12 min, 90% B for 4 min, at 2.0 mL/min. Retention time: 13.71 min. Purity: > 99%. ^{1}H NMR (CD_3OD): δ 7.12-7.31 (m, 5H), 4.64 (m, 1H), 4.27 (m, 1H), 3.66 (s, 3H), 3.12 (m, 1H), 3.00 (m, 1H), 2.00-2.21 (m, 2H), 2.08 (s, 3H), 1.44-1.79 (m, 4H), 1.12-1.43 (m, 7H). ^{13}C NMR (CD_3OD): δ 174.2, 173.7, 173.4, 171.9, 169.8, 136.8, 129.0, 128.9, 128.2, 126.6, 53.8, 52.9, 51.3, 49.0, 36.8, 35.2, 31.7, 28.0, 24.9, 21.1, 16.3, 16.0.